



Industrial application of supercritical carbon dioxide soluble polymers

Alba Castanon Rodriguez

► To cite this version:

Alba Castanon Rodriguez. Industrial application of supercritical carbon dioxide soluble polymers. Polymers. Université de Lyon; University of Nottingham, 2018. English. NNT : 2018LYSE1233 . tel-02026024

HAL Id: tel-02026024

<https://theses.hal.science/tel-02026024>

Submitted on 20 Feb 2019

HAL is a multi-disciplinary open access archive for the deposit and dissemination of scientific research documents, whether they are published or not. The documents may come from teaching and research institutions in France or abroad, or from public or private research centers.

L'archive ouverte pluridisciplinaire **HAL**, est destinée au dépôt et à la diffusion de documents scientifiques de niveau recherche, publiés ou non, émanant des établissements d'enseignement et de recherche français ou étrangers, des laboratoires publics ou privés.



N°d'ordre NNT : 2018LYSE1233

THESE de DOCTORAT DE L'UNIVERSITE DE LYON

opérée au sein de
l'Université Claude Bernard Lyon 1

Ecole Doctorale de Lyon

N° ED206

Spécialité de doctorat : Chimie

Discipline : Chimie des Polymères

Soutenue publiquement le 29/10/2018, par :

Alba Castañón Rodríguez

Application industrielle de polymères solubles dans le dioxyde de carbone supercritique

Devant le jury composé de :

Rapporteur & Président : Andreas Heise, Professeur des Universités, Royal College of Surgeons in Ireland

Rapporteur : Sébastien Perrier, Professeur des Universités, University of Warwick

Examineur : David Amabilino, Professeur des Universités, University of Nottingham

Examineur : Emmanuel Beyou, Professeur des Universités, Université Claude Bernard Lyon 1

Examinatrice : Helen Willcock, Professeur Associé, University of Loughborough

Directeur de thèse : Steven Howdle, Professeur des Universités, University of Nottingham

Co-directrice de thèse : Muriel Lansalot, Directeur de recherche CNRS, Université Claude Bernard Lyon 1.

Invité : Franck D'Agosto, Directeur de recherche CNRS, Université Claude Bernard Lyon 1.



Industrial application of supercritical carbon dioxide soluble polymers

Alba Castañón Rodríguez

Thesis submitted to the University of Nottingham for the
degree of Doctor of Philosophy

September 2018



**University of
Nottingham**
UK | CHINA | MALAYSIA



Declaration

Except where specific reference has been made to other sources, the work presented in this thesis is the original work of the author. It has not been submitted, in whole, or in part, for any other degree or professional qualification.

Date:.....

Signed:.....

Alba Castañon Rodriguez

Acknowledgements

Firstly, I would like to thank my supervisors, Professor Steve Howdle in Nottingham and Dr. Muriel Lansalot and Dr. Franck D'Agosto in Lyon, for giving me the opportunity to work in this project with them and for guiding me through this PhD. I would also like to thank the European Doctoral Programme in Sustainable Industrial Chemistry (SINCHEM) for the funding.

I would like to thank everyone in the Howdle group I shared my time in Nottingham with and were always there to help, especially all the post-docs: Simon Basset, Guping He, Tom Bennet, Liv Monaghan and Andrea Hufendiek, for their guidance and help. I also want to thank my project student, Josh, for his help with some of the work reported in this thesis.

I would also like to thank Rahmet, my partner in crime, for sharing her knowledge and wisdom with me, to Alice for always being willing to help, especially with some of the SEM reported in this thesis, to Mariana for her support during the very stressful period of thesis submission and to Marina for being a friend when I moved to Nottingham. A special thank you to all the B10 galz.

I would also like to thank the team in Lyon for all their help during my time there, especially to Mathieu for helping me in the lab and to the SEC technicians Manel and Olivier. I am also grateful to Daniel Lester at Warwick University for his help with SEC.

I would also like to thank the Workshop staff in Nottingham for their technical support with the equipment used throughout this work, especially Pete Fields and Richard Wilson, who fixed my equipment so many times. Also thank you to Mark Guyler for all

of his help with all things lab related, and to Sue for taking care of all of us during the coffee breaks.

I am also grateful to my SINCEM colleagues who I shared the PhD experience with and supported me and my friends in Spain who were always there for me when I had a bad day. I would also like to thank my partner, Thomas, who not only supported me but also pushed me to keep going when I felt like giving up.

Last but most importantly, I would like to thank my wonderful family, my parents who always supported me even in the decision to leave them and move far away, but especially my brother Alejandro who always encouraged me and made me smile. He was always my role model and since he is sadly no longer with us, I would like to dedicate this thesis to him.

Abbreviations

AIBN	Azobisisobutyronitrile
ATRP	Atom transfer radical polymerisation
CRP	Controlled radical polymerisation
\bar{D}	Dispersity
DCM	Dichloromethane
DMF	Dimethyl formamide
DSC	Differential scanning calorimetry
LAM	Less activated monomer
MADIX	Macromolecular design via interchange of xanthates
MAM	More activated monomer
MMA	Methyl methacrylate
M_n	Number average molecular mass
M_w	Weight average molecular mass
NMP	Nitroxide mediated polymerisation
NMR	Nuclear magnetic resonance
NVP	N-vinyl pyrrolidone
PDMS	Polydimethyl siloxane
RAFT	Reversible addition-fragmentation chain transfer
RDRP	Reversible-deactivation radical polymerisation
scCO ₂	Supercritical carbon dioxide
SCF	Supercritical fluid
SEC	Size exclusion chromatography

SEC RI	Size exclusion chromatography refractive index
SEC UV	Size exclusion chromatography ultraviolet
SEM	Scanning electron microscopy
THF	Tetrahydrofuran
VAc	Vinyl acetate
VPI	Vinyl pivalate

Abstract

Carbon capture has become a major global process, carbon dioxide (CO₂) can be separated as a by-product in the industrial production of ammonia and ethanol using different methods such as cryogenic separation or the use of membranes, reducing the carbon footprint of the process.

Our aim is to make positive use of the captured carbon dioxide as an alternative green solvent for polymer synthesis. Dispersion polymerisation is an industrially relevant technique that provides polymer particles with defined morphology and size that are used in various applications from drug delivery to electronics. However, the main limitation for using supercritical carbon dioxide (scCO₂) as solvent in this technique is the lack of highly soluble, environmentally friendly and affordable stabilisers.

In this thesis the synthesis of hydrocarbon based stabilisers for dispersion polymerisation is explored. Until very recently, only fluorocarbon and silicone based (polydimethylsiloxane, PDMS) polymers showed any significant solubility in scCO₂ but these are expensive and not environmentally friendly. Hydrocarbon stabilisers such as poly(vinyl acetate-*stat*-vinyl pivalate) (P(VAc-*stat*-VPi)) constitute a viable alternative. However they have only worked successfully for one monomer, N-vinyl pyrrolidone (NVP). The application of P(VAc-*stat*-VPi) based stabilisers in dispersion polymerisation of methyl methacrylate (MMA) is thus explored in this work.

A range of P(VAc-*stat*-VPi)-*block*-PNVP block copolymers with different molar masses and compositions were synthesised using controlled radical

polymerisation (RAFT/MADIX) and characterised by different techniques such as nuclear magnetic resonance (NMR) spectroscopy and size exclusion chromatography (SEC) showing narrow dispersities. Solubility of the stabilisers was tested using a variable volume view cell.

Block copolymers of different DP of PNVP were tested in dispersion polymerisation of MMA. Although none of the reactions proceeded to high conversion as expected for this kind of process, micron sized polymer particles of spherical morphology could be observed by scanning electron microscopy (SEM) for some of the stabiliser materials, making them a very promising alternative.

Table of contents

Chapter 1: Introduction	1
1.1 Green chemistry.....	1
1.2 Supercritical fluids.....	3
1.2.1 Supercritical carbon dioxide.....	6
1.3 Introduction to polymers	7
1.3.1 Polymerisation techniques according to mechanism	9
1.3.2 Polymerisation techniques according to process	26
1.4 Aims and objectives	33
Chapter 2: Experimental and characterisation techniques.....	36
2.1 High pressure equipment	36
2.1.1 General high pressure setup.....	36
2.1.2 MK III sealed autoclave	37
2.1.3 Procedure for dispersion polymerisation in scCO ₂	38
2.1.4 High pressure variable volume view cell.....	41
2.1.5 Procedure for determination of phase behavior in scCO ₂	43
2.2 Size exclusion chromatography	45
2.3 Nuclear magnetic resonance	48
2.4 Scanning electron microscopy	49
2.5 Differential scanning calorimetry	50

Chapter 3: Design of P(VAc- <i>stat</i> -VPi)- <i>block</i> -PNVP block copolymers by RAFT/MADIX polymerisation as potential stabilisers for dispersion polymerisation in scCO ₂	50
3.1 Introduction	50
3.1.1 Stabilisers for scCO ₂	51
3.1.2 Design of new hydrocarbon based stabilisers by RAFT/MADIX polymerisation.....	72
3.2 Experimental	73
Materials.....	73
Synthesis of <i>O</i> -ethyl- <i>S</i> -(1-ethoxycarbonyl) ethyl dithiocarbonate (Xanthate X1).....	74
Synthesis of <i>O</i> -ethyl- <i>S</i> -(1-methoxycarbonyl) ethyl dithiocarbonate (Xanthate X2).....	75
Polymerisation of vinyl acetate with X1 and X2.....	76
Synthesis of PVAc- <i>stat</i> -VPi-X1 copolymer.....	77
Synthesis of P(VAc- <i>stat</i> -VPi)-X2 copolymer	77
Synthesis of P(VAc- <i>stat</i> -VPi)- <i>block</i> -PNVP-X2 copolymer	78
Phase behaviour measurements.....	78
Dispersion polymerisation of NVP and MMA	79
3.3 Results and discussion	79
3.3.1 RAFT agent choice	79

3.3.2 Synthesis of P(VAc- <i>stat</i> -VPi)-X2	87
3.3.3 Synthesis of P(VAc- <i>stat</i> -VPi)- <i>block</i> -PNVP block copolymers.....	92
3.3.4 Phase behavior in scCO ₂	97
3.3.5 Dispersion polymerisation experiments	101
3.4 Conclusions	106
Chapter 4: In-depth study of RAFT polymerisation of vinyl acetate, vinyl pivalate and <i>N</i> -vinyl pyrrolidone	107
4.1 Introduction	107
4.1.1 Block copolymer synthesis by RAFT polymerisation	108
4.2 Experimental	109
Materials.....	109
Synthesis of low M_n PVAc-X2	110
Chain extension of low M_n PVAc-X2 with VAc.....	110
Synthesis of low conversion PVAc-X2	111
Chain extension of low conversion PVAc-X2 with VAc	111
Synthesis of low temperature PVAc-X2	112
Chain extension of low temperature PVAc-X2 with VAc	112
Synthesis of low conversion low temperature PVAc-X2	113
Chain extension of low conversion low temperature PVAc-X2 with VAc	113
4.3 Livingness of PVAc polymerisation	113

4.3.1 Low M_n PVAc	114
4.3.1 Head to head addition.....	119
4.4 Livingness of PVPI polymerisation.	137
4.4.1 Conversion.....	140
4.5 Synthesis of P(VAc- <i>stat</i> -VPi)-X2 with improved properties.....	142
4.6 Conclusions	145
Chapter 5: Dispersion polymerisation using P(VAc- <i>stat</i> -VPi)- <i>block</i> -PNVP-X2	146
5.1 Introduction	147
5.2 Experimental	149
Materials.....	149
Synthesis of P(VAc- <i>stat</i> -VPi)-X2.....	150
Synthesis of P(VAc- <i>stat</i> -VPi)- <i>block</i> -PNVP-X2.....	151
Dispersion polymerisation of NVP and MMA	151
Phase Behaviour Measurements	152
5.3. Dispersion polymerisation of NVP with P(VAc- <i>stat</i> -VPi)-X2 stabilisers	152
5.3.3. Dispersion polymerisation with P(VAc- <i>stat</i> -VPi)- <i>block</i> -PNVP-X2 stabilisers.....	159
5.4 Conclusions	175
Chapter 6: Conclusions and future research	177

References	181
------------------	-----

Chapter 1: Introduction

The aim of this chapter is to provide an introduction to polymer chemistry as well as supercritical fluids. It will outline the different polymerisation techniques used throughout the project (RAFT, dispersion polymerisation) and it will discuss the state of the art in the field of stabilisers for dispersion polymerisation.

1.1 Green chemistry

The term *green chemistry*, also known as sustainable chemistry, was coined in 1991 by the chemist Paul Anastas who defined it as *the design of chemical products and processes that reduce or eliminate the use and generation of hazardous substances*.¹ It applies across the life cycle of a chemical product, including its design, manufacture, use and ultimate disposal.

The twelve principles of green chemistry were developed by Anastas and Warner in 1998² and they outline the concept of what would make a greener process, chemical or product. They are listed below.

1. Prevention. It is better to prevent waste than to treat or clean up waste after it has been created.
2. Atom Economy. Synthetic methods should be designed to maximize the incorporation of all materials used in the process into the final product.

3. Less Hazardous Chemical Syntheses. Wherever practicable, synthetic methods should be designed to use and generate substances that possess little or no toxicity to human health and the environment.
4. Designing Safer Chemicals. Chemical products should be designed to affect their desired function while minimizing their toxicity.
5. Safer Solvents and Auxiliaries. The use of auxiliary substances (e.g., solvents, separation agents, etc.) should be made unnecessary wherever possible and innocuous when used.
6. Design for Energy Efficiency. Energy requirements of chemical processes should be recognized for their environmental and economic impacts and should be minimized. If possible, synthetic methods should be conducted at ambient temperature and pressure.
7. Use of Renewable Feedstocks. A raw material or feedstock should be renewable rather than depleting whenever technically and economically practicable.
8. Reduce Derivatives. Unnecessary derivatization (use of blocking groups, protection/deprotection, temporary modification of physical/chemical processes) should be minimized or avoided if possible, because such steps require additional reagents and can generate waste.
9. Catalysis. Catalytic reagents (as selective as possible) are superior to stoichiometric reagents.

10. Design for Degradation. Chemical products should be designed so that at the end of their function they break down into innocuous degradation products and do not persist in the environment.
11. Real-time analysis for Pollution Prevention. Analytical methodologies need to be further developed to allow for real-time, in-process monitoring and control prior to the formation of hazardous substances.
12. Inherently Safer Chemistry for Accident Prevention. Substances and the form of a substance used in a chemical process should be chosen to minimize the potential for chemical accidents, including releases, explosions, and fires.

The work presented in this thesis focuses on principles 4 and 5, the use of green solvents and non-toxic chemical products as a safer and environmentally friendly alternative.

1.2 Supercritical fluids

The replacement of organic solvents by alternative 'green' solvents on an industrial scale has been the focus of much academic research in recent years.³ Supercritical fluids (SCFs) have established themselves as a viable alternative in the case of extraction⁴, chromatography and as a medium in different chemical reactions.⁵ Pfaltz *et al* reported the enantioselective hydrogenation of imines in supercritical carbon dioxide (scCO₂) with enantiomeric excesses up to 81%.⁶ Zhao *et al* reported the hydrogenation of

cinnamaldehyde in scCO₂ with high selectivity and found CO₂ pressure affected both conversion and product selectivity.⁷

A SCF is a phase of a substance above its critical temperature (T_c) and critical pressure (p_c). **Figure 1** shows the phase diagram for pure carbon dioxide.⁸ At the triple point, liquid, solid and gas phases are in equilibrium with one another at a defined pressure and temperature. The critical point represents the highest temperature and pressure at which liquid and gas can co-exist. Above the critical point there is no distinction between the gaseous and liquid phases.

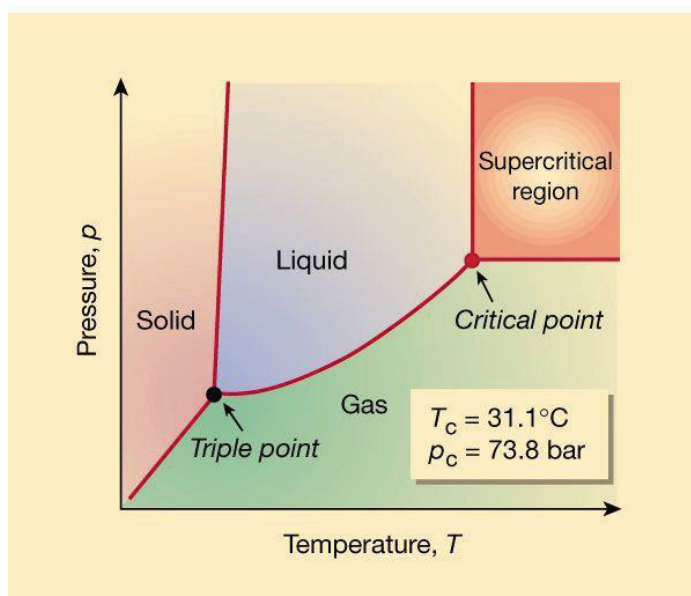


Figure 1: Phase diagram for pure carbon dioxide. Critical temperature and pressure are shown. Reprinted with permission of Springer Nature from ⁸, Copyright 2000.

Licence *et al.* designed an apparatus to observe the transition from a liquid-gas to a supercritical phase in the case of SF₆.⁹ It consisted of a minimal volume sealed optical cell that contained a small amount of liquefied SF₆. The cell was heated and cooled down by changing on the polarity of the

voltage applied by two Peltier devices. **Figure 2** shows the transition that takes place when a gas-liquid mixture is heated above the critical point.

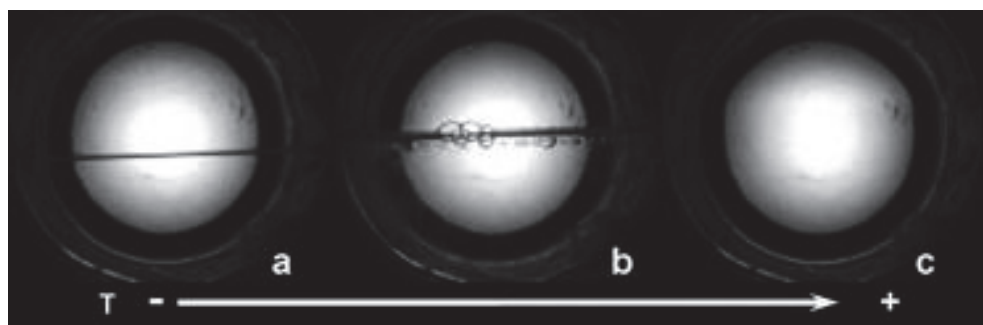


Figure 2: Still photographs illustrating the phase transition observed as SF_6 is heated through its critical temperature (318.7 K); (a) initial 2 phases [liquid + gas]; (b) boiling liquid, and rise in the meniscus as a result of volumetric expansion indicating a drop in the density of the liquid phase; (c) the single phase, SCF, after the temperature has exceeded T_c . Reproduced from ⁹ with permission of The Royal Society of Chemistry.

SCFs have shown real promise due to the unique properties they exhibit. They have lower viscosities than conventional solvents and physical properties intermediate to those of gas and liquids. **Table 1** compares the physical properties of liquids, supercritical fluids and gases respectively.¹⁰

Table 1. Comparison of the physical properties of gases, liquids and SCFs. Adapted from ¹⁰.

Physical Property	Liquid	Supercritical Fluid	Gas
Density (g ml^{-1})	1	0.4	10^{-3}
Viscosity (Pa s)	10^{-3}	10^{-4}	10^{-5}
Diffusivity ($\text{cm}^2 \text{s}^{-1}$)	$10^{-5} - 10^{-6}$	10^{-3}	0.1

SCFs exhibit a high diffusivity, which makes them miscible with gases, and a low viscosity, which makes them highly compressible. One of the most

interesting features these fluids present is their tunable density. This means that density, and therefore solvation power, can be adjusted by varying temperature and pressure, making them suitable for specific reactions where product selectivity can be controlled by changing the SCF density¹¹ and for extraction processes where a compound of interest can be selectively dissolved.¹² This behaviour is especially pronounced around the critical point, where a small change in pressure leads to a dramatic increase in density.¹³

1.2.1 Supercritical carbon dioxide

Supercritical carbon dioxide (scCO₂) is one of the most promising SCFs. Although CO₂ is classified as an asphyxiant and can cause unconsciousness upon exposure to high concentrations, it has a much higher safe exposure limit than organic solvents and it is therefore much less toxic.¹⁴ In addition, it is non-flammable, chemically inert at most reaction conditions and also advantageous from the energy point of view since it has an attainable critical point (31.1 °C, 73.8 bar)¹⁵ compared to other SCFs (374°C, 220 bar for H₂O).¹⁶ Furthermore, it is inexpensive since it can be taken from other processes that produce it as a by-product, like the combustion of fossil fuels (coal, oil, natural gas) and the synthesis of ammonia or ethanol,¹⁷ using methods such as liquid solvent extraction, membrane or cryogenic separation.¹⁸

One of the most significant advantages that CO₂ presents over other conventional solvents is that it can be removed from the reaction media by simple depressurisation. This not only allows the isolation of dry products

without using subsequent energy intensive drying procedures, but also removes the need for solvent waste after treatment. This stands as a great convenience compared to water-based designed processes.

For these reasons, scCO_2 is widely used on an industrial scale for the extraction of spices, flavours and perfumes, and for the decaffeination of coffee beans.¹⁹⁻²⁰

ScCO_2 is a poor solvent for high molecular weight materials.²¹ This makes it suitable for polymer synthesis since it allows an easy recovery of the polymer from the reaction medium. The use of scCO_2 as a reaction medium for polymer manufacturing has been explored by companies such as Dupont (USA) for the synthesis of fluoropolymers, and Xerox (Canada).²²

1.3 Introduction to polymers

A polymer can be defined as a molecule of high relative molar mass (macromolecule), the structure of which comprises the multiple repetition of units derived, actually or conceptually, from molecules of low relative molar mass called monomers.²³

Polymers exist in a number of forms and the use of different combination of monomers will result in a change of the resulting polymer structure and therefore in the physical and chemical properties of the material. Different monomer functionalities lead to a variety of polymer architectures such as linear, branched or network (cross-linked) (**Figure 4**).²⁴

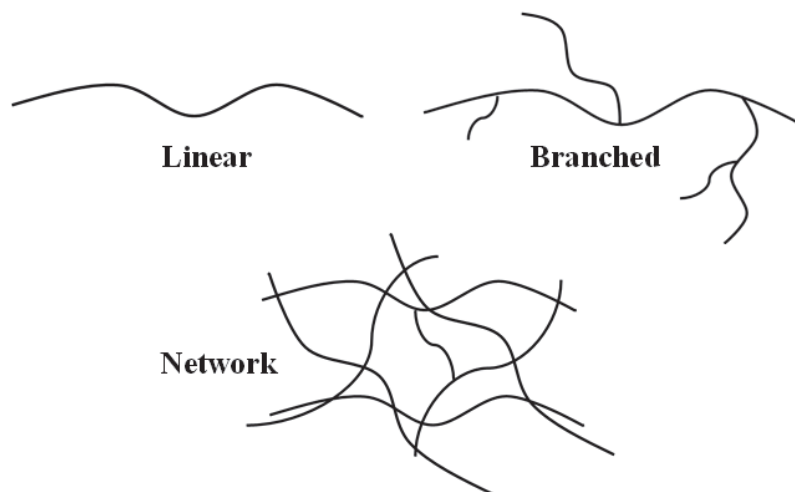


Figure 3: Linear, branched and network polymer architectures.

This thesis focuses on linear polymers. For copolymers, the distribution of the monomer repeat units in the polymer backbone depends on the concentration and reactivity ratios of the different monomers²⁵ and it is used to classify the type of structure (**Figure 4**).²⁶

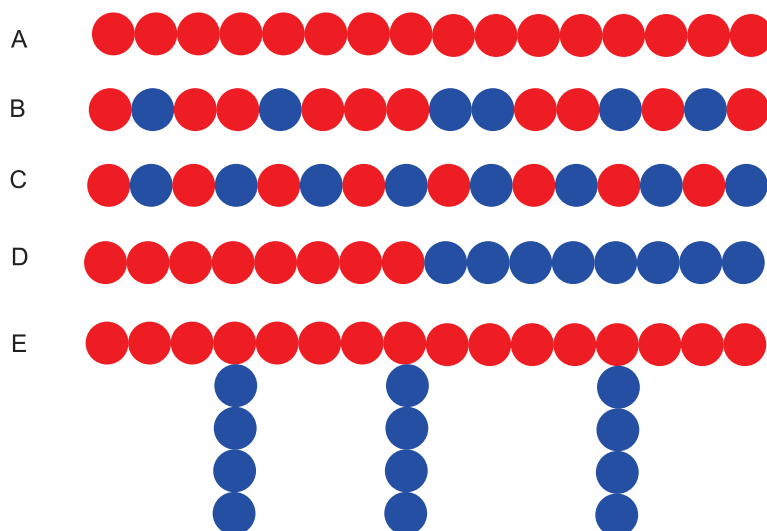


Figure 4: Polymer structures that results from a single monomer (A●) or from the combination of two monomers (A● and B●). a) Homopolymer, b) Statistical Copolymer, c) Alternating Copolymer, d) Block Copolymer, e) Graft Copolymer.

A homopolymer (**Figure 4a**) is formed by polymerisation of a single monomer. A statistical copolymer (**Figure 4b**) is formed from two monomers that arrange following a statistical law. An alternating copolymer (**Figure 4c**) is formed of two monomers that alternate in the structure. Block copolymers (**Figure 4d**) form by polymerisation of a single monomer followed by sequential addition of a second one. Multi-block copolymers can be formed by sequential polymerisation of multiple monomers. Finally, graft copolymers (**Figure 4e**) consist of a linear backbone made from one monomer, and covalently linked side chains coming from the other monomer.

1.3.1 Polymerisation techniques according to mechanism

A process used to convert monomer molecules into a polymer is called polymerization. Polymers can be synthesised using two main methods according to reaction mechanism, referred to as step growth polymerisation and chain growth polymerisation.²⁷⁻²⁸

Step growth polymerisation usually proceeds by intermolecular condensation reactions of the functional groups of monomers such as -OH , -COOH or -COCl , -NH_2 , and the elimination of a small molecule such as H_2O normally takes place.²⁹ Thus, two monomers react to form a dimer, which can react with another monomer to form a trimer or with another dimer to form a tetramer. This process continues producing oligomers first, and eventually polymers by condensation of the oligomers.³⁰ Each reaction of the functional groups proceeds essentially at the same reaction rate until

over a relatively long period of time a high molecular weight polymer is obtained.²⁷

In chain growth polymerisation or addition polymerisation monomer molecules add onto the active site of a growing polymer chain one at a time.³¹ These reactive centers can exist usually in the form of free radicals, but also as anionic or cationic species and organometallic complexes, resulting in different polymerization techniques (**Figure 5**). Chain growth polymerisation involves three main steps; initiation, propagation and termination.

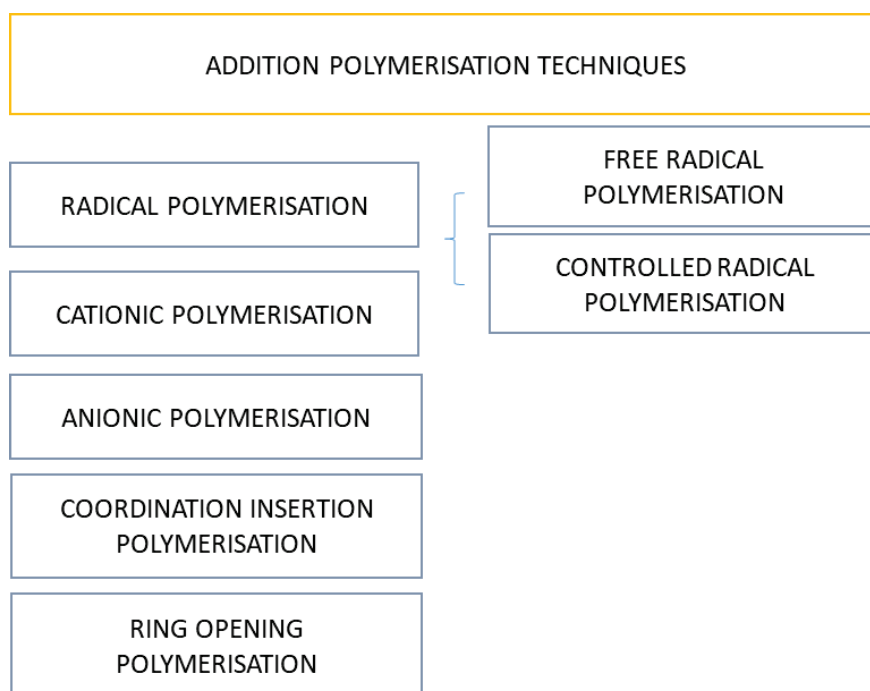


Figure 5: Addition Polymerisation techniques.

Figure 5 illustrates the plot of the number average molar mass (M_n) versus conversion for chain and step growth polymerisation processes. In chain growth polymerisation molar mass increases rapidly at early stage and it remains approximately constant throughout polymerisation. In step growth

polymerisation a high extent of reaction is needed to achieve high molar mass.

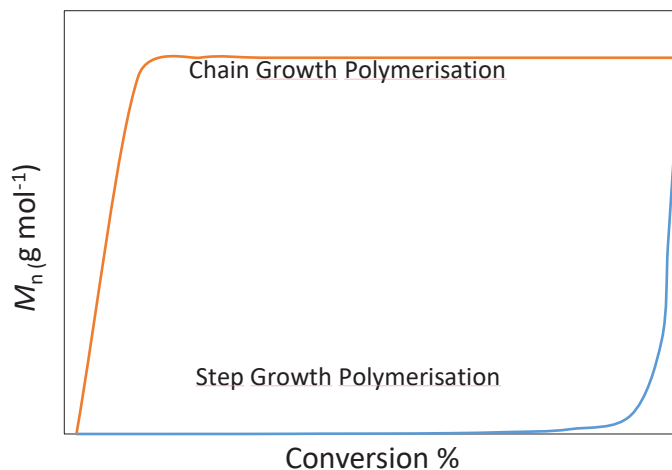


Figure 6: M_n versus conversion for chain and step growth polymerisation.

1.3.1.1 Free radical polymerisation

Free radical polymerisation (FRP) is a widely used technique in the synthesis of a variety of polymeric materials. FRP occurs *via* different steps that can be described using the polymerisation of styrene with 2,2'-azobisisobutyronitrile (AIBN) as the initiator as an example.³²

1. Initiation: In this first step radicals are formed by homolytic cleavage of the covalent bonds of non-radical species called initiators, either thermally, photochemically or by a redox reaction. This is immediately followed by the addition of these generated radicals to the first monomer molecule.

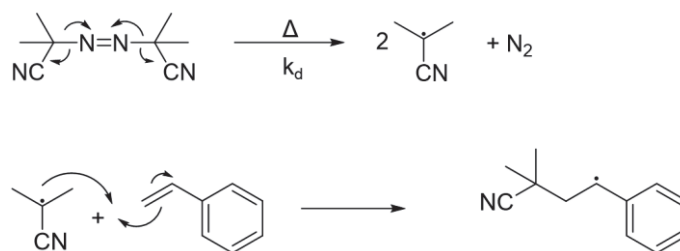


Figure 7: Thermal decomposition of AIBN. Homolytic cleavage leads to the formation of two isobutyronitrile radicals and an N_2 molecule. The generated radicals then add to a first monomer molecule.

Thermal initiators are the most widely used type. Ideally, they should be relatively stable at room temperature but also decompose fast enough in the polymerisation conditions. The decomposition rate of the initiator, k_d , is highly dependent on temperature and solvent. The half-life of the initiator, $t_{1/2}$, can be defined as the time required to decrease its concentration to a half of the starting one at a given temperature and it is a measure of its activity.³³

Decomposition rate, k_d , and half-life, $t_{1/2}$, are related through **equation 1**, assuming first order decomposition kinetics which is true for most initiators.

$$t_{1/2} = \frac{\ln 2}{k_d} \quad (1)$$

Equation 1: Relationship between half-life ($t_{1/2}$) and decomposition rate (k_d) for an initiator that undergoes unimolecular decomposition.

A half-life of 10 hours is often considered practical for most polymerisation reactions which is why initiators are sometimes classified according to the temperatures at which they show a half-life of 10 hours. **Table 2** summarises the required temperatures for a half-life of ten hours for some of the most commonly used commercial thermal initiators.³⁴ The initiators AIBN and V-70 are used throughout this thesis.

Table 2: Thermal initiator required temperature for a half-life of 10 hours.

Initiator	T(°C)-10h(Solvent)
Diisobutyl peroxide	23 (Toluene)
2,2'-Azobis(4-methoxy-2,4-dimethylvaleronitrile) (V-70)	30 (Toluene)
2,2'-Azobisisobutyronitrile (AIBN)	65 (Toluene)
Benzoyl peroxide (BPO)	70 (Toluene)
1,1'-Azobis(cyclohexanecarbonitrile)	88 (Toluene)
tert-Butyl hydroperoxide	120 (Benzene)
Cumene hydroperoxide	135 (Toluene)

2. Propagation: The radical monomers generated during initiation can successively add to more monomer initiating the polymer chains (**Figure 8**). This process will continue until there is no more monomer or termination occurs. Propagation rate is given by k_p .

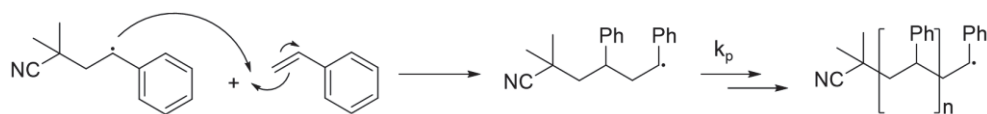


Figure 8: Propagation step in FRP. Addition of monomer radical to more monomer molecules.

3. Termination. Chain termination occurs when the radical species are destroyed via different mechanisms.³³ The main ones are:

a) Combination: It involves the coupling of two propagating polymer chains resulting in a dead polymer (**Figure 9**). It is the most common kind of termination with polystyryl radicals, especially at low temperatures.

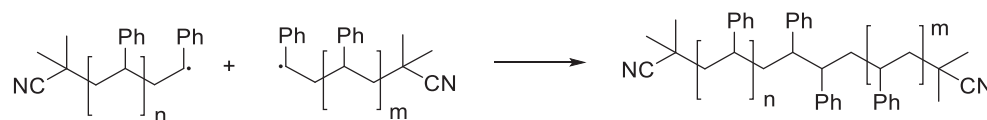


Figure 9: Termination by combination in styrene free radical polymerisation.

b) Disproportionation: it involves the abstraction of one hydrogen atom from one propagating chain to another, leading to the formation of two different chain ends (**Figure 10**). This is a more common termination process for methacrylic radicals.

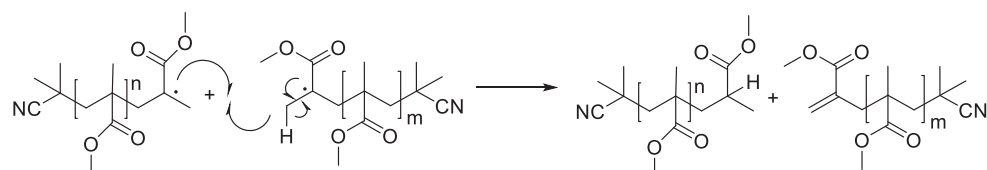


Figure 10: Termination by disproportionation in methyl methacrylate free radical polymerisation.

FRP is a suitable method for a wide range of monomers and polymerisation conditions.³⁵ However, the main limitation is the poor control over some of the key elements of the process that would allow the preparation of well-defined polymers with controlled molecular weight, dispersity, composition and chain architecture.

1.3.1.2 Controlled radical polymerisation

Controlled radical polymerisation (CRP), also defined as reversible-deactivation radical polymerisation (RDRP) by the IUPAC,³⁶ is a technique where the termination reactions are minimised and propagation reactions are favoured. Thus, it allows molar mass to increase linearly with conversion

until all monomer is consumed or the reaction is terminated intentionally. This is achieved by the formation of dormant species that undergo reversible termination or transfer to generate propagating radical chains.³⁷ These dormant species are formed with the help of an additional compound called controlling agent. Controlled polymerisation techniques can be classified depending on the type of reaction (reversible termination or reversible transfer) of the controlling agent with the propagating radical that generates the dormant species.

CRP constitutes a great alternative to FRP since it allows control of the macromolecular architecture, molecular weight and dispersity of the generated polymers.³⁸

Iniferter (initiation-transfer-termination) polymerization was one of the earliest CRP techniques reported by Otsu and co-workers in 1982 as a novel method for preparing well-defined polymers.³⁹ This was later followed by other techniques such as nitroxide mediated polymerisation (NMP)⁴⁰⁻⁴¹, atom transfer radical polymerisation (ATRP)⁴² and reversible addition fragmentation chain transfer (RAFT) polymerisation^{43,44}, which are the most widely used up to date. Among the above techniques, RAFT is the most versatile in terms of the number of different monomers that may be successfully polymerised. Since it is the technique of choice for this thesis it will be explained in more detail than NMP and ATRP.

1.3.1.2.1 Nitroxide mediated polymerisation (NMP)

NMP is a controlled polymerisation technique where a stable nitroxyl radical is used to mediate polymerisation by trapping radical species.⁴⁵ The general mechanism is illustrated in **Figure 11**.

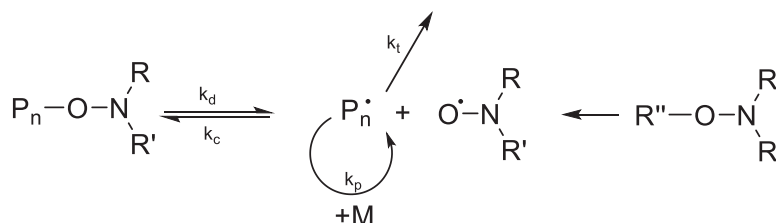


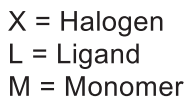
Figure 11: Basic mechanism of NMP polymerisation. Adapted from reference.
⁴⁶

NMP starts with an alkoxyamine initiator that can break homolitically to form a stabilised nitroxyl radical and a carbon radical that can initiate polymerisation with the monomer. The monomer radical generated can then either continue propagation with more monomer or recombine with the nitroxyl radical to form a new alkoxyamine. This limits the radical species present in the reaction, favouring propagation over termination and providing control over the polymerisation.

NMP produces polymer products with controlled architectures and narrow dispersities. The main advantage it presents is the ease of implementation, however, there is a number of monomers that are not compatible with this technique and that limit its application.⁴⁷

1.3.1.2.2 Atom transfer radical polymerisation (ATRP)

ATRP is a catalytic process mediated by redox-active transition metal complexes.⁴⁸⁻⁴⁹ The basic mechanism is shown in **Figure 12**.⁵⁰



Initiation starts when a halogen atom is transferred from the alkyl halide to the transition metal complex. The resulting radical can then add to a monomer molecule starting the polymerisation. The propagating radical chains can undergo reversible deactivation by the higher oxidation state metal complex, setting an equilibrium that controls the radical concentration and therefore the polymerisation process. The reaction proceeds with repetitive transfer of the halogen atom to and from the metal complex.

17

1.3.1.2.3 Reversible addition fragmentation chain transfer (RAFT)

polymerisation

RAFT was first reported in 1998 by Moad *et al.*⁴³ This technique provides control over the molecular weight and dispersity of the polymers by using a chain transfer agent (CTA) or RAFT agent that can be a dithioester (**Figure 13, 1**), a trithiocarbonate (**Figure 13, 2**), a xanthate or dithiocarbonate (**Figure 13, 3**) (in this case it is called MADIX polymerisation: Macromolecular Design *via* the Interchange of Xanthates) or a dithiocarbamate (**Figure 13, 4**).

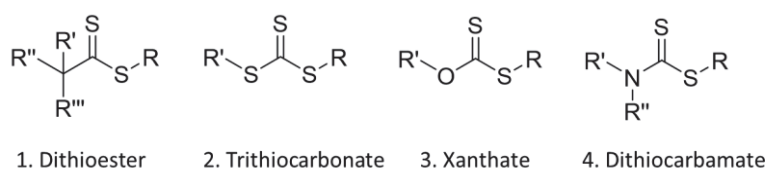


Figure 13: RAFT agent structures. 1: Dithioester, 2: Trithiocarbonate, 3: Xanthate (dithiocarbonate), 4: Dithiocarbamate.

Mechanism of RAFT polymerisation

The reactions associated with RAFT (**Figure 14**) are in addition to those that occur during conventional free radical polymerisation.⁵¹

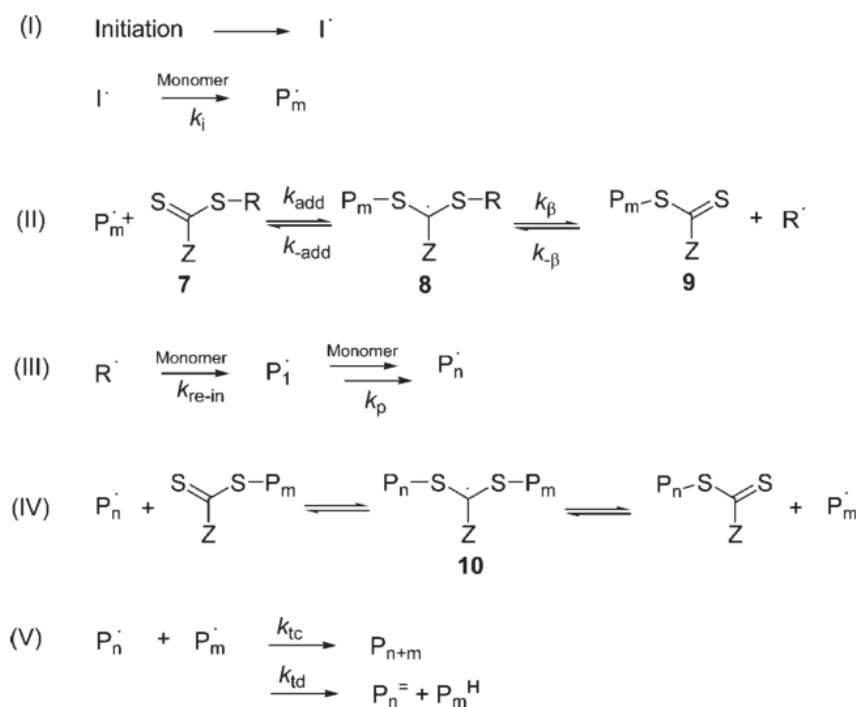


Figure 14: General mechanism for RAFT/MADIX polymerisation. k_i = initiation rate constant, k_{add} = addition rate constant, k_β = fragmentation rate constant, k_{re-in} = re-initiation rate constant, k_p = propagation rate constant, k_t = termination rate constant. Reproduced from reference ⁵¹, with permission of John Wiley and Sons, Copyright 2005.

An external source of radicals is required to initiate and maintain polymerisation. The initiator species I^\bullet initiates the formation of a propagating radical, P_m^\bullet (**Figure 14, I**). After a certain time, addition of the propagating radical to the highly reactive C=S bond of the RAFT agent (**Figure 14, 7**) takes place, resulting in the formation of a stabilised intermediate structure (**Figure 14, II**). Fragmentation of the intermediate radical occurs, leading to the production of a radical species R^\bullet derived from the RAFT agent leaving group, and a temporarily deactivated dormant thiocarbonylthio capped polymer (macromolecular RAFT agent). A second propagating polymeric radical P_n^\bullet is formed as the radical species R^\bullet reinitiates polymerisation (**Figure 14, III**).

The fundamental step in RAFT polymerisation is the equilibrium between the propagating polymer chains and the dormant macromolecular RAFT agent (**Figure 14, IV**).⁵² The rapid exchange between active and dormant chains ensures equal probability for all chains to grow with minimal termination steps since the molar amount of initiator species is here much lower than that of the RAFT agent, so the process leads to narrow molecular weight distributions (**Figure 15**).

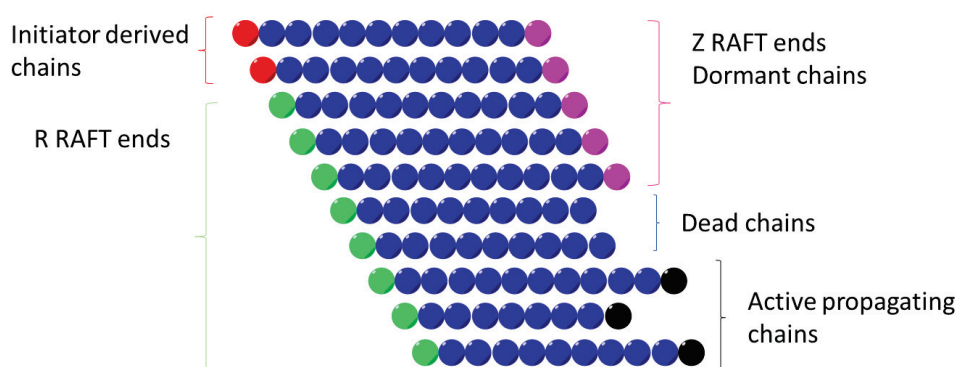


Figure 15: RAFT polymerisation schematic. The number of each type of chains is not representative of a real RAFT polymerisation. Ideally the fraction of dormant thiocarbonyl chains should be far superior than shown in order for the polymerisation to be controlled. Adapted from reference ⁵³.

In RAFT polymerisation molecular weight can be predicted using **equation 2**, if we assume that all RAFT agent has reacted and neglect the chains initiated by the source of radicals, and concentration of monomer (M) and RAFT (T) are known.⁵⁴

$$M_{n,theor} = \frac{(M_0 - M_t)}{T_0} m_M + m_T \quad (2)$$

Equation 2: Determination of theoretical molecular weight ($M_{n,theor}$). M_0 = initial concentration of monomer, M_t = concentration of monomer at time t, T_0 = initial concentration of RAFT agent, m_M = molecular weight of the monomer, m_T = molecular weight of the RAFT agent.

Retention of the thiocarbonylthio groups in the polymeric product is responsible for the living character of RAFT polymerisation. This means that chain termination reactions are highly reduced and polymerisation can further continue by adding more monomer. This allows the straightforward synthesis of a wide variety of architectures such as well-defined homo, block and star polymers.⁵⁵⁻⁵⁹

Kinetics of RAFT polymerisation

As previously mentioned, while NMP and ATRP rely on reversible termination-based activation-deactivation equilibria for controlling polymerisation, in RAFT this equilibrium involves a chain transfer reaction that has no effect on the polymerisation rate since no radical species are lost.⁵⁴ Ideally, this would mean that RAFT follows the same kinetics as conventional FRP, being nondependent on the CTA concentration and half order with respect to the initiator concentration.⁶⁰ However RAFT processes have been reported to be much slower than FRP under similar conditions.⁶¹ Furthermore, most RAFT polymerisations are characterised by a decrease in the rate of polymerisation when the concentration of CTA is increased **(Figure 16)**.⁶²

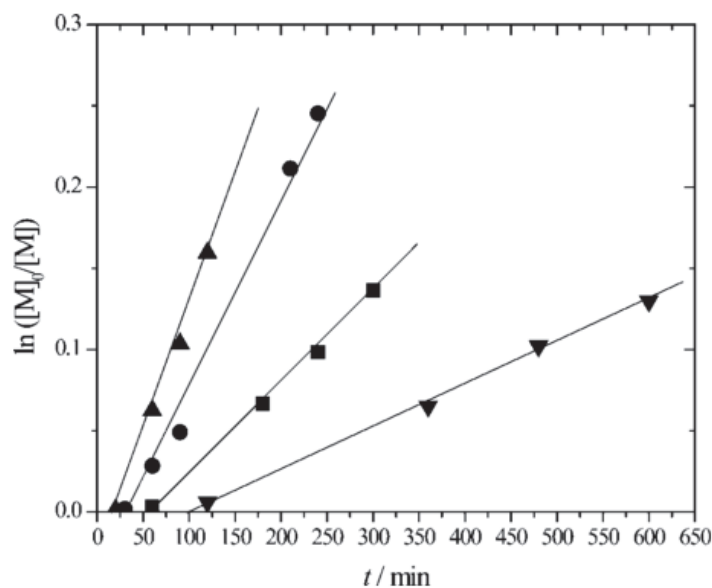


Figure 16: Pseudo-first-order rate plot for the bulk polymerization of methyl acrylate at 60 °C mediated by 1-phenylethyl dithiobenzoate (PEDB) in the following concentrations: (▲) 1.9×10^{-3} , (●) 3.8×10^{-3} , (■) 7.7×10^{-3} , and (▼) $17.4 \times 10^{-3} \text{ mol L}^{-1}$. Note the decrease in the polymerisation rate and the increase in the inhibition/induction period as the CTA concentration increases. Reproduced from reference ⁶² with permission of John Wiley and Sons, Copyright © 2005 Wiley Periodicals, Inc.

There is still a lot of argument on the cause of this rate retardation. Many groups have studied this phenomenon for different monomer/CTA systems. Some of them have attributed it to the slow fragmentation of the polymeric RAFT adduct 10 (**Figure 12, IV**), ⁶³⁻⁶⁶ while others have reported additional side irreversible termination reactions of the adduct 10 with other polymeric radicals or with itself as the cause. ⁶⁷⁻⁶⁸

In addition, a certain degree of inhibition/induction is often observed in RAFT polymerisation, and the effect is enhanced for fast propagating monomers (**Figure 17**). ⁶²

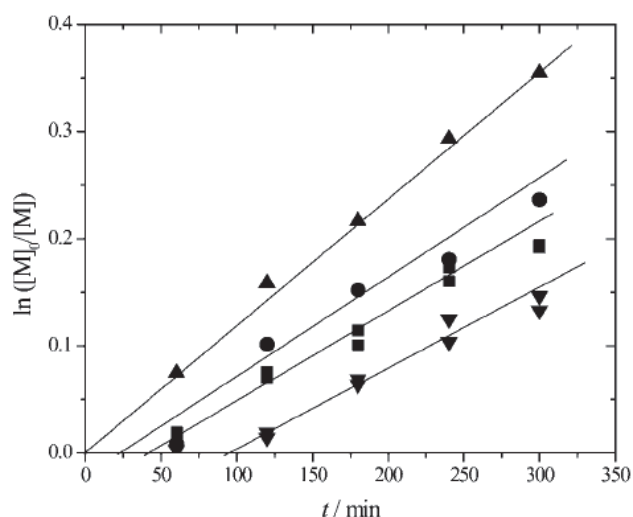


Figure 17: Pseudo-first order rate plot for bulk polymerisation of methyl methacrylate (MMA) mediated by (▲) 1-methoxycarbonyl ethyl dithiobenzoate, (●) cyanoisopropyl dithiobenzoate, (■) phenylethyl dithiobenzoate, and (▼) poly(methyl acrylate) dithiobenzoate at an initial concentration of $7.7 \times 10^{-3} \text{ mol L}^{-1}$. Reproduced from reference ⁶² with permission of John Wiley and Sons, Copyright © 2005 Wiley Periodicals, Inc.

Klumperman and coworkers used ^1H NMR to investigate the processes that take place in the early stages of a retarded/inhibited RAFT polymerisation.⁶⁹⁻

⁷¹ They observed that, rather than an inhibition, an initialization period where all the initial RAFT agent was consumed took place. The critical process in the initialization period was the addition of the first monomer molecule to the RAFT agent to form a single monomer adduct, which was governed by the rate of addition of the initiator derived radical to the monomer and the consequent fragmentation of the leaving group radical from the RAFT agent.

RAFT agent

The structure of the RAFT agent must be chosen carefully since electronic and steric properties of the R and Z groups will determine whether polymerisation of a certain monomer is successful (**Figure 18**). The R group

affects the fragmentation (k_f) and re-initiation (k_{re-in}) rate constants, it must be a good leaving group compared to the monomer and be able to re-initiate polymerisation. The Z group affects the reactivity of C=S double bond towards radical addition (k_{add}).⁷²

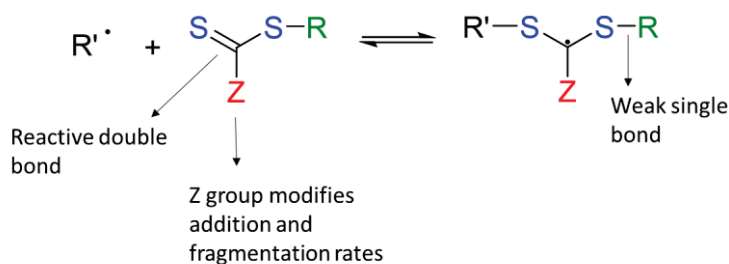


Figure 18: Scheme of radical addition to RAFT agent. RAFT agent structure is described. Adapted from reference ⁷².

It is important to select the RAFT agent according to the monomer being polymerised. There are two types of radical polymerisable monomers, more-activated monomers (MAMs), where the vinyl group is conjugated to an electron withdrawing group such as a carbonyl (e.g. methacrylates) (**Figure 19, left**) or an aromatic ring (e.g. styrene), and less-activated monomers (LAMs), where the vinyl group is adjacent to an electron donating atom such as oxygen (vinyl esters) (**Figure 19, right**).

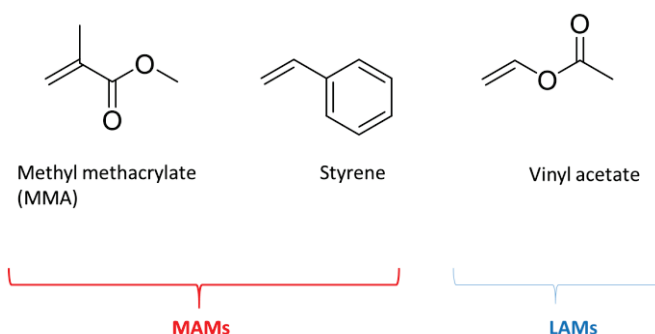


Figure 19: More activated and less activated monomer examples.

Although MAMs react with radicals more readily than LAMs, due to electronic stabilisation by the electron withdrawing group, they also

produce more stable less reactive macro-radicals than LAMs. The polymerisation of MAMs is generally better controlled by more active RAFT agents such as dithioesters or trithiocarbonates that present high rates of reversible addition-fragmentation allowing rapid equilibration of the growing polymer chains.⁵¹

The polymerisation of LAMs, on the other hand, is better controlled by less active RAFT agents such as xanthates. The electron donating Z groups deactivate the RAFT agent towards radical addition, providing control over the polymerisation.

Guidelines for the selection of the R and Z groups are widely available in the literature.^{54, 73}

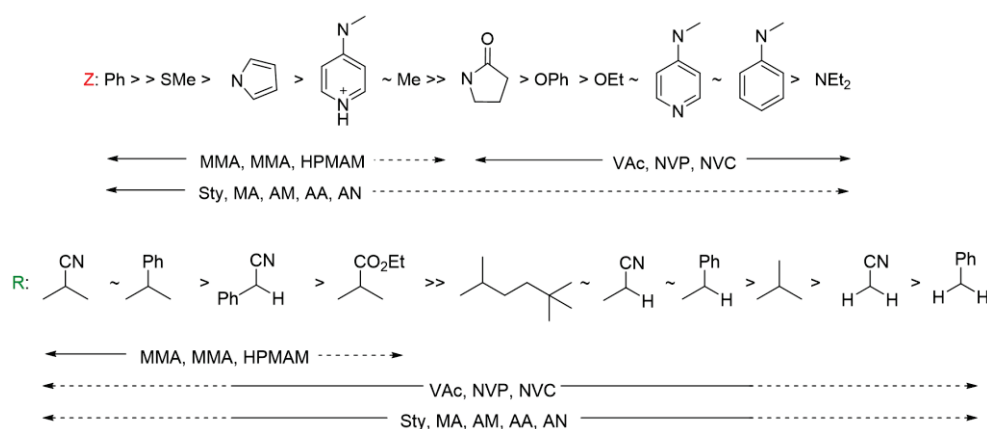


Figure 20: Guideline for the selection of R and Z RAFT agent groups for different monomers. For 'Z', addition rates and transfer constants decrease and fragmentation rates increase from left to right. For 'R', fragmentation rates decrease from left to right. Adapted from reference⁵⁴.

RAFT can be used for a wide range of both functional and non-functional monomers. The high tolerance and compatibility of RAFT towards other functional groups also allows the synthesis of polymers using RAFT agents containing a large range of functionalities, making it possible to target

polymers for different applications, as these groups are retained in the final product⁷⁴⁻⁷⁷ and are also easy to remove or modify by convenience.⁷⁸

1.3.2 Polymerisation techniques according to process

Polymerisation techniques can also be sorted according to the physical process involved in: bulk polymerisation, solution polymerisation, precipitation polymerisation, suspension polymerisation, emulsion polymerisation and dispersion polymerisation.

The first two techniques involve a homogeneous system, this meaning there is only one phase during the process and there is no polymer precipitation. The rest of them take place in heterogeneous systems involving two phases that either can coexist from the beginning of the process or generate as a result of polymer growth. Heterogeneous techniques will be explained in more detailed due to their relevance to this work. The main differences between them is the initial state of the polymerisation mixture, the mechanism of particle formation and the shape and size of the polymer particles formed.⁷⁹

1.3.2.1 Emulsion polymerisation

In emulsion polymerisation the monomer has very limited solubility in the continuous phase, usually water, and it is dispersed in the form of droplets and inside micelles formed with an emulsifier (**Figure 21, left**).⁸⁰ This emulsifier is usually an anionic compound composed of a hydrophilic head and a hydrophobic tail.

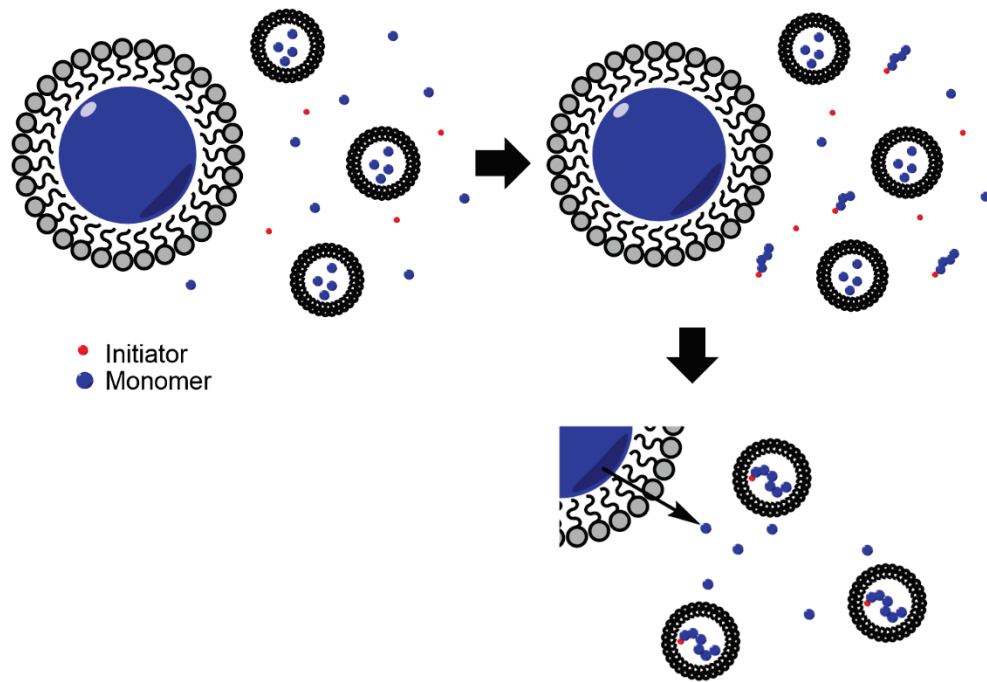


Figure 21: Simplified schematic of emulsion polymerisation. Initially most of the monomer is found as monomer droplets with only a small amount in the continuous phase and in the micelles. As polymerisation starts in the continuous phase, the radicals will add a few monomer units. The formed oligoradicals then become surface active and thus able to migrate into the micelles where propagation with the monomer takes place. As polymerisation continues and chains grow, more monomer migrates from the droplets into the micelles. Adapted from reference.⁸⁰

The initiator is highly soluble in the continuous phase, where the reaction starts with the formation of a propagating radical that can add more monomer to form oligoradicals that become surface active and can then migrate into the micelles where the rest of the polymerisation takes place (**Figure 21, right**).⁶⁰ The polymer particles form a dispersion that is stabilised by the emulsifier, which is called a latex. Since the initiator is insoluble in the monomer, no polymerisation takes place within the monomer droplets, and their only function is to feed the reaction medium with monomer. Particle size ranges from 100 nm to 1µm in conventional emulsion

polymerisation⁸¹ but sizes between 10 and 100 nm can be achieved by microemulsion polymerisation.⁸²

Emulsion polymerization is one of the most widely industrially used techniques to synthesize large quantities of latex for a multitude of applications such as surface coatings (paints, adhesives).⁸³⁻⁸⁴

In addition, it presents several technical advantages. The use of water as the reaction medium is considered environmentally friendly compared to volatile organic solvents and also allows a very efficient heat dissipation during the course of the polymerization. Similarly, the low viscosity of the emulsion allows access to high molecular weight polymers, not readily accessible in solution or bulk polymerization reactions.⁸⁵ Some of the main disadvantages include the need of energy intensive drying procedures in order to remove the water and post-purification processes in order to remove the surfactant that remains with the product.

1.3.2.2 Suspension polymerisation

Suspension polymerisation follows a similar mechanism to emulsion polymerisation, where the monomer is insoluble in the continuous phase, which is normally water, and is dispersed in the way of droplets with the aid of a water-miscible polymer.⁸⁶ However, in the case of suspension the initiator is also insoluble in the continuous phase, and the polymerisation reaction therefore takes place in the monomer phase. The final polymer particles have the size of the monomer droplets.⁸⁷ Although it is a far less industrially relevant technique compared to emulsion, there are some

relevant examples such as the suspension polymerisation of vinyl chloride.⁸⁸ Suspension systems offer advantages such as improved control of heat exchange mechanism and ease of material separation in the product. Furthermore, particle size ranging between 50 and 500 μm can be obtained and easily controlled by the combination of stirring speed and suspending agent concentration.⁸⁹

1.3.2.3 Precipitation Polymerisation

Precipitation polymerisation starts as a homogeneous solution polymerisation, where the monomer and initiator are soluble in the reaction solvent.⁹⁰ After radical initiation, propagation takes place and polymer chains grow until they reach a critical length, J_{crit} , when they become insoluble and precipitate. After precipitation, polymerisation continues by absorption of the monomer into the polymer particles.

The main advantage this technique presents is the absence of a surfactant or stabiliser. Traditionally, that involved a lack of control in the morphology and size of the polymer particles, however in recent years the preparation of micro and nano-beads⁹¹, nanoparticles⁹² and core-shell particles⁹³ by precipitation polymerisation using cross-linkers has been reported.

1.3.2.4 Dispersion polymerisation

Dispersion polymerisation is a heterogeneous technique that involves a medium (scCO_2 for this project) in which monomer and initiator are soluble but the resulting polymer is insoluble.⁹⁴ A radical initiator starts the polymerisation in solution (**Figure 22, 1**). Propagation then follows and the

polymer chains grow (**Figure 22,2**) until a critical point (J_{crit}) when they become insoluble and precipitate out as unstable nuclei leading to phase separation. Agglomeration of these particle nuclei is then prevented with the presence of a stabiliser molecule, which is anchored onto the surface of the polymer particle providing steric stabilisation and forming a stable latex (**Figure 22, 3**). Alternatively, electrostatic stabilisation can take place in the case of charged particles formed from ionic monomers.⁹⁵ This first stage is known as particle nucleation. Polymerisation can then carry on within the particles until all monomer is consumed (**Figure 22, 4**). This second stage is known as particle growth.

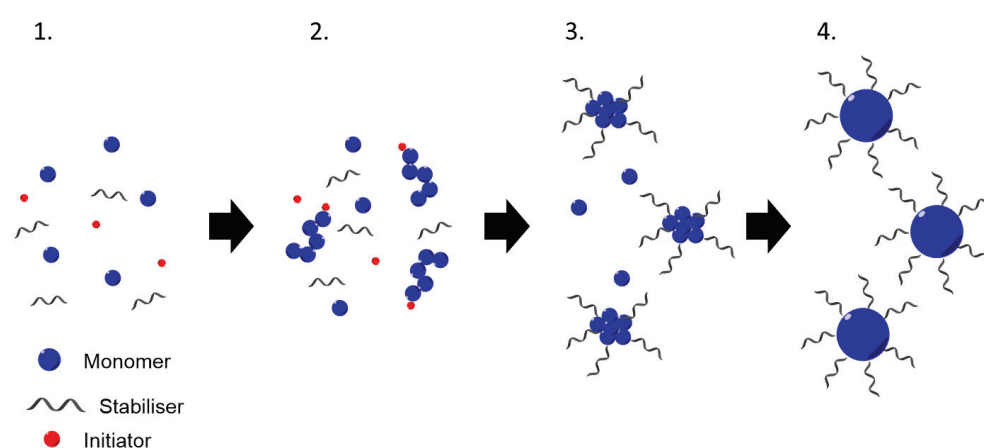


Figure 22: Simplified schematic illustration of a dispersion polymerisation process. Molecule sizes and concentrations do not represent a real scale. 1) Initial homogenous reaction mixture. 2) Polymerisation starts and polymer chains grow until the critical length, J_{crit} . 3) As the polymer precipitates the stabiliser anchors to the particle nuclei, preventing agglomeration. 4) The particle nuclei continue to grow until all the monomer is consumed and the reaction is complete.

The main difference with precipitation polymerisation is the presence of the stabiliser, which is normally a polymer or macromolecule.⁷⁹ A careful choice of stabiliser that bonds chemically or physically to the particles is key to

achieve latex stability during particle nucleation and growth. The most effective stabilisers constitute of both anchor groups and stabilising moieties and they work through a steric stabilisation mechanism (**Figure 22**).⁹⁶

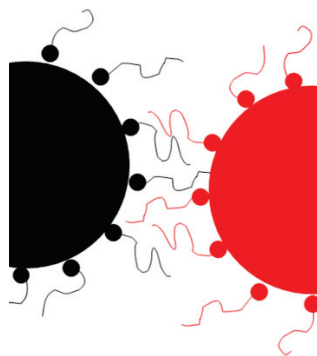


Figure 23: Schematic of steric stabilisation mechanism. When two polymer particles approach, the stabiliser chains can interpenetrate or get compressed. This situation is thermodynamically unfavourable keeping particles apart.

The stabilising moieties must be highly soluble in the dispersion solvent, so they can extend out adopting the most favourable configuration. When two stabilised particles approach the stabiliser chains can either interpenetrate or get compressed, generating a repulsive force that prevents agglomeration. The role of the anchor groups is to prevent the stabiliser from desorbing from the particle surface when a second particle comes into close proximity.

One of the main advantages of dispersion polymerisation is that it provides great control over the particle morphology (generally spherical particles around 0.1-10 μm size)⁹⁷ allowing the preparation of different architectures such as core-shell⁹⁸ and hollow particles.⁹⁹ This makes it suitable for the preparation of micro and nano particles for many applications such as

optoelectronics,¹⁰⁰ drug carriers,¹⁰¹ probes in biomedical analysis,¹⁰² and electrophoretic displays.¹⁰³

Synthesis of poly (methyl methacrylate) by dispersion polymerisation

Among the wide range of polymers that can be synthesised by dispersion polymerisation, this work focuses primarily on poly (methyl methacrylate) (PMMA) due to its industrial relevance.

PMMA is a thermoplastic polymer synthesised from methyl methacrylate MMA (**Figure 24**). It was developed in 1928 in different laboratories simultaneously. Chemists Rowland Hill and John Crawford at Imperial Chemical Industries in England registered it as Perspex, and Otto Röhm of Rohm and Haas AG in Germany, who was trying to produce a safety glass, registered it under the name of Plexiglas and was the first one to commercialise it in 1933.¹⁰⁴ It is also known as acrylic glass, Acrylite or Lucite.

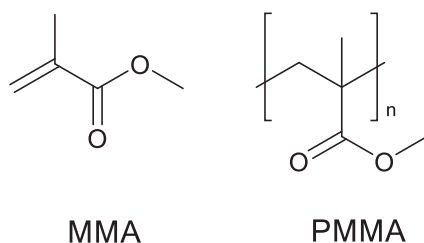


Figure 24: MMA and PMMA chemical structures

The global PMMA market size was valued at USD 4.06 billion in 2015 and its market volume is expected to reach 2.85 million tons by 2020, growing at a CAGR (compound annual growth rate) of 6.1% from 2013 to 2020.¹⁰⁵

PMMA is one of the most widely used thermoplastic substitutes to glass since it is a clear colorless polymer with a melting point of 130°C.¹⁰⁶ It is also

resistant to sunshine exposure and has good thermal stability. It is also one of the hardest thermoplastics with high scratch resistance and reasonable resistance to chemicals. Furthermore, it possesses very good optical properties and a good degree of compatibility with human tissue.¹⁰⁷

As a result, PMMA is used in a broad variety of applications including optical devices, displays,¹⁰⁸ construction, cosmetics, automotive, nanotechnology,¹⁰⁹ biomedicine¹¹⁰, solar cells¹¹¹ or 3D printing.¹¹²

The most common method to produce PMMA in industry is free radical polymerisation³², either performed in solution or dispersed media such as emulsion or dispersion polymerisation. These techniques are normally carried out in water or organic solvents, so the polymer is obtained in a solution, which is not ideal since powder products are required for a lot of the applications mentioned above. In order to remove these solvents, very costly and energy intensive procedures are often required.¹¹³⁻¹¹⁴

1.4 Aims and objectives of the thesis

Dispersion polymerisation in scCO₂ is a much greener alternative to all the aforementioned processes. It produces dry polymer powders since the solvent is completely removed at the end of the reaction upon depressurisation, removing the need for all the costly post-processing.

However, the main challenge in the application of scCO₂ as a solvent in dispersion polymerisation is the design of highly soluble stabilisers that are effective and non-expensive. Stabilisers used for this process are

traditionally fluorinated or silicone based, which is not ideal since they are expensive, not environmentally friendly (fluorinated ones specially) and they bio-accumulate. The use of alternative hydrocarbon based stabilisers has been reported. These are cheaper and more environmentally friendly but have only been successful for one monomer system so far, N-vinyl pyrrolidone.¹¹⁵

The main focus of this thesis is to design efficient hydrocarbon based stabilisers that work in the dispersion polymerisation of MMA, a more industrially relevant monomer.

In chapter 3, the first of the three experimental chapters presented in this thesis, the design and synthesis of hydrocarbon based stabilisers and their use in dispersion polymerisation of methyl methacrylate in scCO₂ is reported. Stabilisers of different molar mass and composition are synthesised using RAFT polymerisation. Solubility of the samples in scCO₂ is investigated using a variable volume view cell. Different stabilisers are tested in dispersion polymerisation of MMA.

Chapter 4 addresses different issues that arise from using RAFT polymerisation, such as the livingness of the polymers described in chapter 3. Head to head addition reactions and their occurrence in RAFT are discussed in detail, as well as different methods to minimise them. The synthesis of hydrocarbon based materials with improved purity by RAFT is investigated.

Chapter 5 focuses on dispersion polymerisation of MMA using the new stabilisers synthesised with improved purity. Solubility in scCO₂ is briefly discussed. Different parameters such as stabiliser loading, temperature or stabiliser composition are studied.

Chapter 2: Experimental and characterisation techniques

2.1 High pressure equipment

All high pressure work described in this thesis was performed in two high pressure systems, an MK III autoclave and a variable volume view cell. These were both designed at The University of Nottingham and are described below.

2.1.1 General high pressure setup

The typical high pressure system is depicted in **Figure 25**.

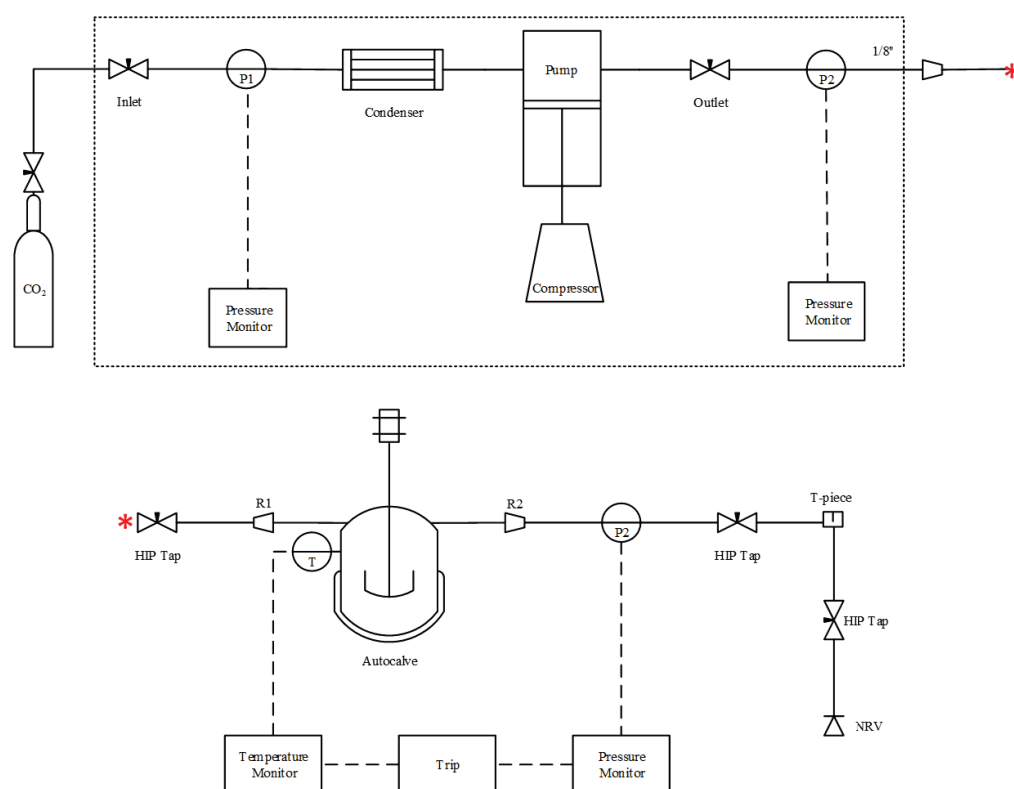


Figure 25: Schematic of high pressure setup.

It consists of a PM-101 SFE Pickel pump that draws gas from a CO₂ cylinder where it is stored as a liquid and feeds it into the system at the desired

pressure by means of a compressor. Stainless steel piping supplied by Swagelok was used to transport liquefied CO₂, with 1/16" piping being used for delivery of liquid CO₂ from the pump to the autoclave and 1/8" piping for the direct delivery of CO₂ into the autoclave head. HIP valves were employed to control the inlet and outlet of CO₂ during reactions. Pressure was monitored using a piezoelectric transducer connected to the inlet pipe and a pressure monitor.

2.1.2 MK III sealed Autoclave

All high pressure polymerisation reactions were performed in a 60 mL stainless steel MK III autoclave. This reactor mainly consists of a head and a base held together by a clamp and sealed with an EPDM O-ring (**Figure 26**). This system can hold pressures up to 340 bar.

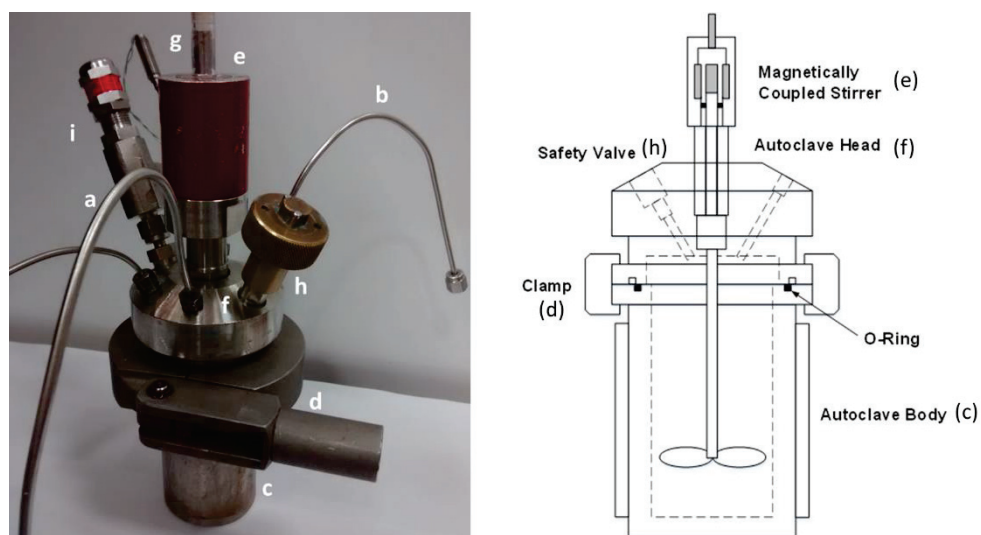


Figure 26: High pressure Mk III autoclave picture (left) and schematic (right). a) CO₂ inlet; b) CO₂ outlet; c) autoclave vessel; d) clamp; e) overhead stirrer; f) autoclave head; g) thermocouple; h) safety key; i) safety valve.

The head is equipped with a magnetically coupled stirrer and five apertures for an inlet, outlet, thermocouple, pressure relief valve and a safety needle. The head of this needle is also a key which is unique to each clamp and opens the autoclave. This safety feature ensures that the autoclave is not opened without removing the safety needle and therefore safely venting any residual CO₂ that may remain. The pressure relief valve is an extra safety feature to prevent the pressure exceeding 345 bar. The valve is sprung, allowing pressure to escape until it falls back, at which point it gets sealed again.

Temperature control is provided by a control box which supplies power to a band heater that is placed around the autoclave body and is also connected to a thermocouple that extends into the autoclave and allows the temperature to be monitored.

2.1.3 Procedure for dispersion polymerisation in scCO₂

A standard operating procedure (SOP) was followed rigorously for the polymerization of NVP and MMA in scCO₂. A simplified schematic outline of the reaction procedure is shown in **Figure 27**. The complete SOP is described below.

1. To assemble the autoclave, place an EPDM O ring in the joint between the base and the head. Clamp and tighten them together using the safety key. Ensure all connections to the inlet and outlet are tightened correctly and all

valves are closed. Fit heating jacket around the base and plug the thermocouple in.

2. Perform a pressure test by slowly filling the vessel with CO₂ to roughly 55 bar. Check each pressure fitting for leaks by covering them with Swagelok Snoop® leak detector. The leak detector is a surfactant solution which will bubble if CO₂ is escaping. In the event of a leak the vessel must be vented to ambient pressure when the leak can be safely fixed by tightening or replacing the fitting. If no leak is found then the pressure can be increased to reaction pressure (276 bar) and the joints checked again for leaks.

3. For extra safety, pressure can be monitored over the course of 1-2 hours in order to detect any leak that might have been missed. If no pressure drop is observed, vent the CO₂.

4. Whilst maintaining a small positive CO₂ pressure of c.a. 2 bar to prevent any air entering the autoclave, remove the safety key and inject a solution of the required monomer, initiator and stabiliser, via a syringe and needle.

5. Seal the autoclave by fitting and tightening the safety key and connect the overhead stirrer. Begin stirring.

6. Increase the pressure to 55 bar. Set the control box to the reaction temperature (35 °C).

7. Once the desired temperature is reached, slowly increase the pressure to 276 bar by opening the inlet tap.

8. After the required reaction time (48 h), set the temperature control box to 0 °C and disconnect the power from the control box to the heating jacket.
9. When the autoclave has reached room temperature, slowly vent the CO₂ into the fume hood.
10. At ambient pressure, remove the safety needle and detach the inlet and outlet connections and thermocouple. Using the safety key, release the clamp and open the autoclave to collect the product.

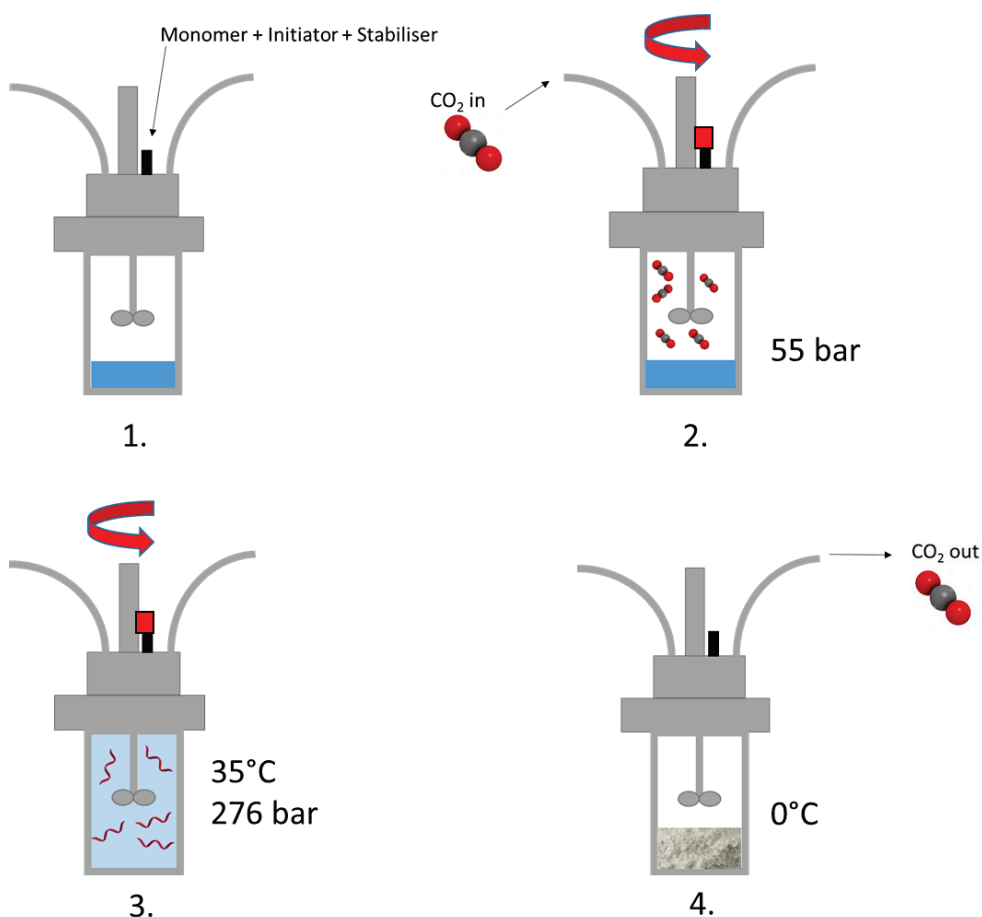


Figure 27: Schematic diagram illustrating the stepwise procedure for a typical dispersion polymerisation conducted in scCO₂. 1. Monomer, initiator and stabiliser are injected through the safety key port, under a small pressure of CO₂. 2. The safety key is fitted in place and the pressure of CO₂ is increased to 55 bar while stirring the vessel. 3. The temperature is increased to 35°C and the pressure to 276 bar. The reaction is then stirred for 48h at that pressure and temperature. 4. The autoclave is cooled down to 0°C, stirring is

stopped and the CO₂ is slowly vented until atmospheric pressure is reached. Product can be collected as a dry powder.

2.1.4 High pressure variable volume view cell

Phase behavior of all the stabilisers in scCO₂ was studied using a high pressure variable volume view cell. It consists of three main units, a stainless steel cell body, a hydraulic intensifier unit and an electronic control box that allows monitoring and adjustment of the vessel temperature and pressure.

Six heating cartridges are inserted into cavities in the walls of the cell body to deliver efficient heating to the cell. A magnetically coupled stirrer located under the body of the view cell is used to rotate a magnetic flea inside the chamber to provide efficient mixing. The main body has three main ports; one at the left for the inlet and outlet of CO₂, one at the right for the thermocouple which is inserted into the cell for monitoring the internal temperature, and a third one at the top for the safety key. The main body of the view cell is constructed of stainless steel and has a static sapphire window at the front, allowing visualization of the phase behaviour (**Figure 28**).

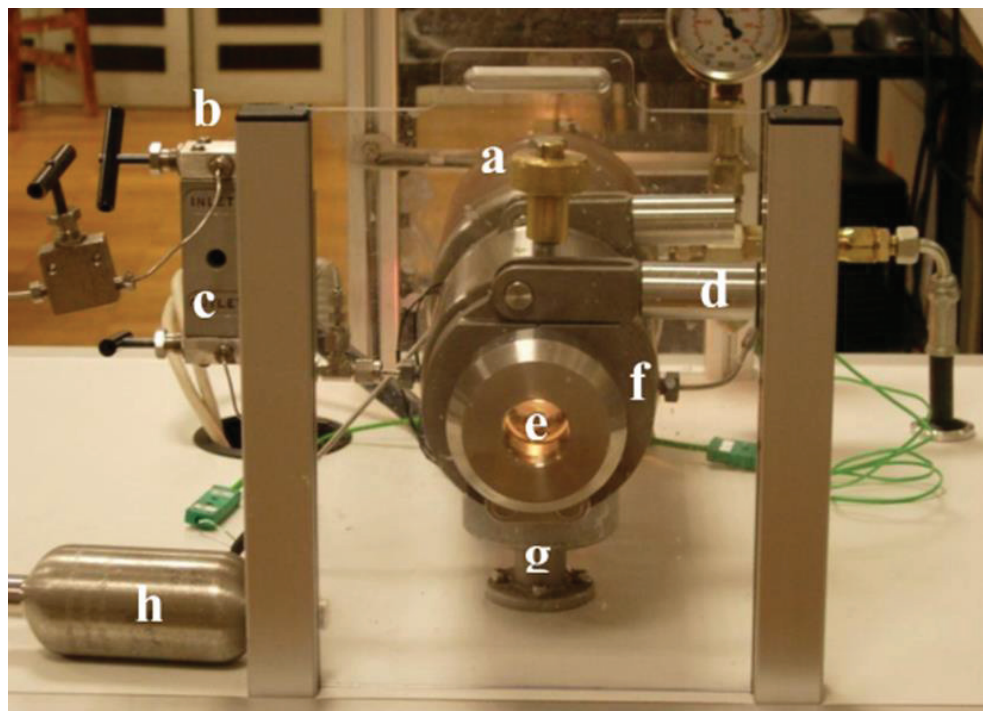


Figure 28: Photograph of front of view cell, which allows direct observation of phase transitions. (a) Safety key; (b) CO₂ inlet; (c) CO₂ outlet; (d) Clamp; (e) Sapphire window (f) Internal thermocouple; (g) Magnetically coupled stirrer; (h) CO₂ bomb for delivery of gas to view cell. Reproduced from reference ¹¹⁵.

The sapphire window sits on a Teflon seat in a stainless steel holder against an EPDM O-ring. Upon pressurising the cell, the sapphire window is forced against both the seat and the O-ring, creating an effective seal. A stainless steel spacer is also used in the window holder to adjust the volume of the vessel.

At the rear of the cell body a hollow hydraulic ram is fitted with a second sapphire window, which forms the piston (**Figure 29, 2**). The rear sapphire piston is fitted with a hydraulic type seal made of PTFE and a PEEK backup ring to provide effective sealing and two additional PTFE rings to aid movement throughout the main cell body as the piston slides backward and

forward. A LED light is also positioned at the rear of the view cell so that the contents of the vessel can be visualised clearly.

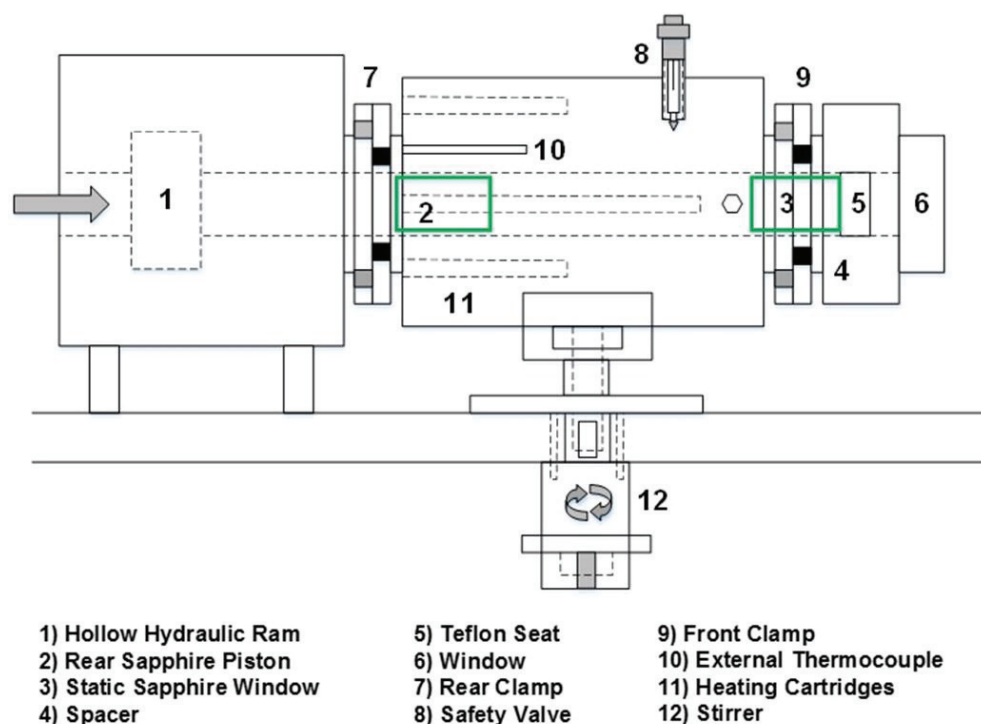


Figure 29: High pressure variable volume view cell schematic.

2.1.5 Procedure for determination of phase behavior in scCO₂

Cloud point experiments were carried out using 15 wt. % of monomer with respect to (w.r.t.) CO₂, and 5 wt. % stabiliser w.r.t. monomer. These quantities were used in order to reproduce initial high pressure dispersion polymerisation conditions in a 60 mL autoclave. A CO₂ loading of approximately 20 g was used in all cloud point measurements. CO₂ was added to the view cell using a stainless steel CO₂ bomb, which was weighed before and after the experiment in order to determine the exact weight.

The procedure for a typical view cell experiment is shown schematically (Figure 30), and is detailed below.

1. The stabiliser is dissolved in the monomer and injected into the view cell through the safety key port using a needle. CO₂ is added to the view cell via the CO₂ bomb connected to the inlet. The bomb is gently heated to aid CO₂ transfer. The cell is half filled, corresponding to a CO₂ weight of around 20g.
2. The view cell is then sealed and its contents stirred. The temperature is then set to the desired value (e.g 35 °C) and the system is allowed to equilibrate. The sapphire piston is pushed forwards via the hydraulic system in order to increase the pressure by decreasing the internal volume. Once a sufficiently high pressure is reached, the stabiliser/monomer mixture will be fully dissolved and the light at the back of the cell will be completely visible.
3. The piston is then slowly moved back to decrease pressure, until the stabiliser starts to precipitate out. The back lights are then obscured. The control box allows accurate recording of the pressure at which the polymer precipitates out of solution at a given temperature. This point is defined as the cloud point. Cloud point measurements were taken from 35-75 °C to produce pressure-temperature phase diagrams.

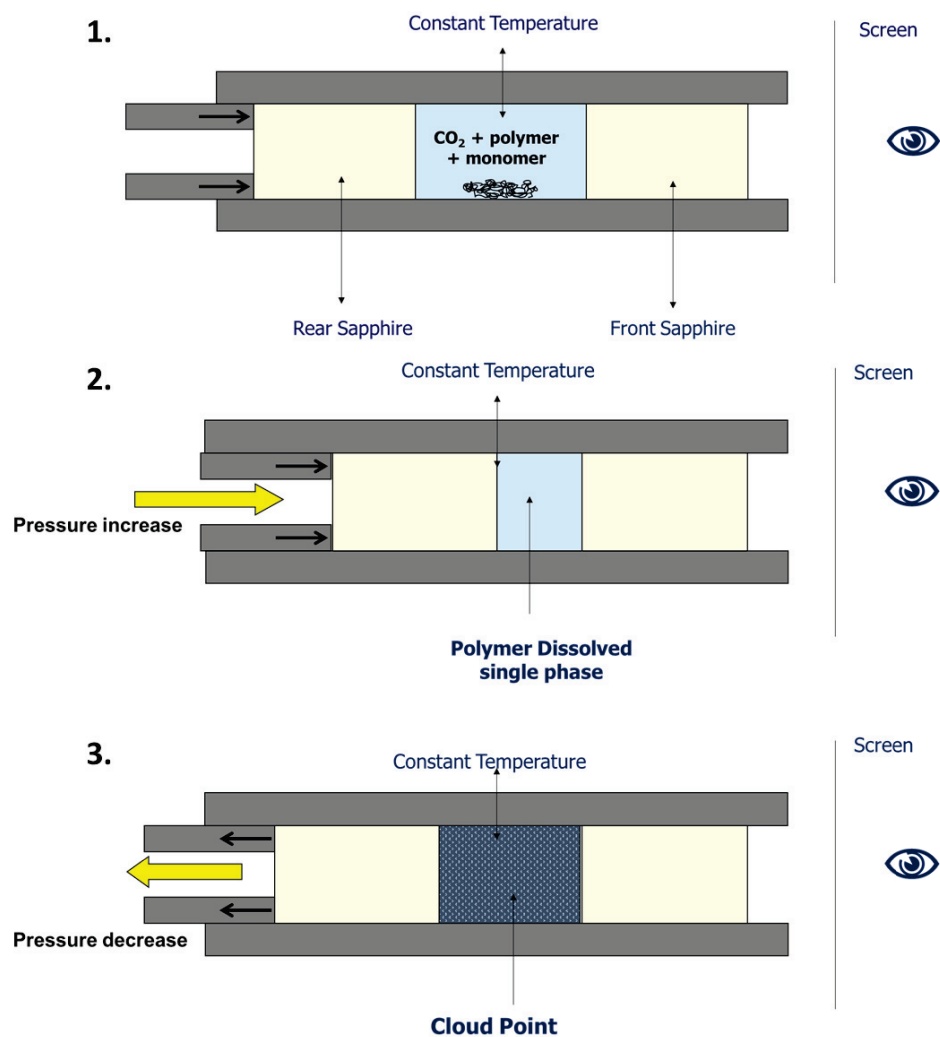


Figure 30: Schematic procedure for the high pressure variable volume view cell. 1. The cell is filled with CO₂, monomer and stabiliser as two separate phases. 2. Once the system reaches the desired temperature, the back piston is moved forwards and cell volume decreases, increasing pressure and solubilising the stabiliser in the continuous phase. 3. The piston is then moved backwards and the pressure is lowered until the cloud point pressure is reached and the stabiliser precipitates.

2.2 Size Exclusion Chromatography

Size exclusion chromatography (SEC), is a widely used polymer characterisation technique that provides key parameters like the number average molar mass (M_n), the weight average molar mass (M_w) and the dispersity ($\mathcal{D} = M_w/M_n$). \mathcal{D} is a measure of the uniformity in molar mass

distribution in a polymer sample. SEC is a type of high performance liquid chromatography.

The SEC instrument consists of a pump to push the mobile liquid phase through the instrument, an injection port to introduce the test sample into the column, a column to hold the solid stationary phase, a detector to detect the components as they leave the column, and a software to control the different parts of the instrument and calculate and display the results.

The separation principle of SEC is based on the size of the hydrodynamic volume of the macromolecules in solution. Polymers adopt a coil conformation in solution, the size of the coil being dependent on the molar mass of the polymer. Small coils flow more slowly through the column (long retention time) because they penetrate deep into the pores of the stationary phase, whereas large coils flow quickly through the column (small retention time) because they do not enter the pores. Consequently, polymers elute from the column according to their molar mass.

The elution behavior of the sample is shown in a chromatogram. The molar mass distribution is calculated by comparison with a calibration graph of standard polymers of known molar mass or using refractive index (dn/dc) values.

In this thesis, SEC samples were analysed using three different systems.

1. At the University of Nottingham two different systems were used. An Agilent 1260 Infinity system equipped with 2 polystyrene columns of 8x300 mm and Wyatt OptilabrEX refractive index detector was used for the

samples reported in chapter 3 and part of the samples reported in chapter 5. DMF and chloroform were used as eluents at 0.5 mL min⁻¹ flow rate. PMMA standards were used for calibration.

SEC measurements of the samples reported in chapter 4 and part of the samples in chapter 5 were performed on an SEC Agilent 1260 Infinity triple detection SEC comprising a Wyatt Optilab multi-angle light scattering (MALS) detector, an Agilent differential refractometer (RI), a Wyatt Optilab viscometer, and an Agilent UV detector. Separation was achieved using 2 PLgel mixed D columns (7.5 mm x 50 mm). The eluent was tetrahydrofuran (THF) at room temperature at a flow rate of 1 mL min⁻¹. Molar mass determination was carried out by the software using the refractive index increment (dn/dc) values taken from the literature.

2. At Warwick University, an Agilent 390-LC MDS instrument equipped with differential refractive index (DRI), viscometry (VS), dual angle light scatter (LS) and UV detectors was used. The system was equipped with 2 x PLgel Mixed D columns (300 x 7.5 mm) and a PLgel 5 μ m guard column. The eluent was DMF with 5 mmol NH₄BF₄ additive. Samples were run at 1 mL min⁻¹ at 50°C. PMMA (Agilent EasyVials) were used for calibration between 955,000 – 550 g mol⁻¹. Analyte samples were filtered through a nylon membrane with 0.22 μ m pore size before injection. Experimental molar mass (M_{nSEC}) and dispersity (\mathcal{D}) values of synthesized polymers were determined by conventional calibration and universal calibration using Agilent GPC/SEC software.

3. At the C2P2 in Lyon, analysis was carried out in a Triple detection set from Viscotek - Malvern Instrument. The system is equipped with a refractometer detector, static light scattering RALS (90 °) and LALS (7 °) and a viscometer detector. The set is thermostated at 35 ° C. A computer drives the set and retrieves the results using software: "OmniSEC" version 4.7 from Malvern Instrument. The set of columns used includes a pre-column (PLgel Olexis Guard 7.5x50mm) followed by three columns in series (PLgel Olexis Guard 7.5x300mm) with a mass range of 500 to 2,000,000 (PS). The mobile phase is THF at a flow rate of 0.8 mL min⁻¹. Samples are injected through a 100 µL loop and filtered in-line before separation on the columns.

All UV measurements were taken at a wavelength of 280 nm.

2.3 Nuclear magnetic resonance

Nuclear magnetic resonance (NMR) is a phenomenon in which nuclei in a magnetic field absorb and re-emit electromagnetic radiation. This occurs at specific resonance frequencies which depend on the magnetic properties of the nuclei. NMR spectroscopy exploits this phenomenon to get information about chemical structure and electronic properties of any molecule or species that contain nuclei possessing spin (¹H, ¹³C, ¹⁹F...).

¹H NMR was used throughout this work to determine structure, molar ratios, conversion and molecular weights of the polymers. We used a Bruker DPX300 spectrometer equipped with a 300 MHz magnet and CDCl₃ as

solvent. Analysis of end groups was carried out at 256 scans to improve the signal to noise ratio. All data were processed using MestRe-Nova software.

2.4 Scanning electron microscopy

Scanning electron microscopy (SEM) is a technique where a focused beam of high-energy electrons is used to generate signals at the surface of a solid sample that can be used to obtain information about the surface topography. SEM was widely used in this thesis to study the morphology of the polymers produced by dispersion polymerisation.

All SEM analyses were carried out using a JEOL 6060L V Variable pressure scanning electron microscope. Image analysis was performed with JEOL analysis software (version 6.57). Samples were prepared by placing the polymer sample on the surface of adhesive carbon tabs. These were attached to aluminium stubs, which were sputter coated with gold using a Balzers SCD 030 gold sputter coater. Particle size was estimated using ImageJ analysis software. This was not straightforward due to particle agglomeration and heterogeneity of the samples and all reported particle sizes should be taken as a very rough estimation. For samples with homogenous size particles size is reported with an error and in the case of samples with very heterogeneous particle size it is reported as a range.

2.5 Differential Scanning Calorimetry

Differential scanning calorimetry (DSC) was used for thermal analysis using a TA Q2000 DSC (TA Instruments) machine. The sample was sealed in an aluminium pan and then cooled to -20 °C and heated to 100 °C at a heating rate of 10 °C min⁻¹ and a N₂ flow rate of 50 mL min⁻¹. The glass transition temperature (T_g) was determined as the midpoint of the change in heat capacity during the second and third heating run for a given sample, and an average value from the two runs was taken. T_g values were analysed by TA Universal Analysis software.

Chapter 3: Design of P(VAc-*stat*-VPi)-*block*-PNVP block copolymers by RAFT/MADIX polymerisation as potential stabilisers for dispersion polymerisation in scCO₂

This chapter discusses the design and synthesis of hydrocarbon based stabilisers and their use in dispersion polymerisation of methyl methacrylate in scCO₂.

3.1 Introduction

As previously discussed in the introduction, the stabilisers most widely used in dispersion polymerisation processes carried out in scCO₂ often contain fluorinated or siloxane based units, which makes them expensive and bio persistent and therefore not suitable for industry scale. There is therefore a need for cheaper and cleaner stabilisers. Hydrocarbon based stabilisers are a very promising alternative. However, they have only been successfully

employed for one monomer system so far, poly (*N*-vinyl pyrrolidone) (NVP).¹¹⁶ The work presented in this chapter focuses on the design and synthesis of new hydrocarbon based stabilisers and their use in dispersion polymerisation in scCO₂. These materials will overcome the previous limitations and work for a wider range of monomers.

3.1.1 Stabilisers for scCO₂

CO₂ is a symmetrical molecule, it does not show a dipole moment. The solvent strength of carbon dioxide for solutes is a result of both its low polarisability (**Figure 3131**) and a strong quadrupole moment.¹¹⁷ Consequently, it is difficult to compare CO₂ to other conventional solvents because of this ambivalent character.

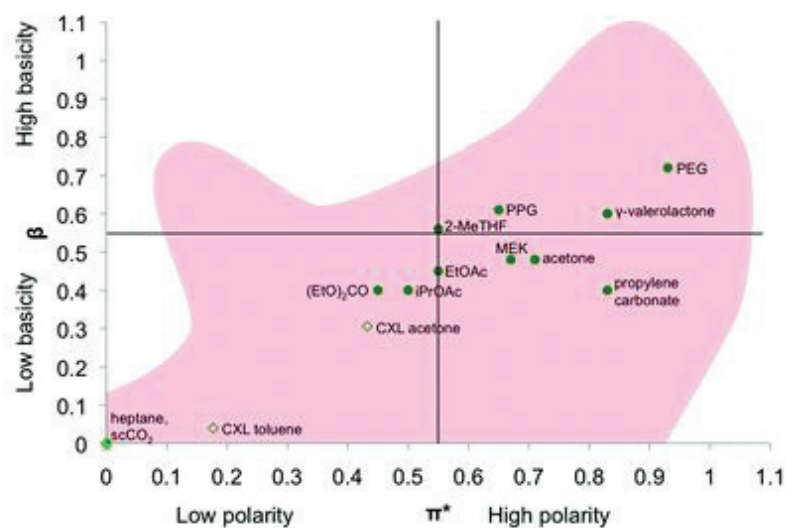


Figure 31: Green aprotic solvents as a function of their polarity and basicity values. Reproduced from reference ³ with permission of The Royal Society of Chemistry.

As a general statement, CO₂ is a reasonably good solvent for small molecules, both polar and nonpolar.¹¹⁸ Complete miscibility can be obtained at elevated pressure for many compounds, with the exception of water. However, this miscibility decreases sharply with increasing molecule size. Consequently, most larger molecules and polymers exhibit very limited solubility in carbon dioxide.¹¹⁹

This might seem like a major drawback for the use of CO₂ as a green solvent, but it can actually be advantageous in heterogeneous processes such as dispersion polymerisation.¹²⁰ However, in such processes a highly soluble stabiliser or surfactant is needed in order to obtain controlled particle morphologies and high conversions.¹²¹

Stabilisers are usually block copolymers, with a polymer-philic block that anchors to the growing particles, and a CO₂-philic block to disperse the particles within the CO₂ phase¹²² (**Figure 32**).

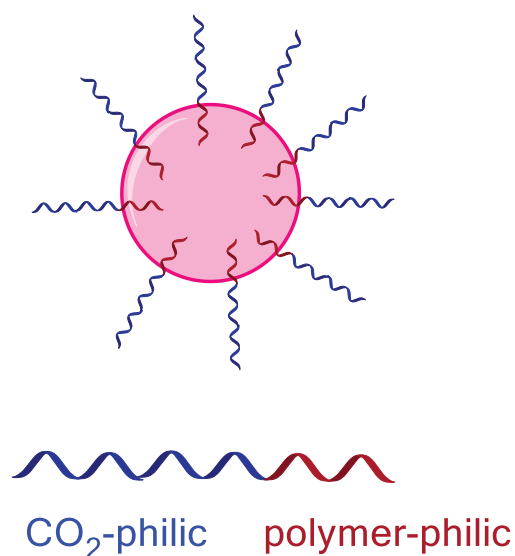


Figure 32: Scheme of a stabilised polymer particle in a dispersion polymerisation in scCO₂ with a block copolymer stabiliser.

One of the biggest challenges when designing block copolymers to use as stabilisers in scCO₂ is to achieve a good compromise between solvation and molar mass of the CO₂-philic block. The ideal stabiliser will have a CO₂-philic block long enough to provide steric stabilisation of the particles so aggregation does not take place. At the same time, it needs to be short enough so it will be soluble in CO₂ and solubilise the polymer-philic group as well.

Furthermore, it is key to have a polymer-philic group that effectively anchors to the growing particles. Different anchoring mechanisms have been reported in the literature, such as chemical grafting, Van der Waals interactions, hydrogen bonding or physical adsorption (**Table 3**). In the case of block copolymers, an optimum anchor soluble balance (ASB) is necessary for a good stabilisation. If the anchoring segment is too short, stabiliser molecules will remain free or associated in the CO₂-phase instead of adsorbing onto the particle surface, leading to insufficient stabilisation.¹²³ Again, if this segment is too long, the stabiliser will not remain soluble in the CO₂-phase.

Most polymers are insoluble in scCO₂ and solubility very often decreases dramatically with the molar mass of the polymer chains.¹²⁴

As discussed in Chapter 1, most of the stabilisers used in scCO₂ have, until recently, been fluorinated or silicone based. Poly(methyl methacrylate), polystyrene or poly(acrylonitrile) polymer particles have been stabilised

using block copolymers with CO₂-philic blocks such as poly(fluoroacrylates) or poly(dimethyl siloxane).

3.1.1.1. Fluorinated and silicon based stabilisers

DeSimone *et al* reported the first dispersion polymerisation of MMA in scCO₂ using a fluorinated polymer as stabiliser in 1994 (**Table 3, entry 1**).¹²¹ It consisted of a polymer-philic acrylic backbone, which adsorbed onto the acrylic particles, and a very CO₂-philic fluorinated side chain that provided steric stabilisation preventing aggregation of the growing particles.

They obtained powder products with spherical morphologies, particle sizes in the range of 0.9-2.7 µm and high conversion and molar mass. In addition, they found that increasing the stabiliser loading led to smaller and more uniform particles. This was attributed to a more successful colloidal dispersion due to more stabiliser situated on the surface of the particles.

Furthermore, increasing the stabiliser molar mass led to an increase in particle size. When using stabilisers of low M_n , more particles with smaller diameters were formed. When using stabilisers of high M_n a lower fixed number of particles were formed and then grew at a uniform rate. This was attributed to a lower amount of stabiliser chains situated on the surface of the particles in the case of higher molar mass materials.

In 1996, DeSimone and co-workers, reported the use of a Poly(styrene-*block*-FOA) (poly(styrene-*block*-fluoro octylacrylate)) (**Table 3, entry 2**) as stabiliser in the dispersion polymerisation of styrene in scCO₂.¹²³ The stabilisation was attributed to a physical adsorption of the PS moiety onto

the growing particles. A white flowing powder with spherical morphology was obtained. Furthermore, they observed that increasing the molar mass of the polymer-philic block decreased the particle diameter. This can be explained by the fact that high molar mass backbones can anchor to the particles faster and more efficiently, leading to the formation of more particles during nucleation.

Shaffer *et al.*, reported the dispersion polymerisation of MMA in scCO₂ using a poly(dimethylsiloxane) (PDMS) macromonomer as the stabiliser for the first time in 1996 (**Table 3, entry 3**).¹²⁵ It consisted of a poly(dimethylsiloxane) chain that acted as a CO₂-philic polymer, terminated with a methacrylate group that copolymerised and therefore grafted onto the forming particles. However, only a very low amount of the PDMS-MA (0.01 to 0.68 wt %) remained in the product after washing with hexane or liquid CO₂, which suggested that only a small part of it was chemically grafted.

In 1998, O'Neill *et al.*, studied in detail the mechanism of particle formation and particle growth in dispersion polymerisation of MMA in scCO₂ using siloxane-based macromonomers.¹²⁶⁻¹²⁷ They used in situ turbidimetry at 65°C from 2000 to 5000 psi for various concentrations of a PDMS-MA stabiliser, and they reported the particle size and surface area versus time. They found that a minimum of 2 wt % stabiliser was necessary to avoid coagulation and that increasing the stabiliser concentration resulted in an increase in surface area and smaller particle sizes during the particle

formation. Furthermore, they reported the partial incorporation of the PDMS macromonomer into the particles at a very early stage of the reaction. However, the role of the unreacted macromonomer was not studied.

In 2000, Giles *et al.* studied the effect of PDMS-MA M_n and concentration in the particle morphology in dispersion polymerisation of MMA in scCO₂. A stabiliser with a molar mass of 2000 g mol⁻¹ produced monodispersed polymer particles at 0.2 wt % loading. In all cases, only 0.08 to 2.91 wt % of the PDMS was incorporated into the final polymer.

In 1997, Beckman *et al.* reported the dispersion polymerisation of MMA in scCO₂ using a series of poly(methyl methacrylate-co-hydroxyethyl methacrylate)-*g*-poly(perfluoropropylene oxide) graft copolymers (**Table 3, entry 4**).¹²⁸ The anchor backbone was insoluble in CO₂ but had good affinity for the forming polymer, while the pendant grafted chains of the fluorinated polymer were highly CO₂-philic.

They found that a balance between the backbone and the soluble side chains was necessary to achieve stabilisation and varying the molar mass of the stabiliser resulted in variations in the particle size and size distribution. Stabilisers with sufficient CO₂-philic component to assure complete solubility, led to smaller and more uniform particles when increasing the backbone molar mass. This was attributed to a more efficient surface anchoring during nucleation, which allows more particles to be stabilised. Further increasing the molar mass of the CO₂-philic side chains had no effect on the particle size.

In 2000, Howdle *et al* reported the use of Krytox 157 FSL as stabiliser for the dispersion polymerisation of MMA in scCO₂ (**Table 3, entry 5**).¹²⁹ It consisted of a CO₂-philic fluorinated chain terminated with a carboxylic acid that provided anchoring to the growing particles. A hydrogen bonding between the acid group from the stabiliser and the ester group from the PMMA was evidenced by FT-IR spectroscopy. Furthermore, ¹⁹F NMR showed that less than 10 wt % of the initial amount of stabiliser was present in the final product.

Only a few years later, in 2003, the former group reported the use of a very similar stabiliser, an ester end-capped perfluoropolyether (**Table 3, entry 6**), for the dispersion polymerisation of MMA in scCO₂.¹³⁰ In this case, the anchor was an ester group that interacted with the forming particles via weak Van der Waals interactions. This resulted in very low amounts of residual stabiliser left in the PMMA product.

In 2005, Howdle and coworkers, prepared perfluoropolyether based stabilisers with different anchor groups (**Table 3, entries 7-10**) and studied their behavior in dispersion polymerisation of MMA in scCO₂ in terms of their anchor group architecture.¹²²

In the case of the stabiliser with the alcohol anchor group (**Table 3, entry 7**), a very poor stabilisation was observed. This was explained by the fact that the hydroxyl group might undergo self-association preventing it from anchoring to the PMMA. When using a stabiliser with an acetate end group instead (**Table 3, entry 8**), the PMMA yield and molar mass improved

substantially. This was explained by a weak interaction between the acetate group and the particles. However, the particles obtained were agglomerated and not spherical.

Stabilisers with a methacrylate anchor group (**Table 3, entry 9**) led to even higher yields and molar mass of the PMMA. This is due to the fact that the methacrylate can chemically graft onto the growing particles. ^1H NMR analysis showed that almost all the stabiliser remained in the PMMA product. The particle morphology was described as a “pearl necklace”.

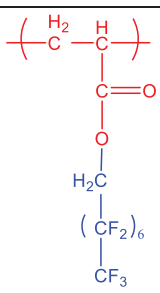
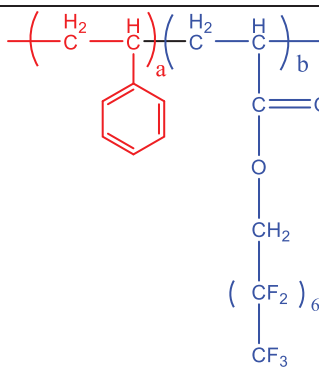
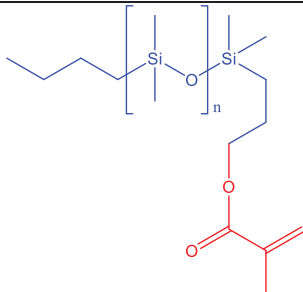
The best results were obtained when using stabilisers with PMMA anchor groups of molar masses between 2 and 3.5 kg mol^{-1} (**Table 3, entry 10**). It was hypothesised that the PMMA group could graft onto the growing PMMA particles either by free radical hydrogen abstraction or by entanglement with the growing polymer chains. Discrete spherical particles were obtained in this case.

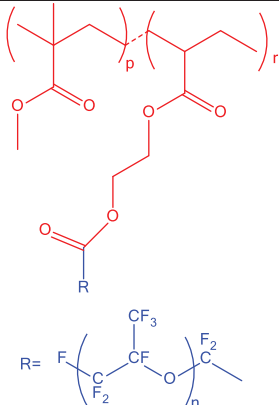
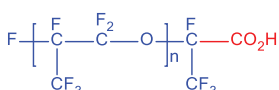
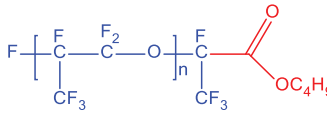
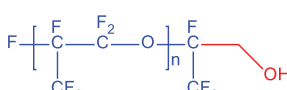
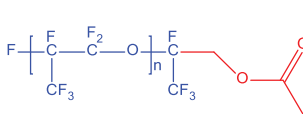
Another example is the use of fluorinated block copolymers of poly(styrene-*r*-acrylonitrile)-*b*-poly(1,1,2,2-tetrahydroperfluorooctyl methacrylate) (PSAN-*b*-PFOMA) (**Table 3, entry 11**) for the copolymerisation of acrylonitrile and vinyl acetate in scCO_2 reported by Yang et al in 2006¹³¹, resulting in uniform, submicron-size spherical particles. In addition, molar mass and particle size could be controlled by changing the initial concentration of monomer and stabiliser.

The dispersion polymerisation of a different monomer, vinylidene fluoride (VDF), using different fluorinated graft stabilisers (**Table 3, entry 12**) was

reported in 2005 by Howdle and coworkers.¹³² High molar mass polymer products with uniform spherical morphology were obtained in all the cases.

Table 3: Stabilisers for dispersion polymerisation in scCO₂. Polymer and CO₂-philic segments are highlighted in red and blue respectively.

Entry	Stabiliser	Chemical Structure	Anchoring mechanism	Prod.	D _n (μm)
1 ¹²¹	[poly(FOA)]		Physical adsorption	PMMA	0.9- 2.7
2 ¹²³	Poly(styrene- <i>block</i> -FOA)		Physical adsorption	PS	0.24- 0.40
3 ¹²⁵	PDMS-MA		Chemical grafting	PMMA	1.1- 2.8

4 ¹²⁸	poly(MMA-co-HEMA)-g-poly(PFP-O)		Physical adsorption	PMMA	0.3-20
5 ¹²⁹	Krytox 157 FSL		Hydrogen bonding	PMMA	~ 2.9
6 ¹³⁰	Krytox 157 FSL Butyl ester		Weak van der Waals interaction	PMMA	2.5
7 ¹²²	PFPE-alcohol		Hydrogen bonding	PMMA	agglomerated
8 ¹²²	PFPE-acetate		Weak Van der Waals interaction	PMMA	agglomerated

9 ¹²²	PFPE- methacrylate		Chemical grafting	PMMA	5
10 ¹²²	PFPE- block- PMMA		Hydrogen abstraction or entanglement	PMMA	3.8
11 ¹³¹	PSAN- block- PFOMA		Physical adsorption	P(Acrylonitrile-co-VAc)	0.09-0.17
12 ¹³²	FGS		Physical adsorption	PVDF	0.2-0.5

However, all the previously mentioned stabiliser polymers contain fluorine and silicone units, which makes them bio-persistent and also expensive, and this is one of the major drawbacks when trying to take polymerisation processes in scCO₂ to industry scale. There is therefore a need to design new materials that are greener and more affordable. Hydrocarbon based stabilisers constitute a very promising alternative and have become the subject of interest in research in recent years.

3.1.1.2 Solubility of hydrocarbon based polymers in scCO₂

There are a number of different factors to consider when evaluating the solubility of a polymer in CO₂ (Figure 33).

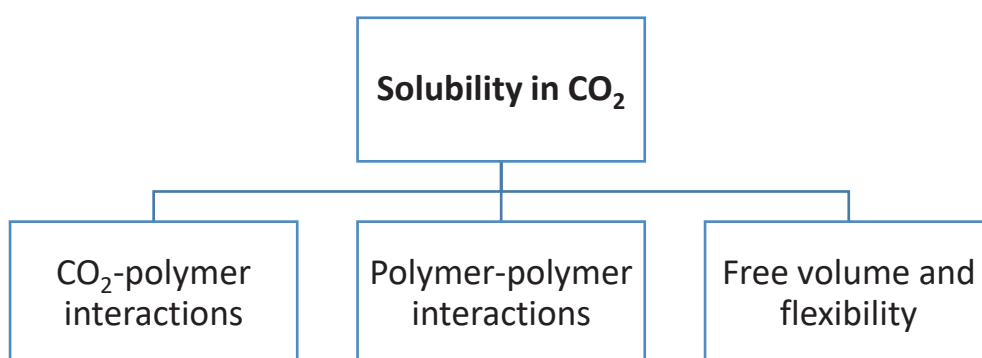


Figure 33: CO₂ solubility chart.

The first is the CO₂-philicity of the polymer, a measure of its interactions with the CO₂. The molecule of CO₂ is charge separated with partial negative charges on the oxygen atoms and positive for the carbon atom. As a result, the oxygen atoms are weak Lewis bases, while the carbon is a Lewis acid.¹³³ CO₂-philic polymers will contain functional groups with a specific interaction with the CO₂, such as fluorinated or carbonyl groups. Dardin *et al.* proved the existence of specific van der Waals interactions between the fluorinated

atoms in different fluorocarbons and CO₂ using high pressure high resolution NMR spectroscopy.¹³⁴

The second thing to consider is the strength of the polymer-polymer interactions. To favour polymer solubility, these must be weaker than the polymer-solvent interactions. Polymer-polymer interactions can be evaluated in terms of the surface tension. A weak surface tension is characteristic of siloxane based polymers, which show extremely good solubility in CO₂.

The third aspect to look at is the flexibility and free volume of the polymer, which is directly related to the glass transition temperature (T_g). The glass transition is a reversible transition of the polymer from a glassy state to a rubber-like state. As a general statement, polymers that are highly branched or contain flexible groups will have a higher free volume and a lower T_g , and will therefore be more soluble in CO₂. Zhang et al demonstrated that, at low molar masses (3500 g mol⁻¹) branching enhances solubility of star-shaped poly(vinyl acetate) (PVAc).¹³⁵

A great amount of research has been devoted to evaluating the solubility of different non-fluorinated non-siloxane hydrocarbon based polymers in scCO₂.¹³⁶ For example, poly(ethylene oxide) shows a very limited solubility in CO₂, with a cloud point of 330 bar at 40°C for a sample with an M_n of 600 g mol⁻¹ at 0.92 wt %.¹³⁷⁻¹³⁸ An analogous polymer, poly(propylene oxide), shows an improved solubility of less than 100 bar at 22°C for a molar mass

of 725 g mol^{-1} .¹³⁹ This is due to the methyl group introduced to enhance the free volume and decrease the surface tension.

Poly(ether carbonates) constitute another example of hydrocarbon based polymers with substantial solubility in CO_2 . Tryznowski *et al* showed that a hyperbranched aliphatic poly(ether carbonate) of M_n around 16000 g mol^{-1} and 15.4 mol% of carbonate was soluble at 130 bar and 22°C at 1 wt %.¹⁴⁰ This can be explained by its low cohesive energy (weak polymer-polymer interactions) and the presence of a Lewis base carbonyl group in the polymer backbone.

Currently, poly(vinyl esters) remain the most promising group of CO_2 -philic hydrocarbon polymers. For example, low molar mass ($M_n = 2060 \text{ g mol}^{-1}$) poly(vinyl acetate) (PVAc) is soluble at 5 wt % in CO_2 at 374 bar and 25°C .¹³⁶ This solubility has been explained by a specific Lewis acid–Lewis base (LA–LB) interaction between the electron-rich carbonyl functionality of the acetate group and the electron deficient carbon atom of the CO_2 molecule. This was confirmed by IR spectroscopy.¹¹⁹ The IR spectrum of CO_2 impregnated PVAc films showed two new absorption bands (661.9 and 654.0 cm^{-1}) that were assigned to the interaction of the CO_2 and the carbonyl group of PVAc. In addition, a cooperative hydrogen bond between the acetate group and the CO_2 molecule was revealed by *ab initio* calculations (Optimized equilibrium structure (CAM-B3LYP/aug-cc-pVDZ) for the complex EtAc– CO_2). Polymer–solvent interactions were calculated using a model structure (ethyl

acetate; EtAc) which is representative of the main functional group of the backbone of PVAc.¹⁴¹⁻¹⁴²

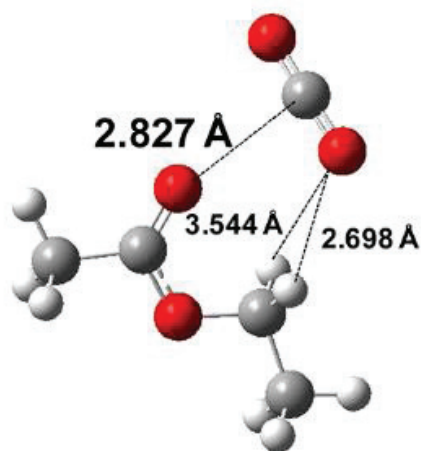


Figure 34: Optimized equilibrium structure (CAM-B3LYP/aug-cc-pVDZ) for the complex EtAc-CO₂. Polymer-solvent interactions were calculated using a model structure (ethyl acetate; EtAc) which is representative of the main functional group of the backbone of PVAc. Reprinted from ¹⁴¹. Copyright 2012 American Chemical Society.

However, these materials do not match the properties of the fluorinated ones that are soluble at mild temperatures and pressures lower than 300 bar.^{143 144} This could be explained by the strong polymer-polymer interactions between PVAc chains and a lower entropy of mixing due to a lower free volume.¹⁴⁵ In addition, the cloud point pressure and solubility are strongly dependent on the chain molar mass, which limits the usefulness of higher molar mass PVAc.

Girard *et al.*, reported the partial fluorination of poly(vinyl esters) as a method for enhancing their solubility in scCO₂.¹⁴¹ They found that, with gradual incorporation of 11, 27, and 50 mol % vinyl trifluoroacetate (VTFAC) units into the polymer chains, the cloud points dramatically decreased from

281 bar for a reference sample of PVAc, to 245, 212, and 177 bar respectively. This was attributed to a decrease in the polymer-polymer interactions, measured in terms of the surface tension. However, this strategy is not an environmentally friendly approach.

Another possible strategy to overcome these limitations is the copolymerisation of VAc with monomers that not only present lower polymer-polymer interactions, but also a higher entropy of mixing, such as monomers with bulkier groups. Howdle and coworkers reported the copolymerisation of VAc with vinyl butyrate, vinyl octanoate¹⁴⁶⁻¹⁴⁷, dibutyl maleate¹⁴⁸ and vinyl pivalate using RAFT polymerisation¹¹⁶.

The best solubility values were found for poly(vinyl acetate-*stat*-vinyl pivalate) (PVAc-*stat*-PVPi) statistical copolymers with molar masses around 10000 g mol⁻¹ and different VAc:VPi ratios that presented cloud points in the range of 132 to 164 bar (1915 to 2379 psi) at 35°C and 5% weight w.r.t. monomer (**Figure 35**).

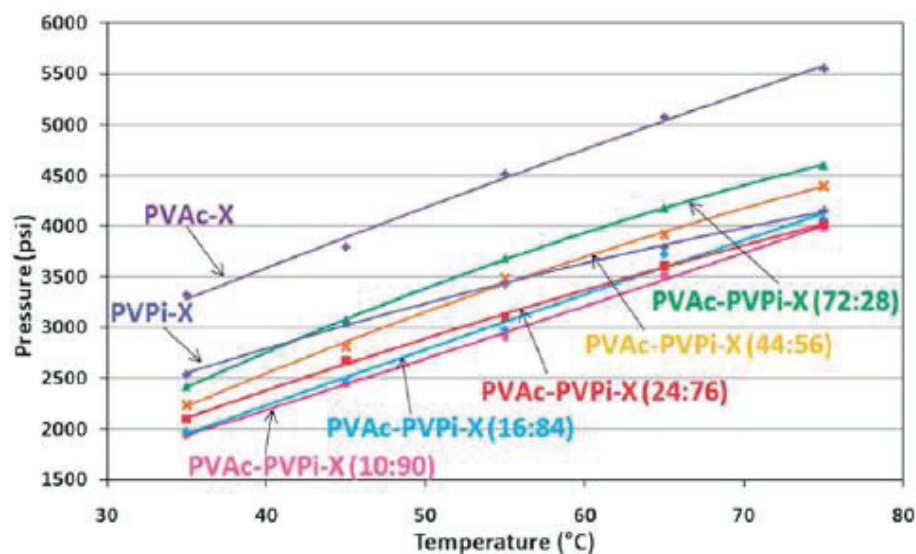


Figure 35: Cloud point curves of PVAc-stat-PVPi-X of $M_n \approx 10000 \text{ g mol}^{-1}$ in CO_2 , with 15 wt% NVP w.r.t. CO_2 . VAc:VPi molar ratios are in the range of 10:90 to 72:28. Reproduced from ¹¹⁶ with permission of The Royal Society of Chemistry.

3.1.1.3 Hydrocarbon based polymers as stabilisers

As previously mentioned, in order to achieve a successful dispersion polymerisation the stabiliser must show a good balance between solubility and steric stabilisation. Stabilisers of higher molar mass provide a more efficient steric stabilisation but they have lower CO_2 -solubility. Furthermore, the stabiliser must interact with the growing polymer in a favorable way.

P(VAc-stat-VPI)-X statistical copolymers synthesised by RAFT polymerisation (Figure 36) have successfully worked as stabilisers for dispersion polymerisation of *N*-vinyl pyrrolidone in scCO_2 , yielding micron size spherical polymer particles.¹¹⁶ The best compromise between the solubility and stabilising ability of the surfactants was found at 25:75 to 50:50 VAc:VPi molar ratios.

Stabilisers with higher VAc content showed a less efficient stabilisation due to a lower solubility. Stabilisers with higher VPi content, although more soluble, showed a less efficient stabilisation. This was attributed to the fact that VAc introduces flexibility into the chain providing a better interaction with the scCO_2 and enhancing the steric stabilisation around the PNVP particles.

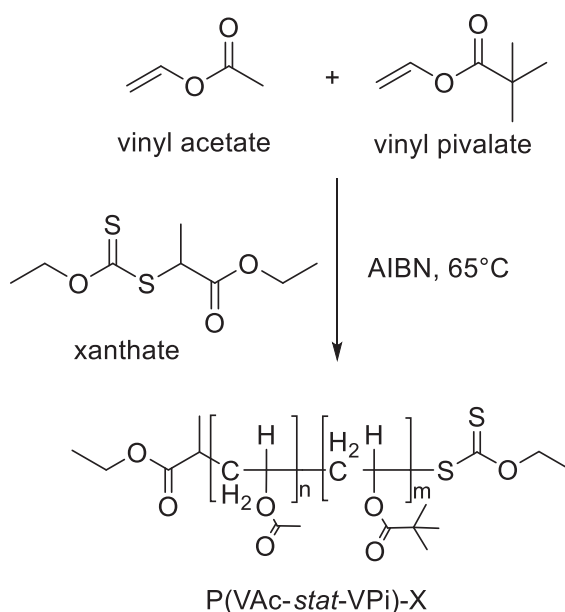
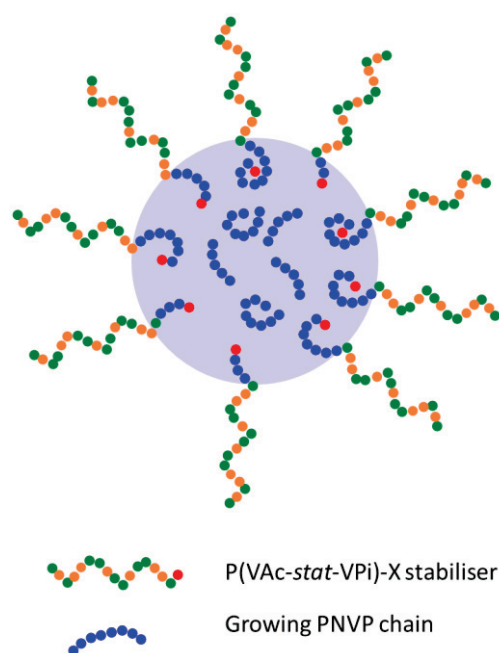


Figure 36: Synthesis of xanthate terminated P(VAc-stat-PVPi)-X statistical copolymer.

However, this kind of stabiliser has only worked for one monomer system so far, PNVP. Attempts to polymerise other monomers such as MMA in scCO_2 using xanthate terminated P(VAc-stat-VPi)-X stabilisers were unsuccessful, resulting in low conversion. This appears to indicate that the stabilisers do not anchor to the growing particles efficiently and precipitation of the polymer takes place.

There is still a lot of discussion about how these materials anchor to the particles. One hypothesis is that the stabiliser can act as a macro-RAFT agent

and chain extend with the monomer to form a P(VAc-*stat*-VPi)-*block*-PNVP block copolymer where the P(VAc-*stat*-VPi) block provides steric stabilisation and the PNVP block is buried in the forming particles. (**Figure 37**). In this anchoring mode, the surfactant is chemically grafted to the polymer particles.



*Figure 37: Anchoring of P(VAc-*stat*-VPi)-X by RAFT chain extension. The RAFT end group provides the opportunity to grow a short PNVP block.*

In the case of MMA this chain extension cannot take place. In order to understand the reason for this, we need to go back to the fundamentals of RAFT polymerisation. Poly (vinyl acetate) and poly (vinyl pivalate) propagating macro radicals are poor leaving groups compared to PMMA macro radical. In consequence, the radical intermediate that would form in the main RAFT equilibrium (**Figure 38, II**) cannot fragment to give free PVAc and chain extension does not take place.

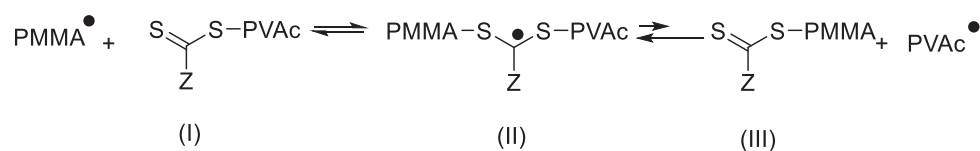


Figure 38: Main RAFT equilibrium for chain extension of PVAc-X with MMA.

PNVP macro radicals have similar reactivity to those of PVAc or PVPI. This hypothesis would explain the formation of a compatibilising block in the case of NVP dispersion polymerisation and why these materials are performing much better in this case compared to dispersion polymerization of MMA.

However, another possible anchoring mode can happen through physical adsorption of the stabilisers to the surface of the particles via weak Van der Waals interactions (**Figure 39**).

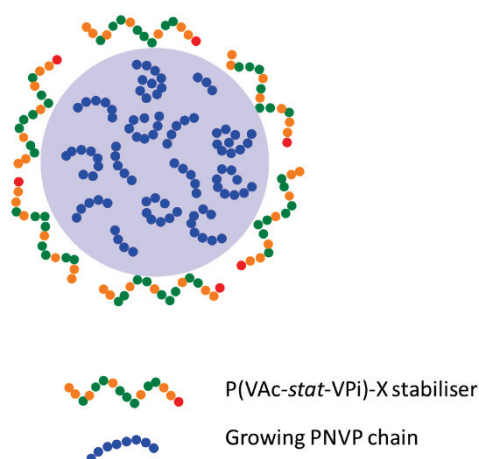


Figure 39: Anchoring of P(VAc-*stat*-VPI)-X by physical adsorption.

Further investigation would be required in order to explain how this anchoring happens in reality. Extraction of the polymer products in scCO₂ can lead to a partial recovery of the stabiliser, which can be used to evaluate if it is grafted, adsorbed through a weak physical interaction, or a combination of both mechanisms like in the case of PDMS-MA.

Independently of this, PVAc based stabilisers do not provide sufficient anchoring in the case of MMA.

In order to try to overcome this limitation, Arrowsmith *et al.* synthesised various hydrocarbon stabilisers with different end groups using a combination of RAFT polymerisation and click chemistry (**Figure 40**).¹⁴⁹

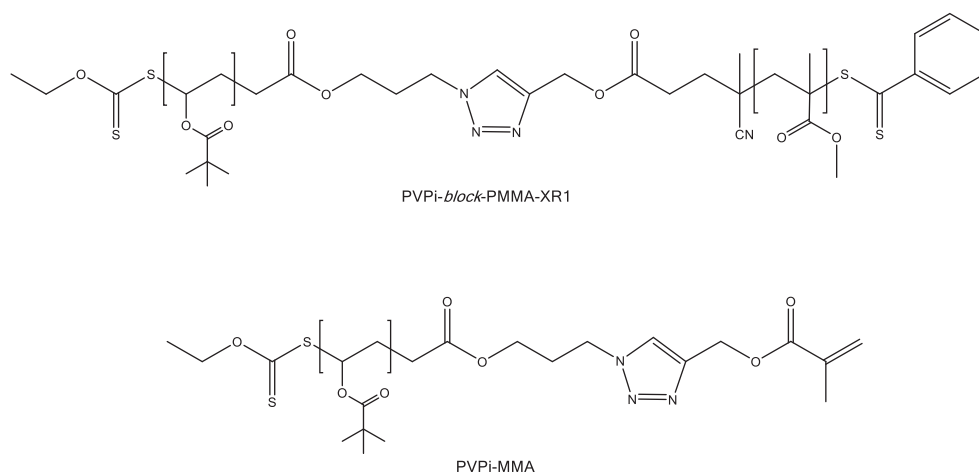


Figure 40: PVPi-block-PMMA-XR1 and PVPi-MMA stabilisers. The PVPi block provides steric stabilisation and the MMA or PMMA block provides an anchor for the forming PMMA particles during dispersion polymerisation.

These stabilisers were tested in dispersion polymerisation of MMA. They were able to produce polymeric products, although the particles were highly agglomerated instead of spherical. This suggests a lack of stabiliser situated on the surface of the growing particles either due to the low solubility of these materials in the reaction conditions or a lack of anchoring of the MMA or PMMA groups.

3.1.2 Design of new hydrocarbon based stabilisers by RAFT/MADIX

polymerisation

The aim of this chapter was to gain a better insight into the mechanism of stabilisation in dispersion polymerisation and design new hydrocarbon based stabilisers that could overcome the limitations of the previous ones by providing effective anchoring for a different monomer system, MMA. Ideally, these materials would be able to produce polymer particles with high conversion and uniform spherical morphologies.

In order to produce a successful stabiliser for MMA dispersion polymerisation in scCO_2 , the stabilisers that had already worked for NVP polymerisation were modified by adding a second block that would act as a polymer-philic group and provide a better anchoring to the MMA growing particles and therefore a better stabilisation. In order to achieve this, we made use of RAFT polymerisation (**Figure 41**).

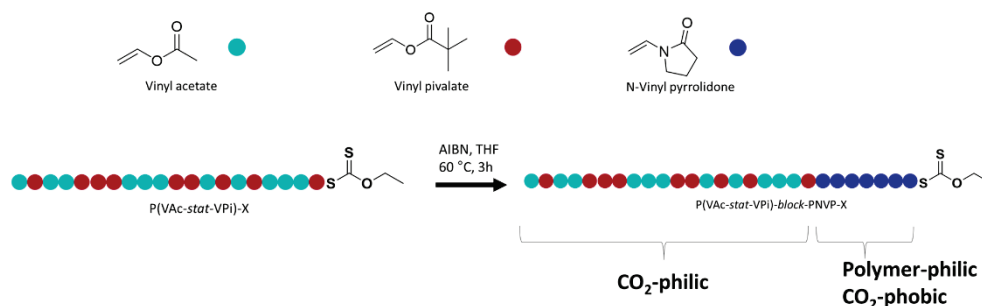


Figure 41: Synthesis of P(VAc-stat-VPI)-block-PNVP-X block copolymers by RAFT.

The monomer of choice for this second block was NVP. There are several reasons for this. PNVP is known to be a highly CO₂-phobic polymer. The solubility range of PNVP in scCO_2 for a M_n of 10 kg mol⁻¹ has been reported to be between 2.03 to 4.85e⁻⁷ mol mol⁻¹, decreasing further when increasing

M_n .¹⁵⁰ It has been hypothesized that in a dispersion polymerisation in $scCO_2$ PNVP will have a tendency to attach to the particles providing anchoring.

Since all of the monomers involved (vinyl acetate, vinyl pivalate and N-vinyl pyrrolidone) belong to the same class (LAMs), they can be polymerised using the same RAFT agent to yield materials with the desired architecture. The synthesis of targeted *P(VAc-stat-VPi)-block-PNVP* by RAFT is thus very straightforward, making them a very good starting point.

3.2 Experimental

Materials

Monomers vinyl acetate (VAc, 99%, with hydroquinone as inhibitor) and methyl methacrylate (MMA, 99%, contains MEHQ as inhibitor) were purchased from Sigma Aldrich. N-vinyl pyrrolidone (NVP, 99%, stabilised with NaOH) and vinyl pivalate (VPi, 99%, with hydroquinone as inhibitor) were purchased from Acros. 2,2'-Azobis(2-methylpropionitrile (AIBN, 98%) was purchased from Sigma Aldrich and 2,2'-Azobis(4-methoxy-2,4-dimethylvaleronitrile (V-70) from Wako. The xanthate RAFT agent (*O*-ethyl-*S*-(1-methoxycarbonyl) ethyl dithiocarbonate) was synthesised as detailed in Chapter 3. All reagents were used without further purification. Dry CO_2 (SFC grade, 99.99%) was purchased from BOC.

**Synthesis of *O*-ethyl-*S*-(1-ethoxycarbonyl) ethyl dithiocarbonate
(Xanthate X1).**

The procedure was adopted from the literature.¹⁵¹ Ethyl 2-bromopropionate (11.12 g, 60.00 mmol) was dissolved in 100 mL of ethanol in a 250 mL round bottom flask. Potassium ethyl xanthate (10.86 g, 70.00 mmol) was added to the solution over a period of 30 minutes. The mixture was then degassed with argon for 30 minutes and stirred at room temperature for 24 hours. The mixture was filtered and the solvent removed under reduced pressure to give a yellow liquid. The product was dissolved in dichloromethane and washed with water (3x75 mL) in a separating funnel and then dried with MgSO₄ and filtered again. The solvent was removed under reduced pressure to give the pure product. Yield = 85%. ¹H NMR (CDCl₃): δ = 4.62 (q, 2H, J_{fa} =7.13 Hz), 4.36 (q, 1H, J_{ec} =7.39 Hz), 4.19, (q, 2H, J_{db} = 7.14 Hz), 1.55 (d, 3H, J_{ce} =7.40 Hz), 1.40 (t, 3H, J_{bd} = 7.12 Hz), 1.26 (t, 3H, J_{af} = 7.13 Hz).

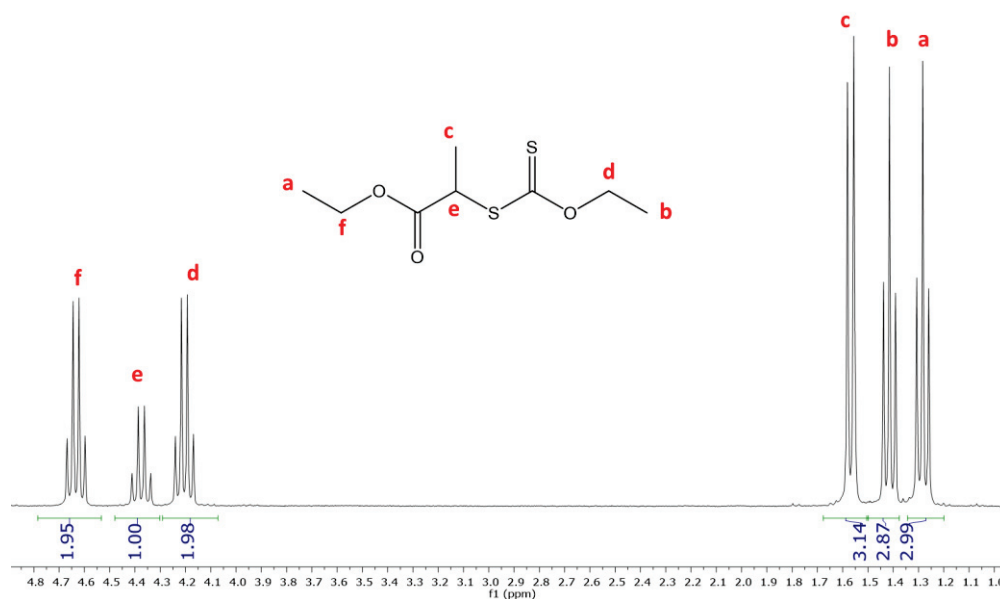


Figure 42: ^1H NMR spectrum of xanthate 1 in CDCl_3 (16 scans).

Synthesis of *O*-ethyl-*S*-(1-methoxycarbonyl) ethyl dithiocarbonate (Xanthate X2)

The procedure was adopted from the literature.¹⁵² Methyl bromoacetate (16.00 g, 104.6 mmol) was dissolved in ethanol (75mL) in a 250 mL round bottom flask with a stirring bar and in an ice bath. Potassium ethyl xanthate (19.52 g, 121.7 mmol) was dissolved in ethanol (100mL) in a beaker for 30 minutes and added dropwise to the flask using an addition funnel. The mixture was stirred at room temperature for 24 hours and filtered to remove KBr salts. The filtrate was evaporated under reduced pressure, dissolved in dichloromethane (50 mL) and washed with water (3x15 mL). The organic phase was dried with magnesium sulfate and dried under vacuum to yield a

yellow liquid. Yield= 79%. ^1H NMR (CDCl_3): δ = 4.5 ppm (q, 2 H, J_{da} = 7.12 Hz), 3.8 ppm (s, 2H), 3.6 ppm (s, 3H), 1.3 ppm (t, 3H, J_{AD} = 7.12 Hz).

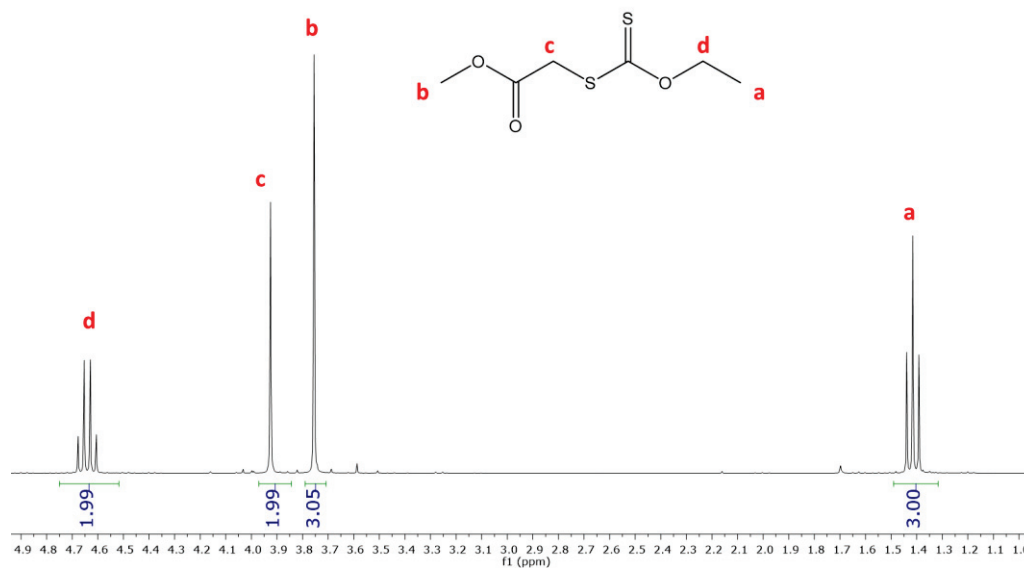


Figure 43: ^1H NMR spectrum of xanthate 2 in CDCl_3 (16 scans).

Polymerisation of vinyl acetate with X1 and X2

Vinyl acetate (20.00 g, 232.3 mmol), xanthate X1 (1.29 g, 5.8 mmol) or X2 (1.10 g, 5.8 mmol) and AIBN (0.09 g, 0.58 mmol) were added to a Schlenk flask and the mixture was degassed with argon for 30 minutes in an ice bath and then stirred at 60° for 4 hours. The product was precipitated into cold petroleum ether and dried under reduced pressure. PVAc-X2: M_{ntheor} = 2.4 kg mol^{-1} , M_{nNMR} = 2.3 kg mol^{-1} , M_{nSEC} (THF) = 2.4 kg mol^{-1} , 64% conversion, 58% yield, \bar{D} = 1.21. ^1H NMR (CDCl_3): δ = 6.5-6.6 ppm (m, 0.75 H), 4.8- 5 ppm (m,

26H), 4.55-4.7 ppm (m, 2H), 3.6 ppm (s, 3H), 2.3-2.4 ppm, 1.6-2.1 ppm (m, 144H), 1.35-1.45 ppm (m, 3H).

Synthesis of PVAc-*stat*-VPi-X1 copolymer

Vinyl acetate (3.73 g, 36.00 mmol), vinyl pivalate (4.67 g, 36.00 mmol), xanthate X1 (0.13 g, 0.57 mmol), AIBN (9.0 mg, 0.06 mmol) and toluene (5 mL) were added to a round bottom flask with a stirrer bar and the mixture was degassed with argon for 30 minutes and stirred at 60°C for 48 hours. The product was purified by precipitation into a mixture of cold methanol:water 4:1 and dried under reduced pressure. $M_{ntheor} = 10.5 \text{ kg mol}^{-1}$, $M_{nSEC}(\text{CDCl}_3) = 11.9 \text{ kg mol}^{-1}$, 76% conversion, 58% yield, VAc:VPi ratio = 57:43, $\bar{D} = 1.36$. $^1\text{H NMR}(\text{CDCl}_3) \delta = 4.65\text{-}5.10 \text{ ppm (m, 1H)}, 1.95\text{-}2.10 \text{ ppm (s, 3H)}, 1.60\text{-}1.90 \text{ ppm (m, 2H)}, 1.10\text{-}1.25 \text{ ppm (s, 3H)}$.

Synthesis of P(VAc-*stat*-VPi)-X2 copolymer

Typical copolymer synthesis: Vinyl acetate (17.99 g, 0.21 mol), vinyl pivalate (2.97 g, 23.23 mmol), xanthate X2 (0.68 g, 3.60 mmol) and AIBN (0.06 g, 0.36 mmol) were placed in a round bottom flask with a stirring bar and degassed with argon for 30 minutes in an ice bath. The mixture was stirred at 60°C for 180 minutes. The product was purified by precipitation into a mixture of cold methanol:water 4:1 and dried under reduced pressure. $M_{ntheor} = 4.5 \text{ kg mol}^{-1}$, $M_{nNMR} = 5.2 \text{ kg mol}^{-1}$, $M_{nexpSEC}(\text{THF}) = 5.8 \text{ kg mol}^{-1}$, 60% conversion, 45% yield, VAc:VPi ratio = 86:14, $\bar{D} = 1.19$. $^1\text{H NMR}(\text{CDCl}_3): \delta = 6.4\text{-}6.7 \text{ ppm (m, 1H)}, 1.95\text{-}2.10 \text{ ppm (s, 3H)}, 1.60\text{-}1.90 \text{ ppm (m, 2H)}, 1.10\text{-}1.25 \text{ ppm (s, 3H)}$.

0.5 H), 4.7-5 ppm (m, 52 H), 4.5-4.7 ppm (m, 2 H), 3.6 ppm (s, 3H), 2.25-2.35 ppm, 1.5-2.1 ppm (m, 228 H), 1.3-1.4 ppm, 1.1-1.3 ppm (m, 161 H).

Synthesis of P(VAc-*stat*-VPi)-*block*-PNVP-X2 copolymer

P(VAc-*stat*-VPi)-X2 of 9.1 kg mol^{-1} (2g, 0.22 mmol) was dissolved in 4 g of THF in a round bottom flask with a stirring bar. NVP (240 mg, mol) and AIBN (20 mg, mol) were added. The flask was sealed and degassed for 30 minutes with argon in an ice bath and then heated at 60°C for 180 minutes. The product was precipitated into a mixture of cold petroleum ether and dried under reduced pressure. DP of PNVP = 7, $M_{\text{nNMR}} = 9.9 \text{ kg mol}^{-1}$, $M_{\text{nexpSEC}}(\text{DMF}) = 12.9 \text{ kg mol}^{-1}$, $\bar{D} = 1.20$.

Phase Behaviour Measurements

Cloud point data were obtained using a hydraulic variable volume view cell described in Chapter 2. 150 mg of the polymer were dissolved in 3 g of monomer (5 wt% polymer with respect to monomer) and injected into the view cell. 20 g of CO₂ (15 wt% wt monomer with respect to CO₂) were then transferred by means of a high pressure stainless steel CO₂ bomb. The contents of the view cell were stirred using magnetic stirring. The system was heated to the desired temperature (35 to 75 °C) and pressure was increased by means of a movable piston to 345 bar when the sample was fully dissolved. To determine the cloud point, pressure was then decreased until the polymer was precipitated and the back light was totally obscured.

All measurements were repeated three times and an average of these values was taken.

Dispersion polymerisation of NVP and MMA

Dispersion polymerisations were carried out in a 60mL high pressure stainless steel autoclave thoroughly described in Chapter 2. The monomer (MMA, 7.2 g, 0.072 mol or NVP, 8 g, 0.072 mol) on one side and 5 wt% of the stabiliser (0.04 mmol) together with V-70 (130 mg, 0.42 mmol) on the other side were degassed with argon for 30 minutes in separate vials, mixed together and then injected into the autoclave through the safety pin, under a small pressure of CO₂. The autoclave was then pressurized with more CO₂ to approximately 55 bar and heated to 35°C. As a result pressure increased to 83 bar. The pressure was then further increased to approximately 275 bar and the reaction proceeded for 48h. The autoclave was then cooled to room temperature and slowly vented. The time needed for pressurising and heating the autoclave to the desired conditions (35°C, 275 bar in this case) will be referred to as setup time.

3.3 Results and discussion

3.3.1 RAFT agent choice

The proposed synthetic path towards P(VAc-*stat*-VPi)-*block*-PNVP-X2 block copolymers is depicted in **Figure 44**. The first step is the synthesis of the xanthate RAFT agent, followed by the copolymerization of vinyl acetate and

vinyl pivalate. The third step is the chain extension of the P(VAc-*stat*-VPi)-X statistical copolymers with a second monomer, N-vinyl pyrrolidone.

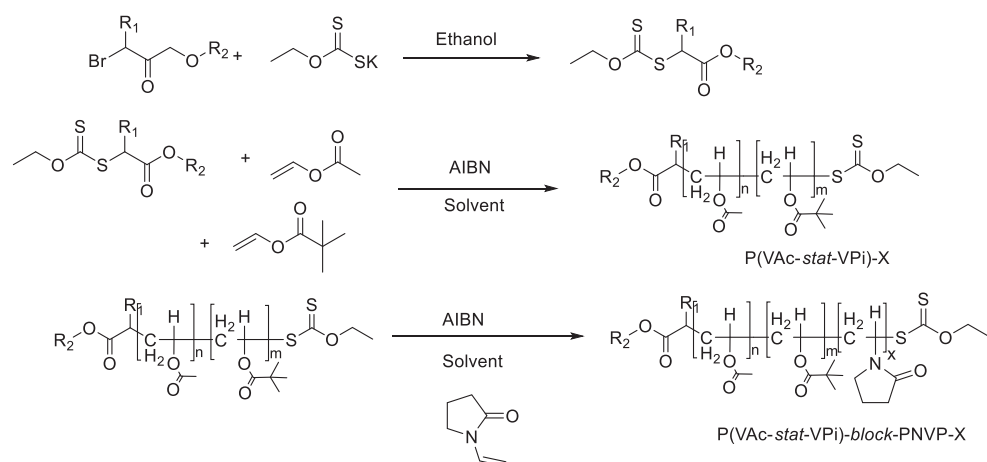


*Figure 44: Synthetic path towards PNVP-based block copolymers. Step one: synthesis of the xanthate. Step two: synthesis of P(VAc-*stat*-VPi)-X copolymers. Step 3: Chain extension of statistical copolymers with NVP.*

As previously discussed in the introduction, the choice of RAFT agent is one of the most important steps in RAFT polymerisation.

Two different xanthate RAFT agents were studied, *O*-ethyl-S-(1-ethoxycarbonyl) ethyl dithiocarbonate (X1) and *O*-ethyl-S-(1-methoxycarbonyl) ethyl dithiocarbonate (X2) (**Figure 45**). The xanthate X1 carrying a secondary 1-ethoxycarbonyl ethyl R reinitiating group has been successfully used previously in the group in the synthesis of vinyl acetate based copolymers, and it was therefore the starting point in this project. The xanthate X2 carrying a primary 1-methoxycarbonyl ethyl R reinitiating group was further employed here.

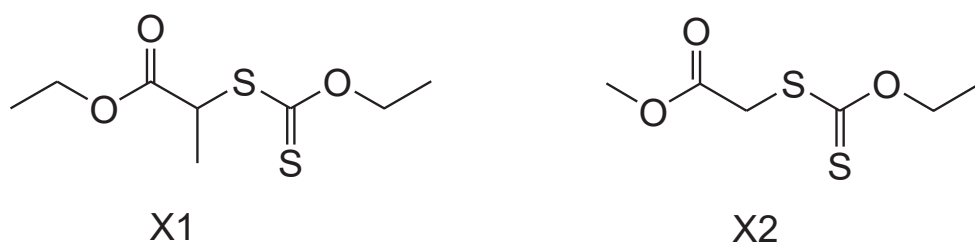


Figure 45: RAFT agent structures.

In order to compare the performance of both RAFT agents, a model polymerisation of vinyl acetate was carried out in bulk for 4h. A number-average molar mass (M_n) of 4 kg mol⁻¹ was targeted for this experiment to ease the analysis of chain ends by NMR.

For the xanthate X1 a conversion of only 26% was achieved after 4h, when the reaction was stopped. A reaction time of 4h was chosen for the kinetic study since longer reaction times can result in the occurrence of side reactions. The product was isolated as a white sticky solid of $M_{nNMR}=1.74$ kg mol⁻¹, $M_{nSEC}=1.2$ kg mol⁻¹ and $\bar{D}=1.35$. ¹H NMR is shown in **Figure 46**.

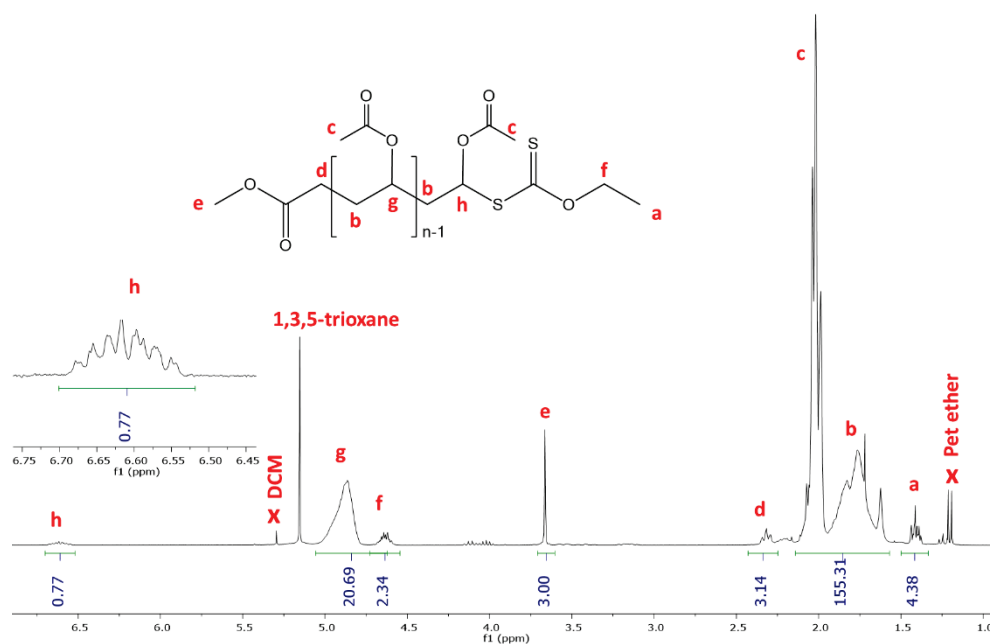


Figure 46: ^1H NMR spectrum of PVAc-X1 in CDCl_3 (256 scans). Non assigned signals at 1.2 and 5.3 ppm correspond to residual precipitation solvents petroleum ether and dichloromethane respectively.

Molar mass was calculated assuming 100% of the chains are functionalized with the methoxy R group and using the integral of this resonance (e) as a reference. The degree of polymerisation then obtained from the integration of the peak g gives the molar mass.

Signals at 1.4 (a), 2.3 (d), 3.6 (e) and 4.6 ppm (f) correspond to the resonances of the protons on chains ends coming from the initial xanthate.

The signal at 6.6 ppm (h) corresponds to the methine proton of the last vinyl acetate unit adjacent to the sulfur atom of the dithiocarbonate end. The integral of this signal can be used to evaluate the percentage of the polymer chains that retain the dithiocarbonate living end. By calibrating the methoxy protons to 3 and assuming all the chains were initiated by the 1-(methoxycarbonyl) ethyl group from X2, the closer the value of the integral

of the resonance h is to 1, the higher percentage of RAFT terminated chains we have, in this case 77%.

Kinetics of the polymerisation was monitored by ^1H NMR (**Figure 47**).

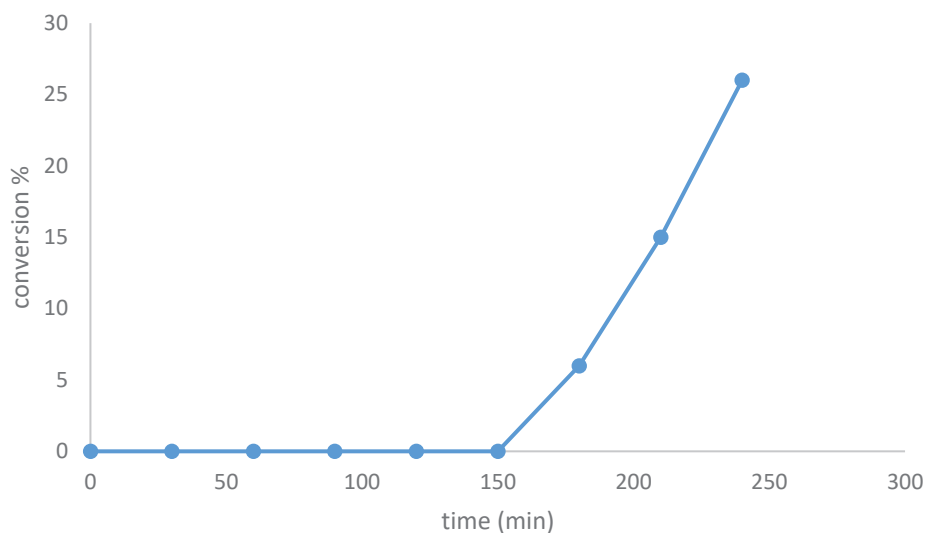


Figure 47: Conversion versus time for vinyl acetate bulk polymerisation with RAFT agent X1. Samples were withdrawn from the reaction mixture every 30 minutes and analysed by ^1H NMR.

The decrease in one of the vinylic monomer resonances ($\delta = 7.1$ ppm) compared to the resonance of an internal reference (1,3,5-trioxane) ($\delta = 4.95$ ppm) gives monomer conversion (**Figure 48**: ^1H NMR of an example VAc polymerisation at $t=0$ before the start of the reaction (A) and final time (B)).

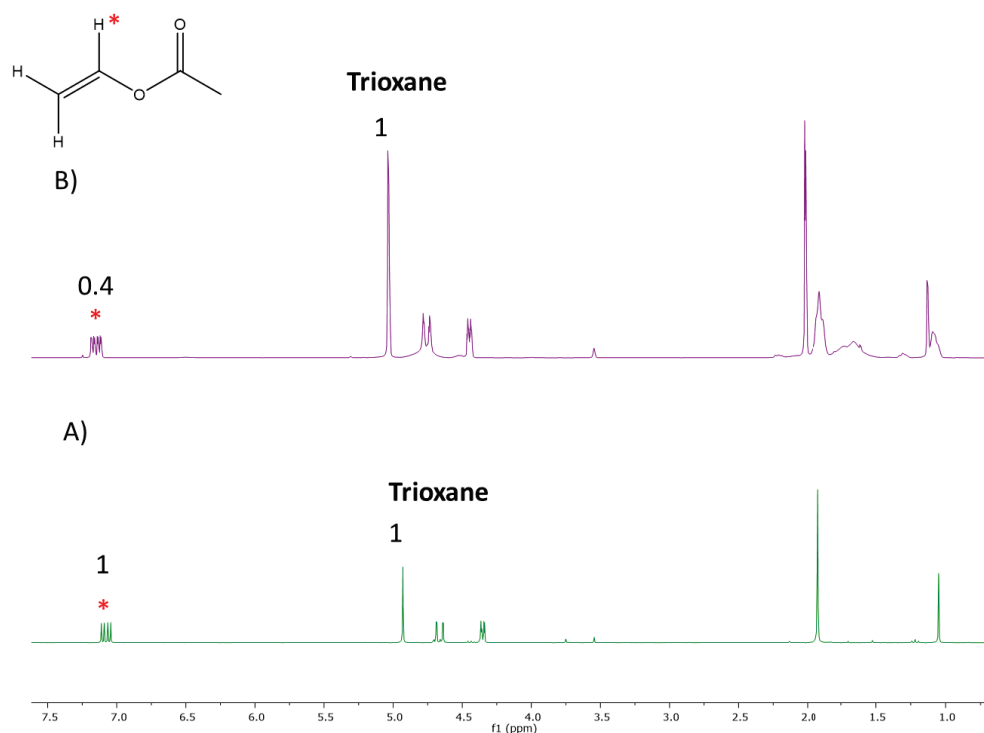


Figure 48: ^1H NMR of an example VAc polymerisation at $t=0$ before the start of the reaction (A) and final time (B) in CDCl_3 (16 scans)

At $t=0$ the integrals of both signals will be 1. As the reaction proceeds, the integral of trioxane stays constant at 1 but the integral of the monomer decreases. At a given time (t) conversion can be calculated using the formula:

$$\text{Conv. \%} = (1 - I_t) \times 100 = (1 - 0.4) \times 100 = 60\%$$

I_t is the value of the integral of the monomer at the given time, 0.4 in our example.

The polymerisation presents a typical kinetic plot for RAFT processes, with an initialisation period that corresponds to the consumption of the RAFT agent to selectively form a R-VAc-X adduct.^{69, 71} Longer chains can then start forming.

For the xanthate X2, a conversion of 64% was achieved in the same reaction time. The polymer product obtained was a white powder of $M_{\text{nNMR}}=2.3$ kg

mol^{-1} , $M_{\text{nSEC}}=2.4 \text{ kg mol}^{-1}$ and a dispersity (\mathcal{D}) of 1.21. ^1H NMR is shown in

Figure 49.

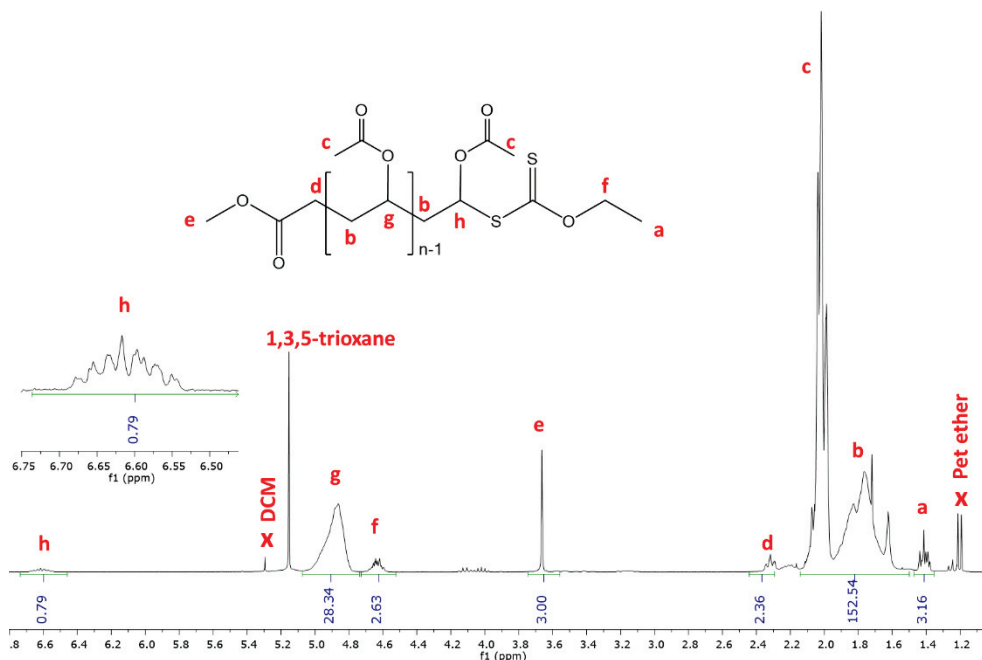


Figure 49: ^1H NMR spectrum of PVAc-X2 in CDCl_3 (256 scans). Non assigned signals at 1.2 and 5.3 ppm correspond to residual precipitation solvents petroleum ether and dichloromethane respectively.

Signals at 1.4 (a), 2.3 (d), 3.6 (e) and 4.6 ppm (f) correspond to the resonances of the protons on chains ends coming from the initial xanthate.

The signal at 6.6 ppm (h) corresponds to the methine proton of the last vinyl acetate unit adjacent to the sulfur atom of the dithiocarbonate end. The integral of this signal can be used to evaluate the percentage of the polymer chains that retain the dithiocarbonate living end. In this case the percentage of RAFT terminated chains is 79%.

As in the previous case, a kinetic plot was obtained by following conversion versus time by ^1H NMR for this reaction (**Figure 50**).

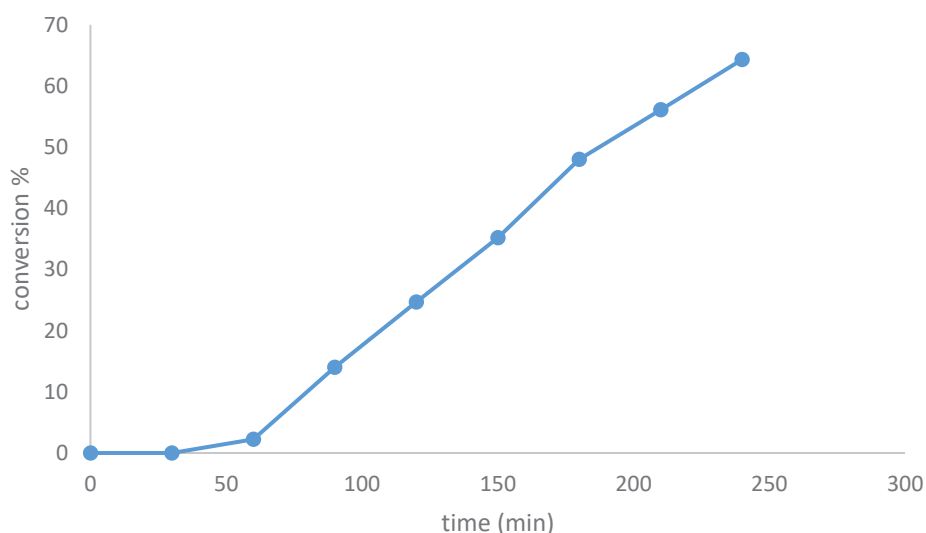


Figure 50: Conversion versus time for vinyl acetate bulk polymerisation with RAFT agent X2. Samples were withdrawn from the reaction mixture every 30 minutes and analysed by ^1H NMR. The decrease in the monomer peak compared to the standard peak (1,3,5-trioxane) gives conversion, as previously explained.

In this case we can observe a much shorter initialisation period,⁷⁰ but a very similar plot to X1 (**Figure 47**), with conversion increasing with time. This along with the low dispersity values, indicates that a controlled radical polymerisation takes place.

The different behavior observed for the two xanthates can be explained by the difference in their structure. Primary radicals are less stable than secondary ones, so the re-initiation step in the RAFT process is faster when X2 is used (**Figure 51**). In consequence, higher conversions are reached in the same reaction times.

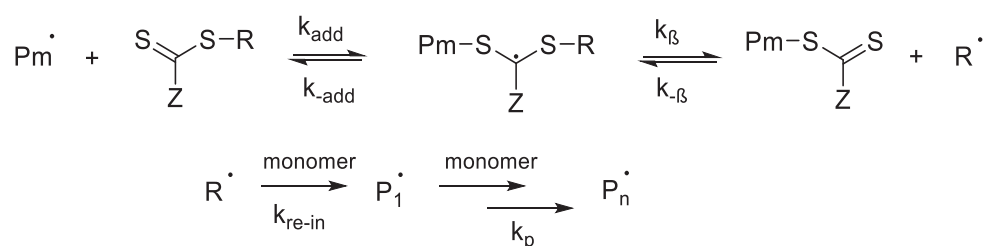


Figure 51: Pre-equilibrium and re-initiation steps in RAFT polymerisation.

We can therefore confirm that xanthate X2 (**Figure 45: RAFT agent structures**). is a much more suitable RAFT agent for the polymerisation of vinyl acetate, hence it was the chosen one for the rest of the project.

Xanthate 2 was also tested as a RAFT agent for NVP polymerization. Conversion of 60% was reached in a period of 3 hours. A kinetic plot was obtained by following the conversion versus time in the same way as for VAc. The process is also controlled by RAFT. Molar mass cannot be determined by NMR end group analysis since there is an overlap of the end group and the polymer peaks. Differences observed between the theoretical molar mass calculated by conversion ($M_{n\text{theor}} = 4 \text{ kg mol}^{-1}$) and the experimental one obtained from SEC ($M_{n\text{SEC}} = 7.2 \text{ kg mol}^{-1}$), as well as the high dispersity ($\mathcal{D} = 1.67$), can be explained by the fact that the hydrodynamic behavior of PNVP differs very much from most standards used in SEC such as PMMA and polystyrene, making it difficult to accurately determine the molar mass and dispersity using this technique.¹⁵³

3.3.2 Synthesis of P(VAc-*stat*-VPi)-X2

P(VAc-*stat*-VPi)-X2 samples of targeted molar masses around 9 kg mol^{-1} and varying VAc:VPi molar ratios ranging from 30:70 to 60:40 were synthesised using RAFT polymerisation. Statistical copolymers with molar mass close to 10 kg mol^{-1} and VAc:VPi molar ratios around 50:50 have shown the best compromise between solubility and stabilising ability in previous studies

carried out in our group on dispersion polymerisation of NVP in scCO₂. These copolymers were therefore chosen for this project.²⁰

Reactions were carried out in bulk and stopped when approximately 60% conversion was reached to ensure low dispersity values and thus maximize dithiocarbonate end retention for further optimum chain extension with NVP. Higher conversions result in higher viscosities and increase the probability of irreversible termination side reactions due to the decrease of monomer concentration. The characterization results are shown in **Table 4**.

Table 4: Key parameters of P(VAc-stat-VPi)-X2 copolymer stabilisers synthesised by RAFT polymerisation in bulk at 60°C for 5 hours.

Entry	Feed ratio ^a	Expt. Ratio ^b	M_n theor kg·mol ⁻¹ c	Conv. % ^d	RAFT end % ^e	M_n NMR kg·mol ⁻¹ f	M_n SEC kg·mol ⁻¹ g	\bar{D}	T_g °C
A1	30:70	23:77	9.8	65	60	10.8	8.3	1.22	37.9
A2	40:60	39:61	8.8	63	55	9.2	8.4	1.25	41.4
A3	50:50	46:54	8.5	61	57	9.5	10.0	1.20	40.9
A4	60:40	57:43	8.4	60	50	8.3	10.0	1.17	45.2
A5	60:40	54:46	9.0	60	40	9.1	11.5	1.13	44.0

a: Theoretical VAc:VPi molar ratios.

b: Experimental VAc:VPi molar ratios calculated by NMR.

c: Theoretical molar mass calculated from conversion.

d: Conversion of the crude sample calculated by NMR by comparing monomer and polymer resonances.

e: Livingness of the chains calculated from end group analysis by NMR comparing polymer chain end and main chain resonances.

f: Experimental molar mass calculated from end group analysis by NMR comparing polymer chain end and main chain resonances.

g: Experimental molar mass calculated by SEC in DMF using PMMA standards.

^1H NMR was used to confirm the structure of the polymer and to calculate conversion, molar mass, VAc:VPi molar ratios and the livingness of the chains.

All products show low dispersity (<1.25), and good agreement between theoretical and experimental molar mass values.

It is important to note that in all cases the VAc:VPi experimental molar ratio is lower than the expected one. This can be explained by looking at the reactivity ratios of both monomers. Considering M_1 and M_2 two monomers, the reactivity ratio, r , is the ratio between the rate a propagating macro-radical terminated with a M_1 unit, M_1^\bullet , adds to more monomer M_1 , to the rate at which it adds to a second monomer M_2 (**Figure 52**).

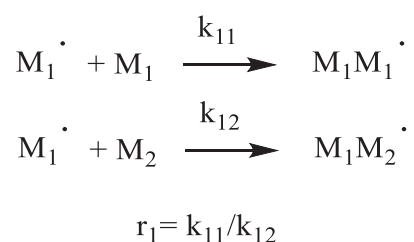


Figure 52: Monomer addition reactivity ratio.

When reactivity ratios of two monomers are similar and close to 1, the copolymerisation of both results in random copolymers. This is the case of vinyl acetate and vinyl pivalate which have reported reactivity ratios of 0.79 and 0.96 respectively for a copolymerisation at 60°C in bulk.¹⁵⁴ The slightly higher reactivity ratio of vinyl pivalate, explained by the *tert*-butyl group in VPi (**Figure 53**) that increases the electron density making it more reactive

towards radical attack, explains the higher VPi content in all the copolymer samples.

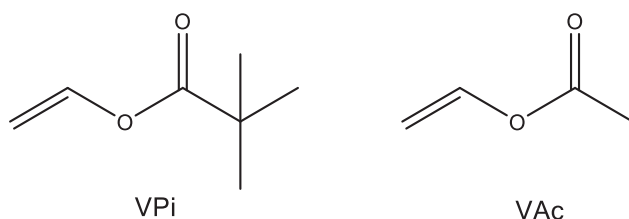


Figure 53: Vinyl acetate (right) and vinyl pivalate (left) chemical structure.

Since the aim is to make a library of copolymers with different VAc:VPi ratios to study their behavior in scCO₂, this is not necessarily a negative outcome.

The difference between molar masses obtained by NMR and SEC can be explained by the inadequacy of the PMMA calibration used for the latter technique and the difference in the hydrodynamic volume of P(VAc-*stat*-VPi)-X₂ and PMMA standards.

The glass transition is a reversible transition of the polymer from a glassy state to a rubber-like state. Glass transition temperature, T_g , gives an idea of the polymer chain flexibility which also has an impact on its solubility in CO₂. T_g values are in agreement with previous results published in our group for very similar polymers.²⁰

VAc:VPi ratios were calculated by comparison of the peaks b, c and d (**Figure 54**). Example from **Table 4 entry A2**. In this case it is also necessary to subtract the residual amount of VPi monomer, given by the peak at 7.3 ppm.

$$\text{VPi (9H from } ^t\text{Bu)} = I_b/9 = 601/9 = 67.7$$

$$5\text{VAc (3H from CH}_3 + 2\text{H from CH}_2) + 2\text{VPi (2H from CH}_2) = I_c = 354$$

$$5VAc + 2 \times 67.7 = 354 \rightarrow VAc = 43.72$$

$$\% VAc = [VAc / (VAc + VPi)] \times 100 = [43.72 / (43.72 + 67.7)] \times 100 = 39\%$$

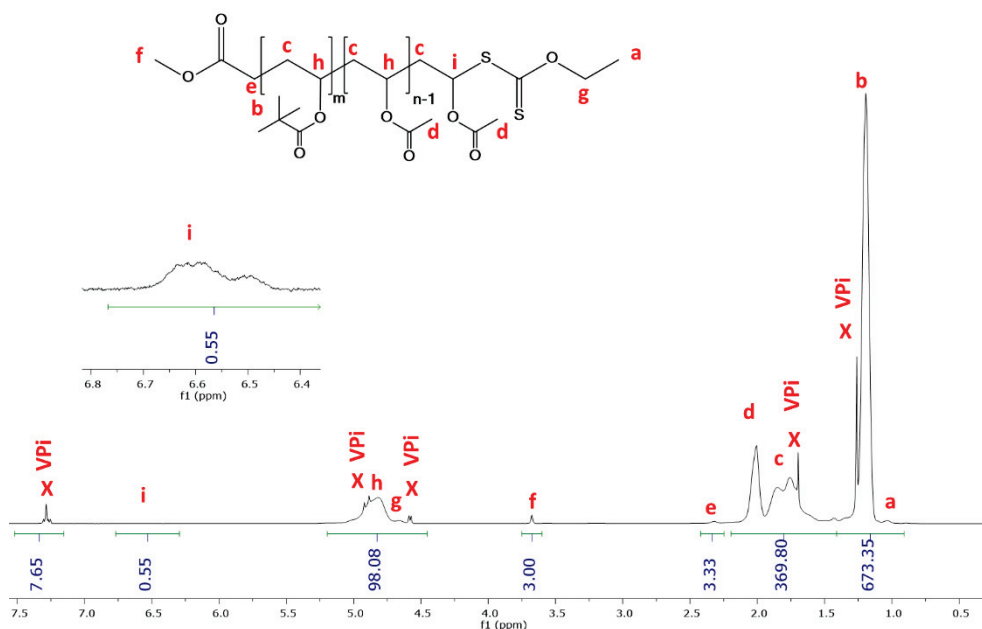


Figure 54: 1H NMR of $P(VAc\text{-}stat\text{-}VPi)$ in $CDCl_3$ (256 scans). The last monomer unit attached to the sulfur can be either a VAc or VPi unit. Residual VPi signals are marked with an X 1.3, 1.7, 4.6 and 5 ppm)

Molar mass was calculated from the degree of polymerisation obtained from the integration of the resonance h when calibrating signal f to 3 and subtracting the amount of residual VPi given by the signal at 7.3 ppm.

Resonances at 4.9, 2.0, 1.8 and 1.2 ppm correspond to the protons of vinyl acetate (c , d , h) and vinyl pivalate (b , c , h) units. The signal at 3.67 ppm corresponds to the protons from the dithiocarbonate end from the xanthate. The signal at 6.60 ppm (f) corresponds to the methine protons of the last monomer unit adjacent to the dithiocarbonate chain end and therefore has a much higher chemical shift than the rest of the units. Its shape is less defined than in **Figure 49** since this unit can be either VAc or

VPI. The integral of this signal can be used to determine the percentage of the polymer chains that retain the dithiocarbonate living end. Consequently, the closer this value is to one, the higher percentage of living chains we have, in this case 57%.

All samples have a RAFT end functionality much lower than expected (**Table 4**). This could dramatically affect the synthesis of the second block. A possible explanation has to do with the inaccuracy of integration of the resonances for higher molar mass polymers. In **Figure 54**, the signal used for integration (*i*) corresponds to a single proton in a long chain of 99 units (i.e. 99 protons) in this case, which could make this integration less accurate due to a low signal/noise ratio, therefore giving a lower value than the real one.

The RAFT end functionality of the samples made was further tested by chain extending them with a second monomer, NVP, in order to make P(VAc-*stat*-VPI)-*block*-PNVP block copolymers.

3.3.3 Synthesis of P(VAc-*stat*-VPI)-*block*-PNVP block copolymers

P(VAc-*stat*-VPI)-*block*-PNVP block copolymers were synthesised as previously discussed by chain extension of the P(VAc-*stat*-VPI) macro-RAFT agents (**Figure 55**).

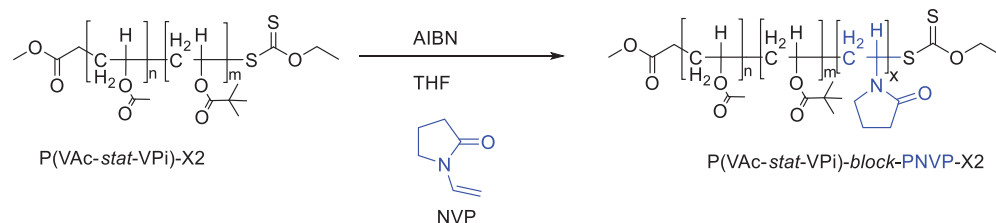


Figure 55: Chain extension scheme of $P(\text{VAc-stat-VPI})\text{-X2}$ with NVP .

The number-average degree of polymerisation (DP_n) is defined as the average number of structural units per polymer chain and can be calculated using **Equation 3**, knowing the molar mass of the polymer, RAFT agent and monomer. The characterisation results are shown in **Table 5**.

$$\text{DP} = \frac{M_n \text{ polymer} - M_w \text{ RAFT}}{M_w \text{ monomer}} \quad (3)$$

Equation 3: Degree of polymerisation calculation.

The determination of the conversion of the crude sample by NMR was not possible in this case due to overlapping signals. All samples show the expected increase in the molecular mass measured both from NMR and SEC and dispersity values are below 1.5 in most cases, indicating good control. Glass transition temperatures show an increase with respect to the starting macro-RAFT agents (**Table 5**). This is probably better shown when looking at the chromatograms obtained after size exclusion chromatography with DMF as eluent (**Figure 56**). For samples coming from the same macro-RAFT agent we can see a shift in the retention time towards lower values with increasing the number of NVP units, which indicates an increase in the molar mass.

Furthermore, there is a broadening of the peaks (higher Đ) when the DP of PNVP block increases, which could indicate a lack of control of the

polymerisation. In particular, this broadening is visible on the low molar mass side showing that a proportion of the starting macro-RAFT has probably not been chain extended. However, most of the samples maintain dispersity values below 1.5. These results match those found by NMR. All results together confirm the formation of the block copolymers.

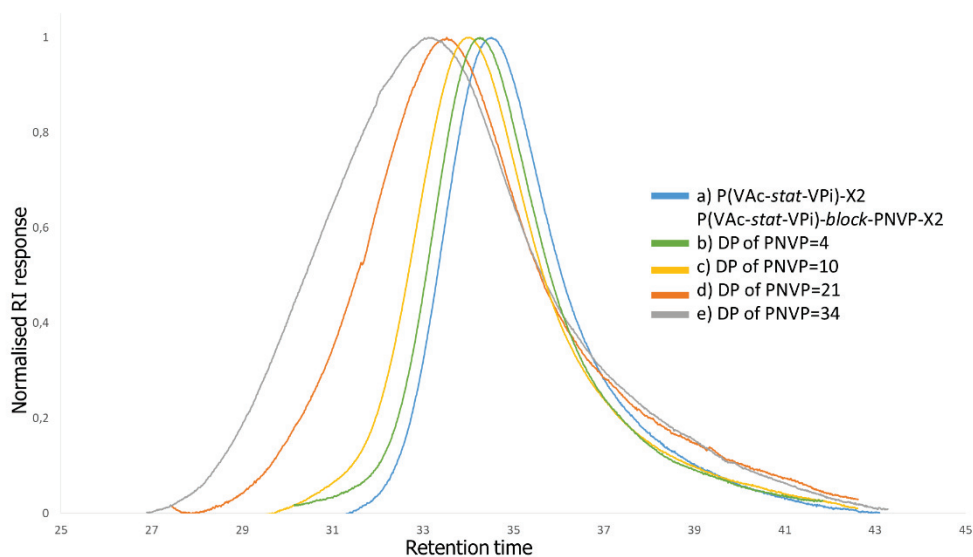


Figure 56: SEC trace overlay of a) *P(VAc-stat-VPI)-X2* (Table 4, A2) and its *P(VAc-stat-VPI)-block-PNVP* block copolymers with increasing DP of PNVP, b) DP of PNVP= 4 (Table 5, B5), c) DP of PNVP= 10 (Table 5, B8), d) DP of PNVP= 21 (Table 3, B11) and e) DP of PNVP= 34 (Table 5, B13).

Table 5: Key parameters of *P*(VAc-stat-VPi)-block-PNVP blocks synthesised by RAFT polymerisation in THF at 60°C for 3-5 hours.

Entry	Macro-RAFT ^a	M_{nNMR} kg mol ⁻¹ ^b	M_{nSEC} kg mol ⁻¹ ^c	DP PNVP target	DP PNVP _d	\bar{D}	T _g °C
B1	A1	11.2	12.0	5	4	1.21	43.2
B2	A4	8.7	11.0	5	4	1.17	46.8
B3	A5	9.5	12.4	5	4	1.20	44.1
B4	A3	9.9	10.7	5	3	1.22	48.0
B5	A2	9.6	12.0	5	4	1.16	52.1
B6	A5	9.9	12.9	12	7	1.20	46.6
B7	A3	10.4	10.9	12	8	1.28	46.4
B8	A2	10.3	9.4	12	10	1.39	52.3
B9	A5	10.9	13.6	25	16	1.24	48.6
B10	A3	11.7	11.3	25	20	1.48	47.4
B11	A2	11.5	8.8	25	21	1.70	49.9
B12	A3	13.2	12.7	37	33	1.50	47.0
B13	A2	12.9	10.0	37	34	1.80	55.3

a: Macro-RAFT agent used, key parameters shown in Table 1.

b: Molar mass calculated from NMR by comparison of *N*-vinyl pyrrolidone unit resonance in the polymer versus vinyl acetate and vinyl pivalate unit resonance.

c: Molar mass calculated from SEC using DMF as solvent and PMMA calibration standards.

d: Degree of polymerisation calculated by integration of the NVP repetitive unit resonances and the resonance of the VAc and VPi units.

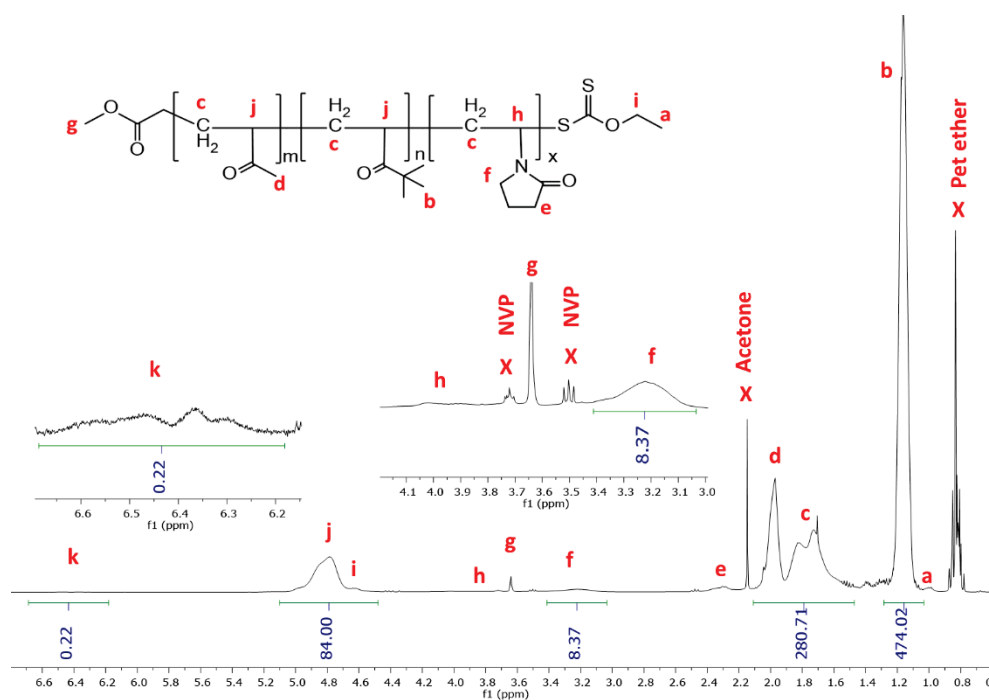


Figure 57: ^1H NMR of $\text{P(VAc-stat-VPI)-block-PNVP}$ in CDCl_3 (256 cans). DP of PNVP is calculated by comparing resonances f and j , knowing the molar mass and DP of the starting material and assuming all starting chains extend. The signals at 3.5 and 3.7 ppm correspond to residual N -vinyl pyrrolidone and the signals at 0.9 and 2.17 ppm to residual petroleum ether from precipitation and acetone respectively.

The analysis of the block copolymers by ^1H NMR shows signals at 4.8, 2.3, 1.8 and 1.2 ppm that correspond to the vinyl acetate (j , c , d) and vinyl pivalate (j , c , b) units, while signals at 4.8, 3.2 and 2.4 ppm belong to the N -vinyl pyrrolidone unit. Signals at 4.6, 3.7 and 1.0 ppm correspond to the dithiocarbonate chain ends coming from the RAFT agent. It is thought that the signal between 6.2 and 6.7 ppm (k) belongs to $\text{P(VAc-stat-VPI)-X}_2$ chains that have not extended with NVP (**Figure 54, signal i**).

The RAFT functionality of the block copolymers cannot be calculated since the resonance of the methine proton of the last NVP unit adjacent to the dithiocarbonate chain end is believed to appear around 4.6 ppm from previous experiments and is therefore covered by other signals.

The presence of resonances from PNVP and P(VAc-*stat*-VPi)-X2 and the single population of chains obtained by SEC, the molar mass of which increases with the targeting PNVP polymerization degree, is consistent with the formation of a P(VAc-*stat*-VPi)-*block*-PNVP-X2 block copolymer. However, some of the starting macro RAFT does not seem to be chain extended. As a result, chain extended chains may exhibit a higher DP of PNVP than targeted.

3.3.4 Phase behavior in scCO₂

The solubility of the samples in **Table 5** (entries B1-B12) was measured using a hydraulic variable volume view cell. Both the cell and the cloud point experiment are described in detail in chapter 2. Cloud point measurements at different temperatures resulted in cloud point curves.

The results of the study of different parameters that affect CO₂ solubility are presented and discussed.

3.3.4.1 Influence of the composition of the CO₂-philic block on the cloud points

A series of cloud point experiments were carried out over a range of VAc:VPi molar ratios in order to study the influence of this parameter on the solubility of these materials. For this set of measurements the DP of PNVP in the second block was kept constant at 4 and the molar mass of the block copolymers was kept constant close to 10 kg mol⁻¹. MMA was used as a co-

solvent to reproduce dispersion polymerisation conditions (15 wt% MMA with respect to CO₂).

Figure 58 shows an increase in the cloud point pressure (therefore a decrease in solubility) with increasing VAc content in the polymer. This agrees with previously published results for the statistical copolymers.¹¹⁶ The cloud point curve of polydimethyl siloxane macromonomer (PDMS-MA), a highly soluble stabiliser very commonly used in dispersion polymerisation of MMA, is shown for comparison.

All samples are soluble in scCO₂ at dispersion polymerisation conditions (35°C, 276 bar). These data show that the solubility can be slightly tuned by optimising the molar ratios of VAc and VPi.

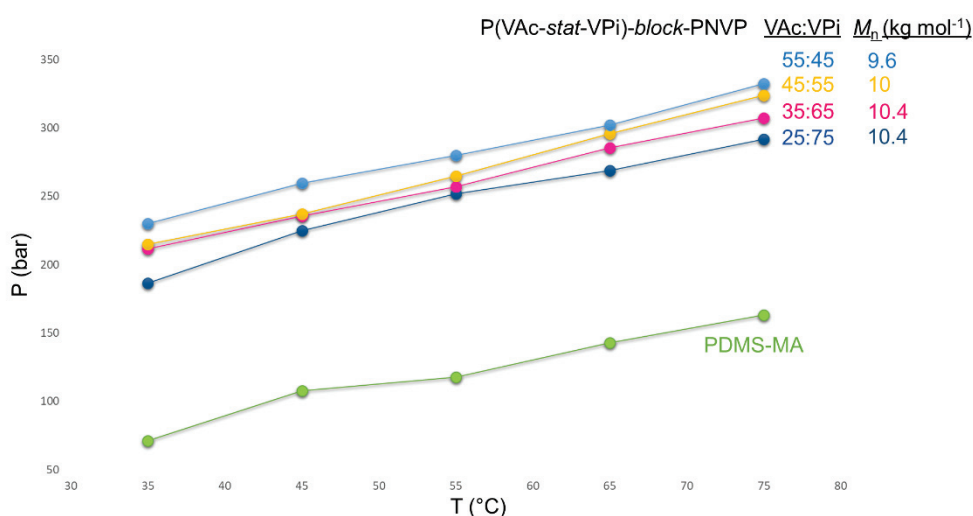


Figure 58: *P-T* diagram of *P*(VAc-stat-VPi)-block-PNVP samples with a DP of PNVP 4, molar mass around 10 kg mol⁻¹ and varying VAc:VPi molar ratios and similar molar mass, versus PDMS-MA in scCO₂. a) PDMS-MA of 10 kg mol⁻¹ molar mass. b) *P*(VAc-stat-VPi)-block-PNVP **Table 3, B1**. c) *P*(VAc-stat-VPi)-block-PNVP **Table 3, B5**. d) *P*(VAc-stat-VPi)-block-PNVP **Table 3, B4**. e) *P*(VAc-stat-VPi)-block-PNVP **Table 3, B3**.

3.3.4.2 Influence of the degree of polymerisation of the PNVP polymer-philic block on the cloud points

A different set of cloud point measurements was carried out to study the influence of the DP of the second PNVP block on the solubility of these copolymers. Although a VAc:VPi molar ratio of 25:75 has shown the highest solubility, molar ratios were kept constant at 35:65 for this experiment, for sample availability reasons. The goal here is not to make the most soluble polymer but to study the influence of the DP of PNVP.

The VAc:VPi molar ratio will greatly affect the stabilising ability of the material since the second block is thought to act as polymer-philic group, and therefore as the anchoring group for stabilising the particles during dispersion polymerisation. Hence it is necessary to determine the DP limit for the blocks to remain soluble in dispersion polymerisation conditions while optimising its interaction with the targeted PMMA particles. **Figure 59** shows the increase in the cloud point pressures when adding a second block. Cloud point curve of PDMS-MA and of the CO₂-philic block are shown for comparison.

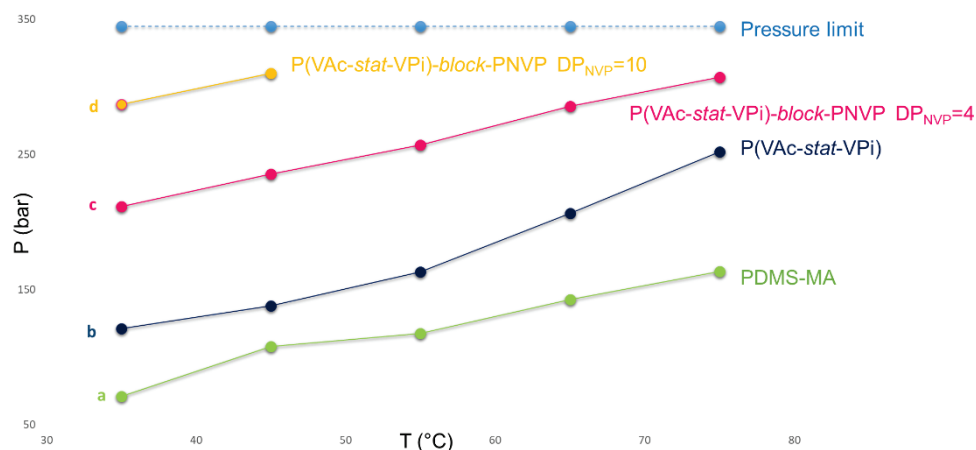


Figure 59: P-T diagram of a) PDMS-MA of 10 kg mol⁻¹ molar mass, b) P(VAc-stat-VPI) of 8.8 kg mol⁻¹ and VAc:VPi molar ratio of 35:65 (**Table 2, entry A2**), c) P(VAc-stat-VPI)-block-PNVP of 9.2 kg mol⁻¹, VAc:VPi molar ratio of 35:65 and a DP of PNVP of 4 (**Table 3, entry B5**) and d) P(VAc-stat-VPI)-block-PNVP of 9.9 kg mol⁻¹, VAc:VPi molar ratio of 35:65 and a DP of PNVP of 10 (**Table 3, entry B8**)

As expected since PNVP is a CO₂-phobic polymer, adding a second block of PNVP to the statistical copolymer resulted in a very significant increase in the cloud point pressure and therefore in a decrease in solubility. The DP of the second block has much bigger impact than other parameters such as the molar mass or composition of the first block, so it will be the limiting parameter. The limit in the degree of polymerisation of NVP that allows the polymer to be fully soluble at 35°C and 276 bar would be 10 units for a VAc:VPi molar ratio of 35:65.

Determination of the solubility of longer blocks is not possible because the pressure values required to fully solubilise these samples would be outside of the operating pressure limits of the view cell.

It is also necessary to highlight that the DP of PNVP is expected to be higher than the reported one. As previously discussed, this is due to the fact that

not all of the chains have extended and it results in a substantial decrease of the solubility.

3.3.5 Dispersion polymerisation experiments

To get a good hand on the equipment, we first started to perform conventional dispersion polymerisation of MMA in scCO₂ in the presence of 5 wt. % PDMS-MA, a commercially available stabiliser (**Figure 60**). The experimental procedure has been previously detailed in the experimental part.

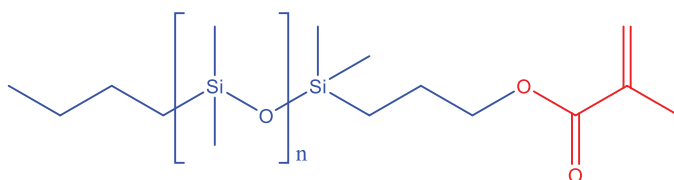


Figure 60. PDMS-MA chemical structure.

Upon optimisation of the setup time, a powder product was obtained and characterised by SEM (**Figure 61**). The picture shows spherical particles uniform in shape and size, which is consistent with the expected product.¹²⁵

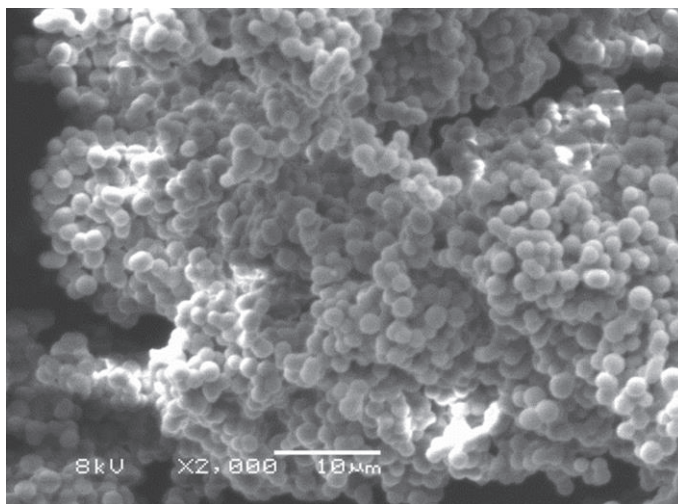


Figure 61: SEM analysis on PMMA particles using 5 wt % of PDMS-MA.

The stabilising ability of the block copolymers with a DP of PNVP of 4 was then investigated in the dispersion polymerisation of MMA in scCO_2 under the same conditions (**Table 6**). All reactions yielded aggregated products instead of the typical flowing powders obtained in successful dispersion polymerisation. In addition, full conversion was not reached.

SEC analysis of the products shows very low molar masses for the synthesis of PMMA (**Table 6**), which is far from the values expected for this kind of process in the range of 100 to 300 kg mol^{-1} .¹⁵⁵ This suggests that precipitation takes place instead of the expected dispersion. Varying the VAc:VPi molar ratios in the stabiliser does not seem to have any effect in the polymerisation.

Table 6. Key parameters of PMMA products made by dispersion polymerisation in $scCO_2$ at 35°C and 276 bar using block copolymers of varying VAc:VPi ratios.

Entry	Stabiliser ^a	Stabiliser VAc:VPi molar ratios	Stabiliser DP PNVP	Product M_n (SEC) ^b kg mol ⁻¹	Product \bar{D}
1	B4	55:45	4	12	1.90
2	B1	35:65	4	11	2.60
3	B2	46:54	4	18	1.85

a: Stabiliser used in the dispersion polymerisation, key parameters are shown in Table 4.

b: Molar mass calculated by SEC in chloroform, using PMMA calibration standards.

Scanning electron microscopy was used to analyse the product morphology (Figure 62). None of the SEM images shows any defined morphology. This along with the SEC results suggests a total lack of stabilisation.

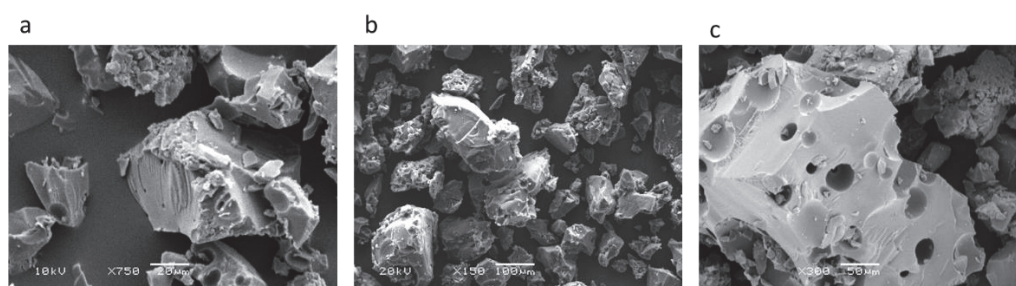


Figure 62: SEM analysis on PMMA samples using 5 wt% of block copolymers with varying VAc:VPi ratios. a) Table 6, entry 1. b) Table 6, entry 2. c) Table 6, entry 3.

The next step was to try stabilisers with higher DP of PNVP segment and study how this parameter affected the dispersion reaction (Table 7).

Although traditionally it is believed that insoluble stabilisers lead to particle agglomeration and therefore unsuccessful dispersion polymerisations,¹²⁸ the use of only partially soluble stabilisers has also been reported.¹⁵⁶ Hence,

a partially soluble stabiliser with a DP of PNVP of 21 (**Table 7, entry 3**) was also used in this experiment.

Table 7: Key parameters of PMMA products made by dispersion polymerisation in scCO₂ at 35°C and 276 bar using block copolymers of increasing DP of PNVP.

Entry	Stabiliser ^a	Stabiliser VAc:VPi molar ratios	Stabiliser DP PNVP	Product M_n (SEC) ^b kg mol ⁻¹	Product \bar{D}
1	B1	35:65	4	11	2.60
2	B7	34:66	10	11	2.70
3	B10	35:65	21	13	2.19

a: Stabiliser used in the dispersion polymerisation, key parameters are shown in Table 2.

b: Molar mass calculated by SEC in chloroform, using PMMA calibration standards.

Molar masses calculated with SEC are again much lower than expected, and

SEM evidences the lack of morphology (**Figure 63**).

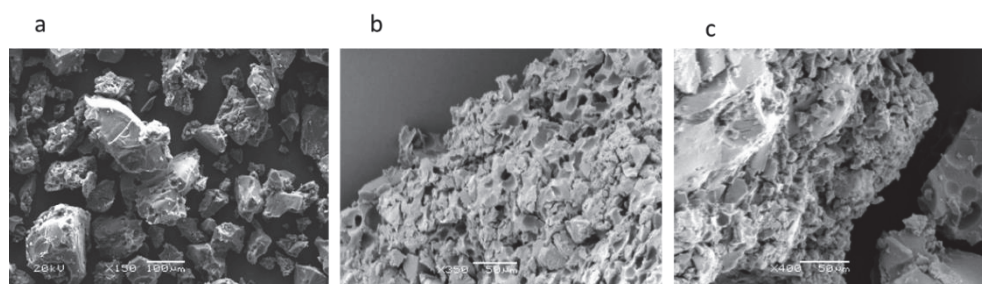


Figure 63: SEM analysis on PMMA samples using 5 wt % of block copolymers with increasing DP of PNVP segment. a) Table 7, entry 1. b) Table 7, entry 2. c) Table 7, entry 3.

We can therefore conclude that the DP of PNVP segment has no effect on the stabilisation for the samples that we used.

The failure of these macromolecules to ensure stabilisation during the dispersion polymerisation process may be related to the way they are

synthesised. As mentioned above, it is possible that the starting macro-RAFTs have lost part of their RAFT functionality or that other side reactions are taking place contaminating the sample. Other variables such as reagent purity, stirring speed and faults in the equipment were previously ruled out by performing a dispersion polymerisation with a commercial stabiliser.

In order to test the performance of our stabilisers, they were used in dispersion polymerisation of NVP, a monomer that has been previously reported to work with P(VAc-*stat*-VPi)-X1 stabilisers.¹¹⁶ A powder product was obtained. The SEM image of this samples shows spherical morphology, however the particles are neither well defined nor homogeneous in size (**Figure 64, I**). Most importantly, they do not match the results for dispersion polymerisation of this monomer using previous P(VAc-*stat*-VPi)-X1 stabilisers of very similar M_n and composition (**Figure 64, II**).

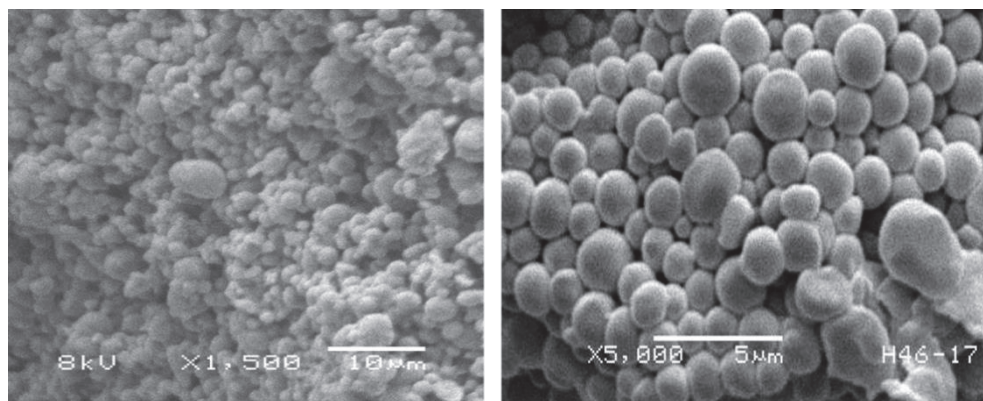


*Figure 64: SEM analysis on PNVP particles (I) using 5 wt % of P(VAc-*stat*-VPi)-block-PNVP (Table 3, Entry 1), (II) using 5 wt % P(VAc-*stat*-VPi)¹.*

This confirms that there actually is an issue with the RAFT synthesis of the stabilisers that has already been pointed out.

3.4 Conclusions

This chapter has shown that it is possible to synthesise P(VAc-*stat*-VPi)-*block*-PNVP block copolymers using RAFT/MADIX polymerisation with VAc:VPi molar ratios ranging between 25:75 and 55:45 and degree of polymerisation of the PNVP block between 4 and 30. SEC and ^1H NMR showed that not 100% of the starting macro RAFT chain extended to form the block copolymers, however products showed dispersities below 1.5 in all cases.

Furthermore, T_g values are in agreement with previous data reported for this type of polymers and they show an increase for the block copolymers compared to the statistical ones.

The solubility of our block copolymers in scCO_2 has been evaluated by measuring the cloud points using a variable volume view cell designed at The University of Nottingham. All samples were found soluble up to a degree of polymerisation of NVP of 10 units at dispersion polymerisation conditions (35 °C, 276 bar, 5 wt %). The solubility is thought to be greatly affected by the DP of PNVP, which might be higher than the calculated one.

However, these materials have not been able to produce PMMA particles with spherical morphology nor do they match the performance of previous stabilisers in the dispersion polymerisation of NVP. This suggests an underlying issue with the way they are synthesised and the purity of the samples that has already been pointed out and will be discussed in future chapters.

Chapter 4: In-depth study of RAFT polymerisation of vinyl acetate, vinyl pivalate and *N*-vinyl pyrrolidone

This chapter addresses different issues that arise from using RAFT polymerisation, such as the livingness of the polymers described in chapter 3. Head to head addition reactions and its occurrence in RAFT are be discussed in detail.

4.1 Introduction

The mechanism of the RAFT process has been thoroughly discussed in previous chapters as well as other considerations such as the RAFT agent choice, the monomer compatibility, or the different possible architectures that this technique allows.

The synthesis of *P(VAc-stat-VPI)-block-PNVP-X2* has been discussed in Chapter 3. However, the application of these materials in dispersion polymerisation processes has not been as successful as expected, which has raised some questions about their purity and the RAFT polymerisation process itself.

In order to answer these questions, an in-depth study of RAFT polymerisation of the monomers involved becomes necessary.

4.1.1 Block copolymer synthesis by RAFT polymerisation

The formation of defects and side products during the synthesis of block copolymers by RAFT polymerisation is inevitable. All of them have been discussed in detail by Keddie (**Figure 65**).⁵¹

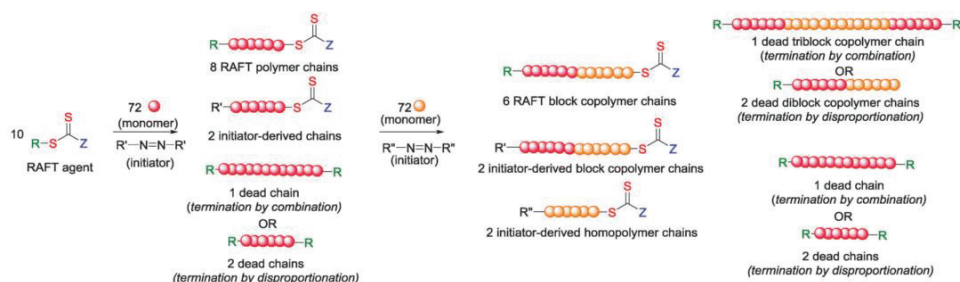


Figure 65: The various polymer species formed during synthesis of block copolymers via stepwise RAFT polymerisation. Reproduced from reference⁵¹ with permission of The Royal Society of Chemistry.

The first one of them is the generation of initiator derived chains, as opposed to the ones generated from the R group of the RAFT agent. This happens both in the synthesis of the homopolymer and the block copolymer, and it can be minimised by lowering the initiator concentration.

The second defect is the formation of dead chains by irreversible radical termination, either by combination or disproportionation. Dead chains cannot chain extend and remain as an impurity in the subsequent reaction steps. This defect can be reduced substantially both by lowering the initiator concentration and the conversion to about 60%.

In addition, during the synthesis of the block copolymer, some monomer can form a homopolymer rather than being incorporated into the macro-RAFT to form the block. This is favoured when the livingness of the macro-RAFT is low.

All these defects together can decrease the purity of the materials and contribute to an increase in the dispersity. In addition and in the particular context of this work, the formation of these side polymeric populations may strongly impact the efficiency of our stabilisers in dispersion polymerisation. Although the reaction conditions used to synthesise the polymers in chapter 1 (60% conversion, 10:1 RAFT to initiator molar ratios) are already designed to minimise these defects, it is necessary to study the reactions in more detail and analyse them using different techniques such as NMR and SEC using RI and UV detectors. In order to make the analysis easier low molar mass polymers will be synthesised.

Furthermore, different reaction parameters will be tested, such as temperature, conversion and molar mass of the polymer to reduce the formation of defects and achieve better quality materials.

4.2 Experimental

4.2.1 Materials

Vinyl acetate (VAc, 99%, with hydroquinone as inhibitor) was purchased from Sigma Aldrich. *N*-vinyl pyrrolidone (NVP, 99%, stabilised with NaOH) and vinyl pivalate (VPi, 99%, with hydroquinone as inhibitor) were purchased from Acros. 2,2'-Azobis(2-methylpropionitrile (AIBN, 98%) was purchased from Sigma Aldrich and 2,2'-Azobis(4-methoxy-2,4-dimethylvaleronitrile (V-70) from Wako. All reagents were used without further purification. The

xanthate RAFT agent (*O*-ethyl-*S*-(1-methoxycarbonyl) ethyl dithiocarbonate) (Xanthate X2) was synthesised as described in Chapter 3.

4.2.2 Synthesis of low M_n PVAc-X2

VAc (10 g, 0.12 mol), AIBN (21mg, 0.13 mmol) and the RAFT agent Xanthate X2 (249mg, 1.28 mol) were added into round bottom flask with a stirring bar and degassed for 30 minutes in an ice bath. The mixture was then heated to 60°C for 180 minutes. A conversion of 55% was reached. The product was precipitated into cold petroleum ether and dried under reduced pressure. $M_{n\text{theor}} = 4.4 \text{ kg mol}^{-1}$, $M_{n\text{NMR}}(\text{CDCl}_3) = 4.6 \text{ kg mol}^{-1}$, RAFT functionality (NMR)= 53%, $M_{n\text{SEC}}(\text{THF}) = 6.5 \text{ kg mol}^{-1}$, $D = 1.05$.

Low M_n PVPI-X2, P(VAc-*stat*-VPI)-X2 and PNVP-X2 were synthesised using the same procedure.

4.2.3 Chain extension of low M_n PVAc-X2 with VAc

Low M_n PVAc-X2 (1.7 g, 0.37 mmol, $M_{n\text{NMR}} = 4.6 \text{ kg mol}^{-1}$) was dissolved in VAc (3 g, 0.03 mol) in a schlenk flask with a stirring bar. AIBN (5.3 mg, 0.03 mmol) and 1,3,5-trioxane (1.06 g, 0.01 mol) were added. The mixture was degassed for 30 minutes in an ice bath and then heated and stirred at 60°C for 180 minutes. Samples were withdrawn at $t = 0, 60, 120$ and 180 minutes and they were precipitated in cold petroleum ether and dried under reduced pressure after calculating conversion. Results are summarised in Table 8.

Low M_n PVPI-X2, P(VAc-*stat*-VPI)-X2 and PNVP-X2 were chain extended using the same procedure

4.2.4 Synthesis of low conversion PVAc-X2

VAc (2g, 0.02 mol), AIBN (21mg, 0.12 mmol) and RAFT agent X2 (249mg, 1.28 mmol) were added into a round bottom flask with a stirring bar and degassed for 30 minutes in an ice bath. The mixture was then heated to 60°C for 110 minutes. The product was precipitated into cold petroleum ether and dried under reduced pressure. $M_{n\text{theor}} = 4 \text{ kg mol}^{-1}$, 22% conversion, $M_{n\text{NMR}} = 3.3 \text{ kg mol}^{-1}$, $M_{n\text{SEC(THF)}} = 4.5 \text{ kg mol}^{-1}$, $D = 1.08$

Low conversion PVPI-X2 and P(VAc-*stat*-VPI)-X2 were synthesised using the same procedure.

4.2.5 Chain extension of low conversion PVAc-X2 with VAc

Low conversion PVAc (130 mg, 0.04 mmol) was dissolved in VAc (715 mg, 8.31 mmol) in a glass vial with a stirring bar. AIBN (3.6 mg, 0.02 mmol) and 1,3,5-trioxane (125 mg, 1.39 mmol) were added and the vial was sealed and degassed with argon for 30 minutes in an ice bath. The mixture was then heated at 60°C and stirred for 150 minutes. The product was precipitated into cold petroleum ether and dried under reduced pressure. $M_{n\text{theor}} = 10.5 \text{ kg mol}^{-1}$, 18% conversion, $M_{n\text{NMR}}(\text{CDCl}_3) = 8 \text{ kg mol}^{-1}$, $M_{n\text{SEC(THF)}} = 10 \text{ kg mol}^{-1}$, $D = 1.10$.

Low conversion PVPI-X2 and P(VAc-*stat*-VPi)-X2 were chain extended using the same procedure.

4.2.6 Synthesis of low temperature PVAc-X2

VAc (10 g, 0.11 mol), V-70 (40mg, 0.13 mmol) and RAFT agent X2 (249mg, 1.28 mmol) were added into a round bottom flask with a stirring bar and degassed for 30 min in an ice bath. The mixture was then heated to 35°C for 110 minutes. The product was precipitated into cold petroleum ether and dried under reduced pressure. $M_{n\text{theor}} = 3.4 \text{ kg mol}^{-1}$, 43% conversion, $M_{n\text{NMR}}(\text{CDCl}_3) = 3.6 \text{ kg mol}^{-1}$, $M_{n\text{SEC}}(\text{THF}) = 4.5 \text{ kg mol}^{-1}$, $\bar{D} = 1.09$.

4.2.7 Chain extension of low temperature PVAc-X2 with VAc

Low temperature PVAc (800 mg, 0.22 mmol) was dissolved in VAc (3.77 g, 0.04 mol) in a glass vial with a stirring bar. V-70 (37 mg, 0.12 mmol) and 1,3,5-trioxane (675 mg, 7.49 mmol) were added and the vial was sealed and degassed with argon for 30 minutes in an ice bath. The mixture was then heated at 60°C and stirred for 150 minutes. The product was precipitated into cold petroleum ether and dried under reduced pressure. $M_{n\text{theor}} = 9.7 \text{ kg mol}^{-1}$, 30% conversion, $M_{n\text{NMR}}(\text{CDCl}_3) = 8.4 \text{ kg mol}^{-1}$, $M_{n\text{SEC}}(\text{THF}) = 10.5 \text{ kg mol}^{-1}$, $\bar{D} = 1.12$.

4.2.8 Synthesis of low conversion low temperature PVAc-X2

VAc (10 g, 0.12 mol), V-70 (20 mg, 0.06 mmol) and RAFT agent X2 (125 mg, 0.64 mmol) were added into a round bottom flask with a stirring bar and degassed for 30 min in an ice bath. The mixture was then heated to 35°C for 110 minutes. The product was precipitated into cold petroleum ether and dried under reduced pressure. $M_{n\text{theor}} = 4.2 \text{ kg mol}^{-1}$, 26% conversion, $M_{n\text{NMR}}(\text{CDCl}_3) = 3.7 \text{ kg mol}^{-1}$, $M_{n\text{SEC}}(\text{THF}) = 4.9 \text{ kg mol}^{-1}$, $\bar{D} = 1.05$.

4.2.9 Chain extension of low conversion low temperature PVAc-X2 with VAc

Low temperature low conversion PVAc (450 mg, 0.12 mmol) was dissolved in VAc (3.60 g, 0.04 mol) in a glass vial with a stirring bar. V-70 (18 mg, 0.06 mmol) and 1,3,5-trioxane (628 mg, 6.97 mmol) were added and the vial was sealed and degassed with argon for 30 minutes in an ice bath. The mixture was then heated at 60°C and stirred for 150 minutes. The product was precipitated into cold petroleum ether and dried under reduced pressure. $M_{n\text{theor}} = 11.7 \text{ kg mol}^{-1}$, 20% conversion, $M_{n\text{NMR}}(\text{CDCl}_3) = 10.8 \text{ kg mol}^{-1}$, $M_{n\text{SEC}}(\text{THF}) = 13 \text{ kg mol}^{-1}$, $\bar{D} = 1.15$.

4.3 Livingness of PVAc polymerisation

The kinetics of RAFT polymerisation has already been discussed in Chapter 1. All RAFT polymerisation reactions carried out using xanthate X2 were found to be controlled, according to the kinetic plots and dispersity data.

However, the end group analysis by ^1H NMR showed a low RAFT functionality. Whether these values represent reality or it is just a limitation of the NMR technique due to the macromolecular species was unclear.

4.3.1 Low M_n PVAc

In order to answer this, a model RAFT polymerisation of VAc was designed (**Figure 66**).

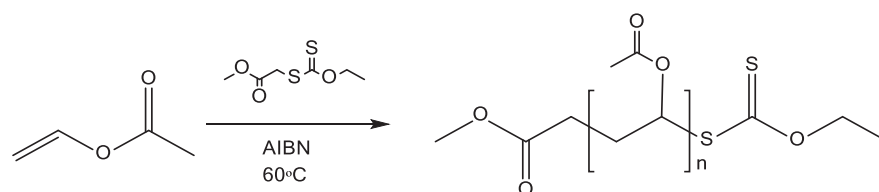


Figure 66: RAFT polymerisation of vinyl acetate

A conversion of 60% was achieved in 4 h. Removing one of the monomers (VPi) simplifies the ^1H NMR spectrum (**Figure 67**) and a target M_n of 4 kg mol^{-1} (instead of 10 kg mol^{-1}) simplifies the end group analysis.

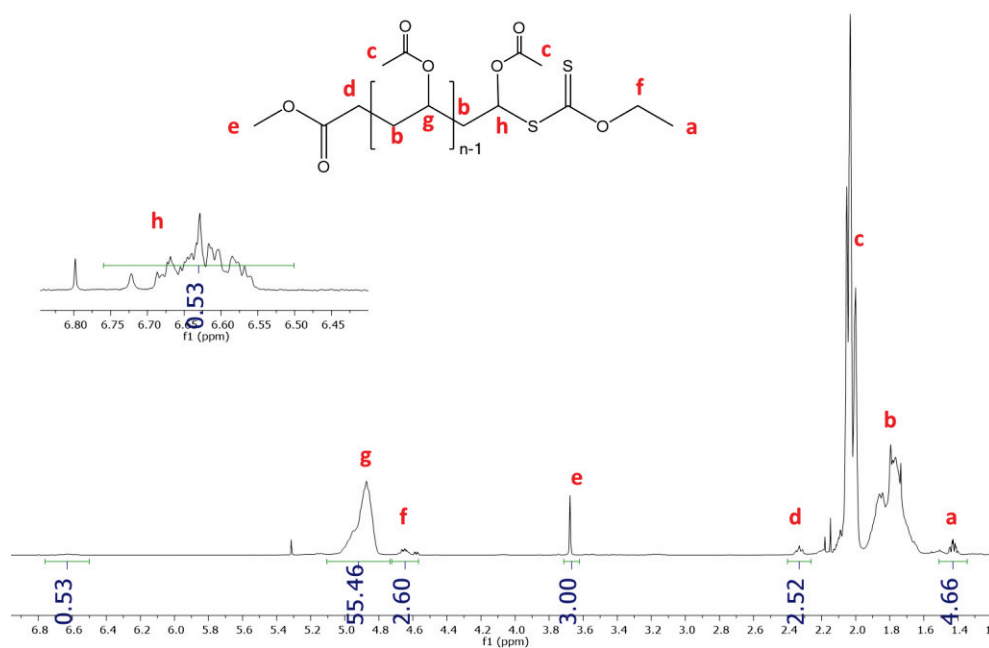


Figure 67: ^1H NMR of PVAc in CDCl_3 , 256 scans.

Signals that previously appeared overlapped in **Figure 54** (g and f, a and b) become clear, which allows a more accurate integration.

The RAFT functionality has been previously calculated in this thesis by integration of the signal at 6.65 ppm (signal h) that belongs to the methine proton in the last unit of the chain attached to the sulfur atom from the dithiocarbonate. This was due to the fact that it did not overlap with any other signals. Although this integral (h) appears to be low (53%), the integrals of the signals that belong to the ethoxy group at the same chain end (signals a and f) that also come from the dithiocarbonate, are close to the expected values, and determining the molar mass of the polymer gives a value (4.6 kg mol^{-1}) that is consistent with the expected one (4.4 kg mol^{-1}). This seems to indicate that it is more a limitation of the NMR technique than a lack of functionality.

In order to confirm this, the PVAc previously made was further chain extended with more VAc (**Figure 68**).

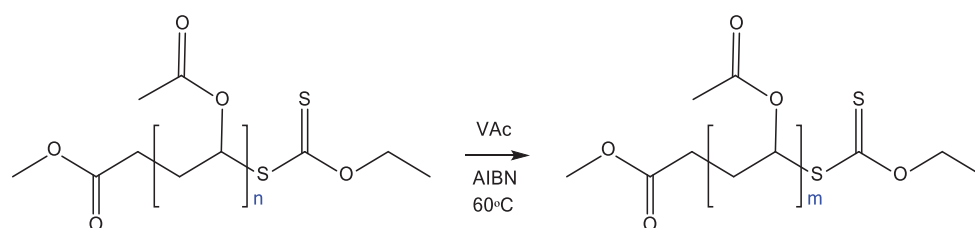


Figure 68: Chain extension of PVAc with VAc.

If all the PVAc chains were functional, they would all grow with monomer in a controlled manner, and hence a very clear shift in the SEC would be observed, corresponding with the increase in molecular weight. Samples were taken at different reaction times and the reaction was followed both by SEC and NMR. Results are summarized in **Table 8**.

Table 8: Key parameters of samples withdrawn at different times from the chain extension reaction of PVAc with VAc.

Entry	time	Conversion ^a	M_{nNMR} kg mol ⁻¹ ^b	RAFT Functionality % ^c	M_{nSEC} kg mol ⁻¹ ^d	\bar{D}
1	0	0	4.6	53	6.5	1.05
2	60	39	7.6	32	12	1.11
3	120	43	9.5	30	15.7	1.15
4	180	58	14.7	26	20	1.22

a: conversion of the crude sample calculated by ¹H NMR by comparing monomer and polymer resonances.

b: experimental molar mass calculated from end group analysis by ¹H NMR comparing polymer chain end and main chain resonances.

c: Livingness of the chains calculated from end group analysis by NMR comparing polymer chain end and main chain resonances.

d: experimental molar mass calculated by SEC in THF using PMMA standards.

Although there was an increase in the molecular weight with conversion, there also seemed to be a loss in the RAFT functionality determined by ^1H NMR. If these values represent the real ones or are a consequence of an inaccuracy in the integration due to the increase in molecular weight is unclear just by using this technique.

SEC (**Figure 69**) shows the expected shift in the molecular weight as the polymer grows and the M_n increases.

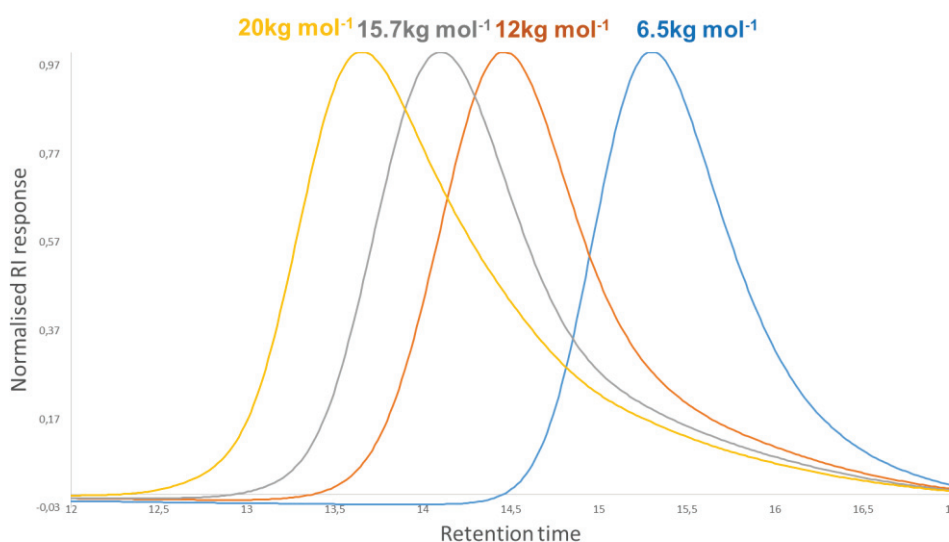


Figure 69: SEC RI chromatograph in THF of kinetic samples withdrawn at different times from PVAc chain extension reaction with VAc.

However, there is also a small overlap of the final polymer with the starting one, which indicates that not all of the chains are growing. This is also highlighted by the increase in the dispersity values and could be explained by a low RAFT functionality, which also agrees with the NMR results.

The RI detector in SEC does not differentiate between functional and non-functional polymer chains for a particular trace. However, since the RAFT

xanthate functionality of the polymer has a UV absorption at 290 nm, we can use SEC UV detection to determine if the chains we see in a particular trace are functional. Results are shown in **Figure 70**.

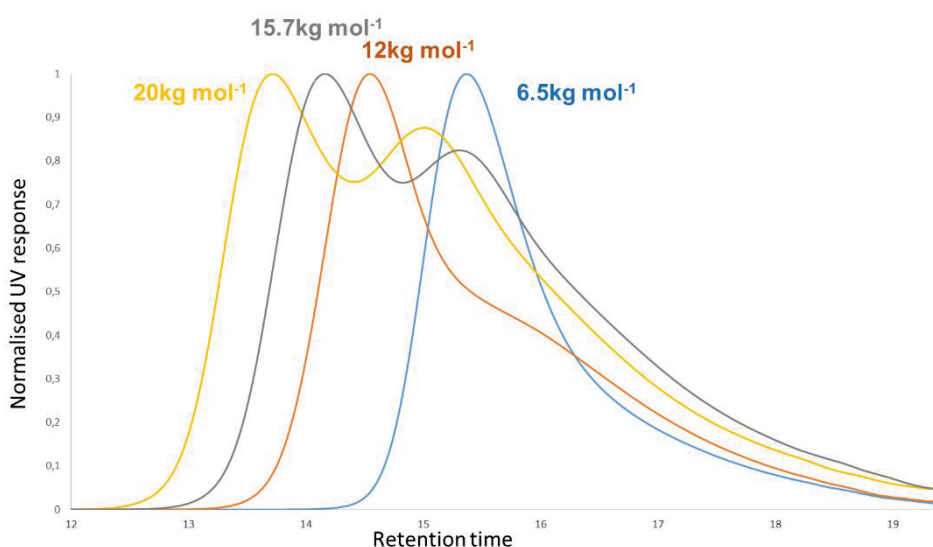


Figure 70: SEC UV chromatograph in THF of kinetic samples withdrawn at different times from PVAc chain extension reaction with VAc.

The same trend as in the RI is observed, there is an increase in the molecular weight and an overlap with the starting material that is much more obvious in this case. The reason for this is that the RI is dependent on the mass of the sample, so for the same number of chains high molar mass polymer chains have more representation in the trace than lower molar mass ones even if there is a significant number of the later ones. The UV, however, only looks at the RAFT functionality, so all the chains count the same in the trace independently of their molar mass and as long as their response coefficient to the detector is the same. This is why we observe a bigger peak for the low molecular weight material.

But what it really is interesting in this SEC is that, contrary to initial thoughts, the material that overlaps with the starting polymer is not dead material that has lost its functionality, but a functional polymer that has not grown.

4.3.1 Head to head addition

In order to fully understand what this undesired material was, a better understanding of the monomer addition mechanism in radical polymerisation was necessary. Flory *et al.* discussed this mechanism in free radical polymerisation of vinyl polymers.¹⁵⁷ They reported two possible addition modes, head to tail and head to head addition (**Figure 71**).

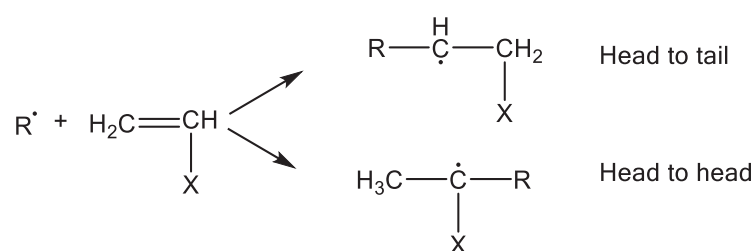


Figure 71. Head to tail and head to head monomer addition modes.

Head to tail addition happens when the propagating radical attacks the unsubstituted carbon of the monomer double bond. It is the most common addition mode because it is thermodynamically favoured. But the radical can occasionally attack the substituted carbon, in a head to head addition mode where the monomer is added to the chain in opposite orientation.

They accounted this head to head addition chains in 1.23% in moles for vinyl alcohol polymerisation at 25°C and 1.95% when the temperature was increased to 110°C.

Debuigne *et al.* also discussed the occurrence of head to head addition in the controlled radical polymerisation of vinyl acetate.¹⁵⁸ PVAc-CHOAc-CH₂-X chains formed from head to head addition have a stronger chemical bond with the control agent and are therefore much more difficult to reactivate. These chains grow at a lower rate than the others and this results in an increase of the dispersity values with conversion.

Matyjasewski and coworkers also reported the presence of head to head chains in the controlled radical polymerisation of vinyl acetate by degenerative transfer with alkyl iodides.¹⁵⁹ They found this defect to increase with conversion, with a proportion of 0.7% of head to head units at 17% conversion and 1% at 37% conversion.

Kamigaito and coworkers also investigated this issue in the synthesis of PVAc by Mn₂(CO)₁₀-induced RAFT polymerisation.¹⁶⁰ They identified head to head units using ¹H NMR and quantified them in 11% at 18% conversion and 90% at 93% monomer conversion. The accumulation of this less reactive chains was held responsible for the broadening of the molecular weight distributions.

More recently, Ladmiraal *et al.* reported the same observation when they were making PVAc-*block*-PVDF copolymers by RAFT polymerisation.¹⁶¹ They synthesised three different PVAc macro-CTAs of molar mass of 1.8, 10.1 and 8.5 kg mol⁻¹ using different reaction conditions and quantified 28, 90 and 67% of head to head terminated chains by ¹H NMR respectively.

They then used this macro-CTAs to make block copolymers with VDF and found that the quality of these was dependent on the amount of head to head chains in the CTA. Relatively well-defined block copolymers were obtained from the CTA with 28% head to head, while the other two yielded products with higher dispersities and quantities of PVDF homopolymer.

These results are in agreement with the previous literature and altogether they highlight the fact that head to head chains are re-initiated much more slowly or not re-initiated at all.

A more in-depth analysis of the ^1H NMR of our synthesised PVAc was then carried out (**Figure 72**).

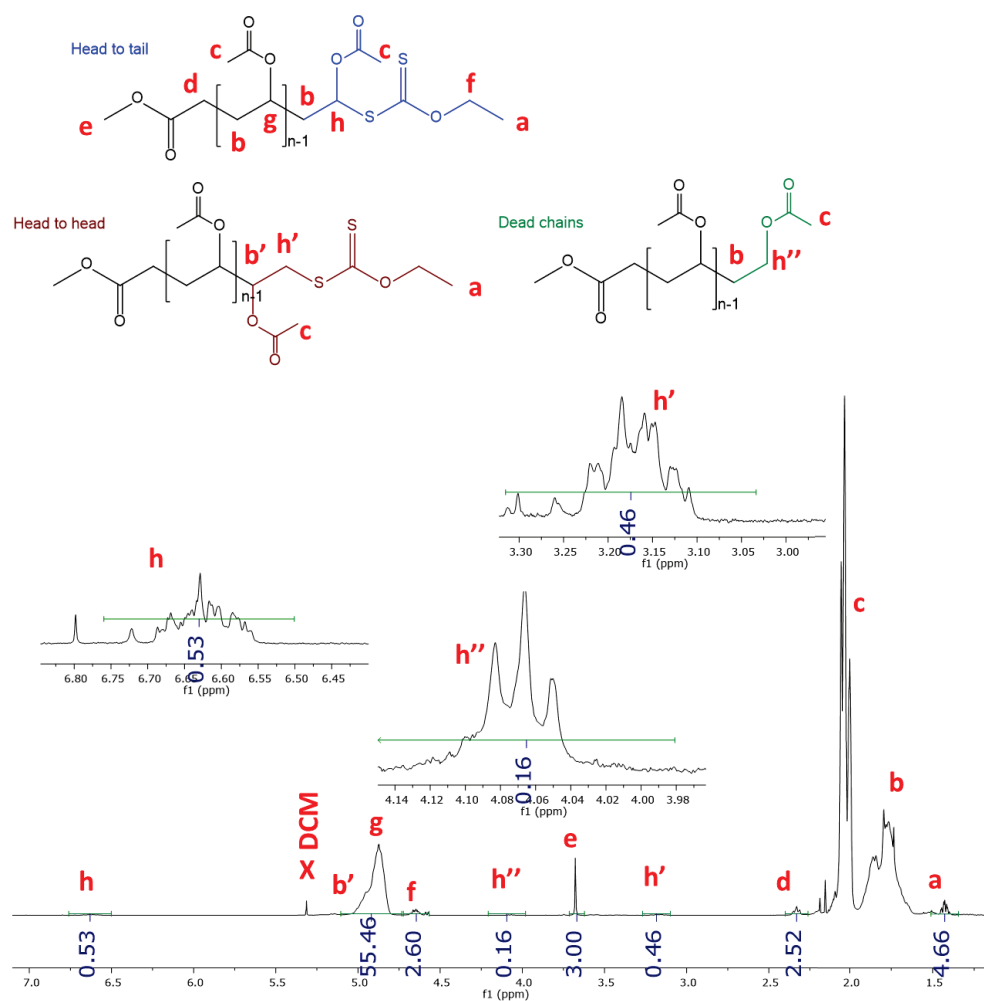


Figure 72: ^1H NMR of low M_n PVAc in CDCl_3 , 256 scans.

There is a signal at a chemical shift between 3 and 3.3 ppm that was assigned to the CH_2 from the head to head units (h') and a signal in between 4 and 4.15 ppm that was assigned to the CHOAc end units from the dead chains by comparison with the literature (h'')¹⁶¹. Integration of the different signals gave a percentage of 53% of head to tail, 23% of head to head and 16% of dead chains.

In order to confirm these results, the polymer was also analysed by ^{13}C NMR (Figure 73).

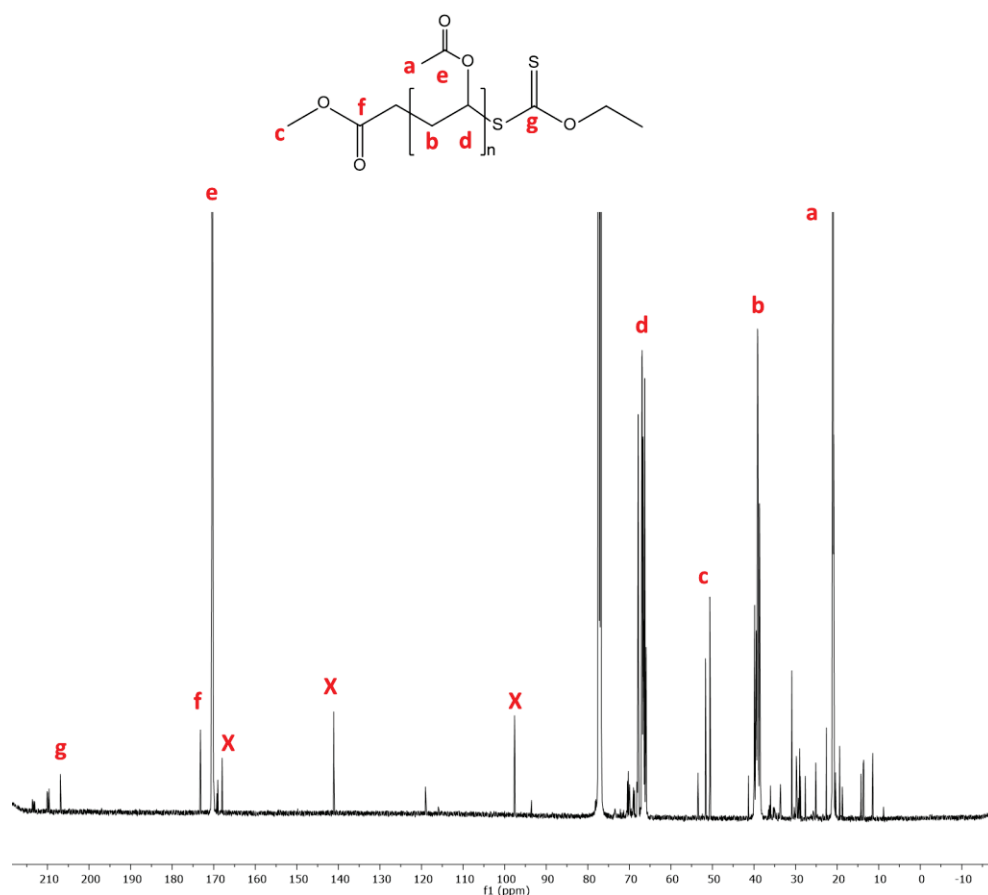


Figure 73: ^{13}C NMR spectrum of PVAc in CDCl_3 . Signals labelled X correspond to leftover VAc monomer.

Due to the complexity of the spectra, only the main signals of a PVAc head to tail chain are shown. Assignment has been done by comparison with the values reported in the literature for PVAc.¹⁶²

However, by focusing in specific areas of the spectrum it is also possible to assign some signals that correspond to head to head chains according to the literature (**Figure 7474**).¹⁶³

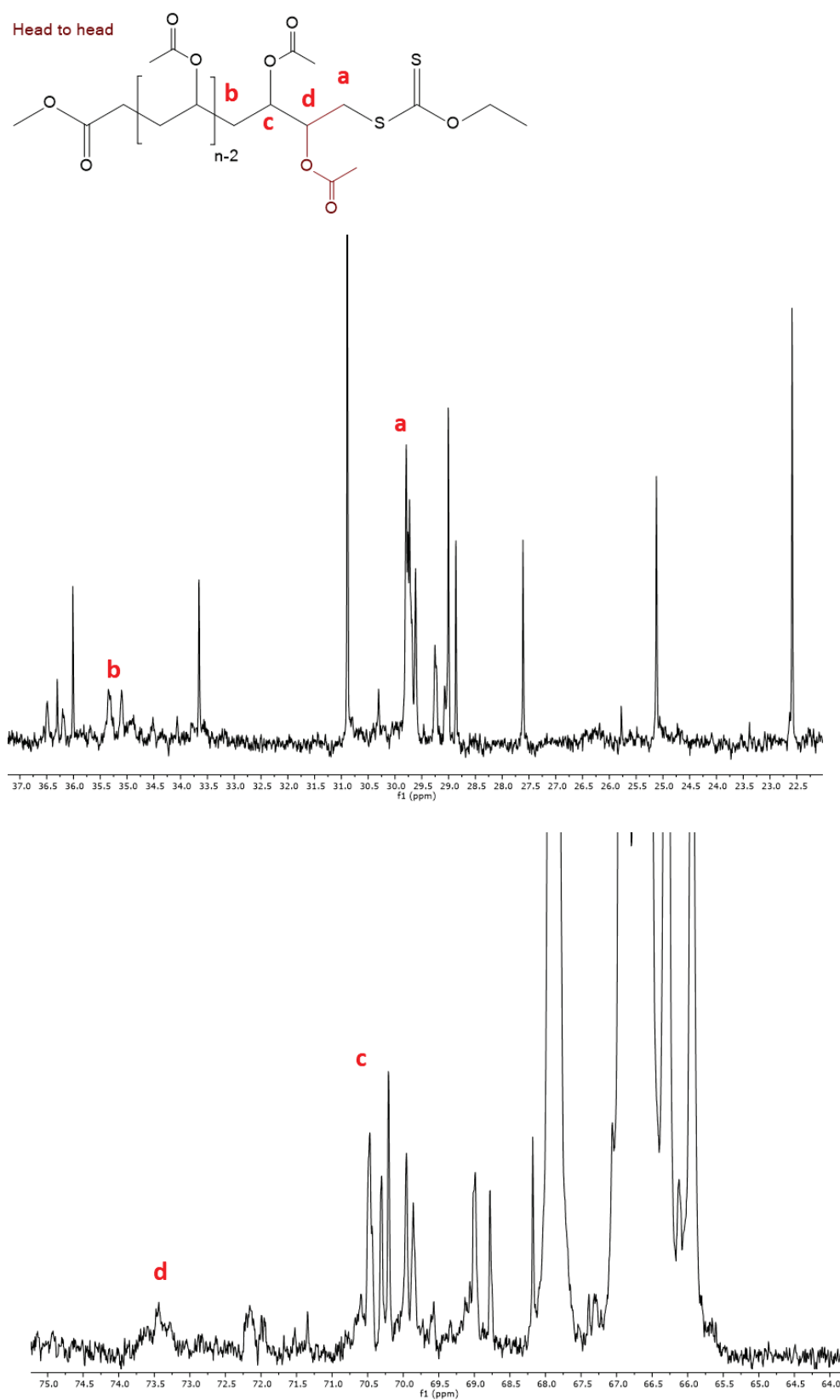


Figure 74. ^{13}C NMR spectrum of PVAc in CDCl_3 .

^1H and ^{13}C NMR together, as well as SEC RI and UV observations confirm the presence of head to head and dead chains in our synthesised PVAc material. In order to reduce the proportion of these defects, different reaction parameters were tested.

4.3.1.1 Conversion

According to the literature, the DP_n of the polymer directly relates to the population of head to head chains.^{158, 164} However, it is not possible in our case to decrease the DP_n of the samples any further since they will be used as stabilisers. In addition, no substantial decrease in head to head addition was observed when synthesising a low Mn (4 kg mol^{-1}) PVAc.

As an alternative to this, conversion was reduced from 60 to 20%.

A PVAc sample of target Mn of 4 kg mol^{-1} was synthesised. Reactions were stopped at 22% conversion and the product was analysed by ^1H NMR.

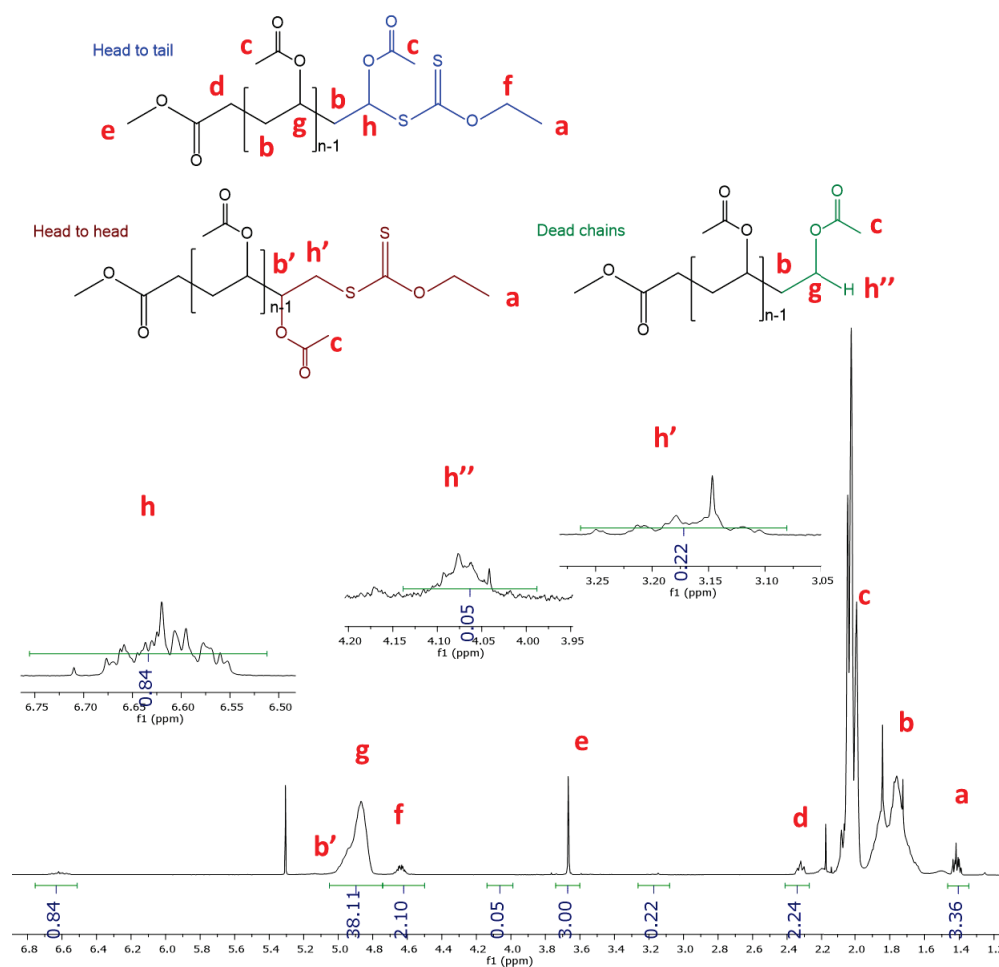


Figure 75. ^1H NMR spectrum of low conversion PVAc in CDCl_3 . 256 scans.

We observed a substantial decrease in the proportion of head to head chains from 23 to 11%, and the dead chains were also reduced from 16 to 5%. As a result, the proportion of head to tail chains increased from 53 to 84%, making a much better quality PVAc.

This material was then chain extended with VAc (**Figure 76**) and the reaction was followed by SEC UV in THF. Results are shown in **Table 9** and **Figure 77**.

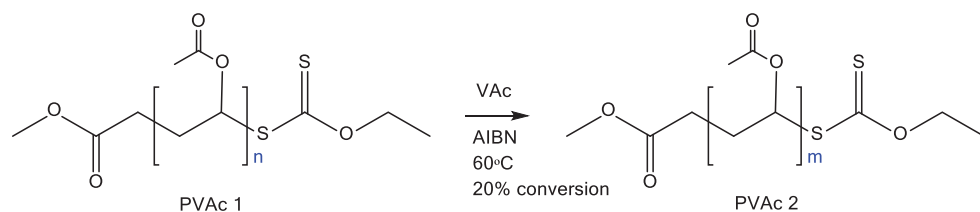


Figure 76: Chain extension of PVAc with VAc at 20% conversion.

Table 9: Key parameters of low conversion PVAc before and after chain extension.

M_{nNMR} PVAc 1 $\text{Kg mol}^{-1\text{a}}$	M_{nSEC} PVAc 1 $\text{Kg mol}^{-1\text{b}}$	\bar{D}	Conv. % ^c	M_{ntheor} PVAc 2 $\text{Kg mol}^{-1\text{d}}$	M_{nNMR} PVAc 2 $\text{Kg mol}^{-1\text{e}}$	M_{nSEC} PVAc 2 $\text{Kg mol}^{-1\text{f}}$	\bar{D}
3.3	4.5	1.08	18	10.5	8	10	1.1

a: experimental molar mass of PVAc 1 calculated from end group analysis by ^1H NMR comparing polymer chain end and main chain resonances.

b: experimental molar mass of PVAc 1 calculated by SEC in THF using PMMA standards.

c: conversion of the chain extension from the crude sample calculated by ^1H NMR by comparing monomer and polymer resonances.

d: theoretical molar mass of PVAc 2 calculated from conversion.

e: experimental molar mass of PVAc 2 calculated from end group analysis by ^1H NMR comparing polymer chain end and main chain resonances.

f: experimental molar mass of PVAc 2 calculated by SEC in THF using PMMA standards.

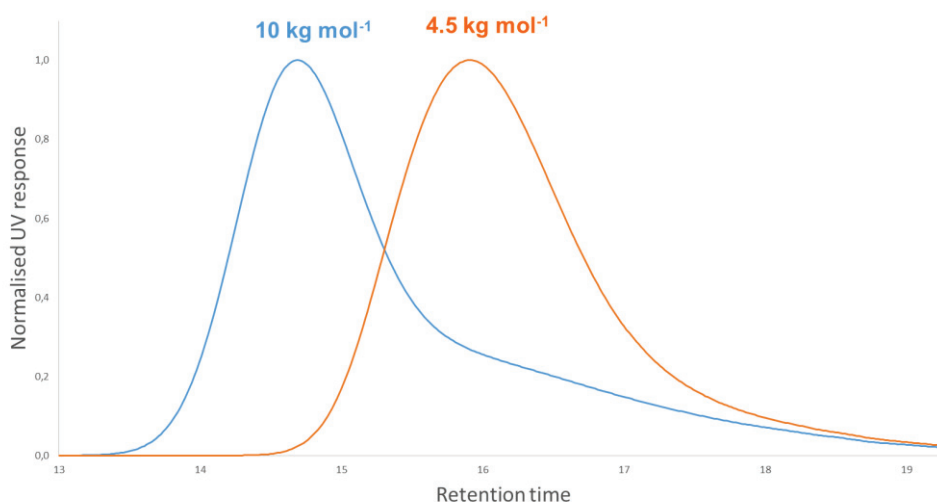


Figure 77. SEC UV chromatograph in THF of chain extension of PVAc with VAc at 20% conversion.

The peak that overlaps with the starting polymer, which has been assigned to head to head and dead chains, is much lower in this case. Furthermore, dispersity values are lower than the previous ones. Lowering the conversion of the reaction is therefore a valid approach to make materials with improved quality.

4.3.1.2 Temperature

The next parameter that was tested was the reaction temperature. According to the literature, temperature enhances the formation of head to head and dead chains.¹⁵⁷ In order to test this, the temperature of the reactions was reduced from 60 to 35°C. A different initiator that decomposes at a lower temperature than AIBN, V-70, was used in this case. A model polymerisation of VAc with a target M_n of 4 kg mol⁻¹ was carried out. Reaction temperature was set at 35°C and the reaction was stopped at 60% conversion. The product was analysed by ¹H NMR (**Figure 78**).

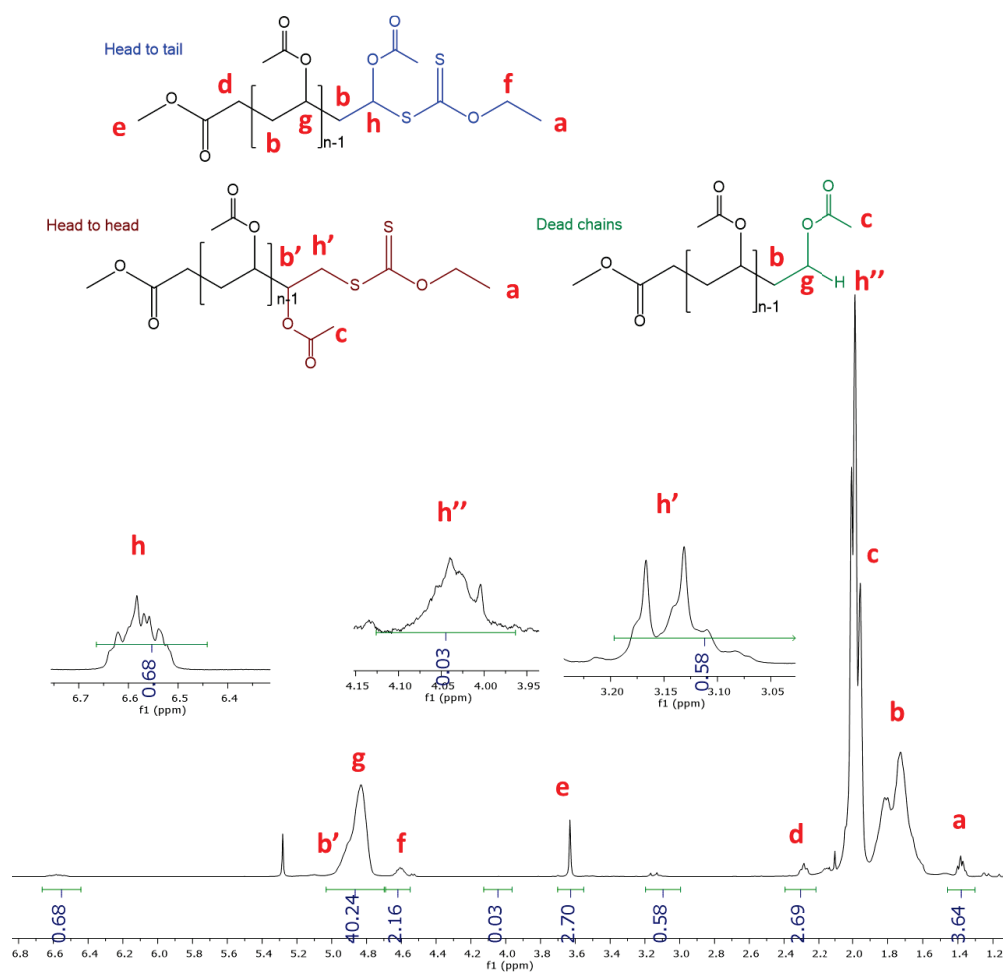


Figure 78. ¹H NMR spectrum of low temperature PVAc in CDCl₃, 256 scans.

In this case a completely different outcome was observed. Dead chains were greatly reduced from 16 to 3%. However, the proportion of head to head chains was not reduced but slightly increased from 23 to a 29%. This contradicts the literature, but it can be explained by the fact that, although temperature does reduce the occurrence of head to head addition, it also slows down the reactivation of these chains substantially, resulting in a higher accumulation of this defect over the course of the reaction.

As an outcome, head to tail accounts for 68% of the chains, which is a slightly higher proportion than the one obtained in conventional reactions, but is much lower than the one obtained when conversion was lowered to 20%.

This material was chain extended with VAc and the reaction was followed by SEC in THF. Results are summarised in **Table 10** and **Figure 79**.

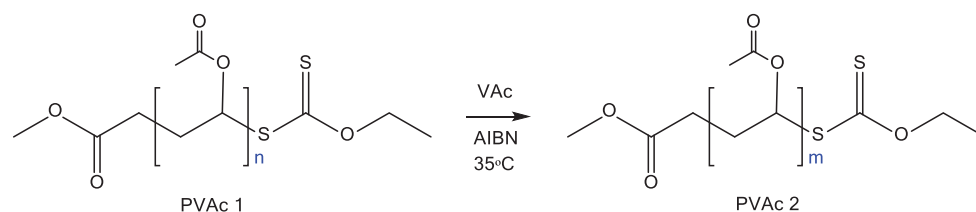


Figure 79: Chain extension of low temperature PVAc with VAc at 35°C.

Table 10: Key parameters of low temperature PVAc before and after chain extension with VAc at 35°C.

$M_{n\text{NMR}}$ PVAc 1	$M_{n\text{SEC}}$ PVAc 1	\bar{D}	Conv. % ^c	$M_{n\text{theor}}$ Kg mol ^{-1 d}	$M_{n\text{NMR}}$ PVAc 2	$M_{n\text{SEC}}$ PVAc 2	\bar{D}
Kg mol ⁻¹ a	Kg mol ⁻¹ b				Kg mol ⁻¹ 1 e	Kg mol ⁻¹ f	
3.6	4.5	1.09	30	9.7	8.4	10.5	1.12

a: experimental molar mass of PVAc 1 calculated from end group analysis by ¹H NMR comparing polymer chain end and main chain resonances.

b: experimental molar mass of PVAc 1 calculated by SEC in THF using PMMA standards.

c: conversion of the chain extension from the crude sample calculated by ¹H NMR by comparing monomer and polymer resonances.

d: theoretical molar mass of PVAc 2 calculated from conversion.

e: experimental molar mass of PVAc 2 calculated from end group analysis by ¹H NMR comparing polymer chain end and main chain resonances.

f: experimental molar mass of PVAc 2 calculated by SEC in THF using PMMA standards.

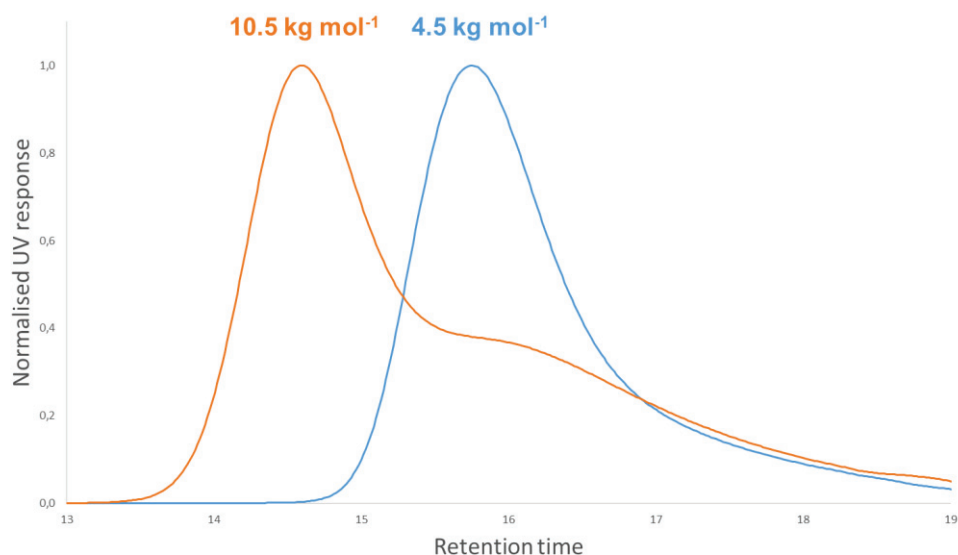


Figure 80: SEC UV chromatograph in THF of chain extension of low temperature PVAc with VAc at 35 °C.

SEC showed a very similar plot to the chain extension reaction of PVAc made at 60°C and 60% conversion (**Figure 70**), with a substantial amount of head to head and dead chains. This is also in agreement with the NMR results. This is hence not the best strategy to decrease the proportion of head to head chains in our materials.

4.3.1.3 Temperature and conversion

In order to study the effect of lowering the temperature and conversion simultaneously, a model PVAc with a target M_n of 4 kg mol⁻¹ was synthesised at 35°C and 20% conversion. The product was analysed by ¹H NMR (**Figure 81**).

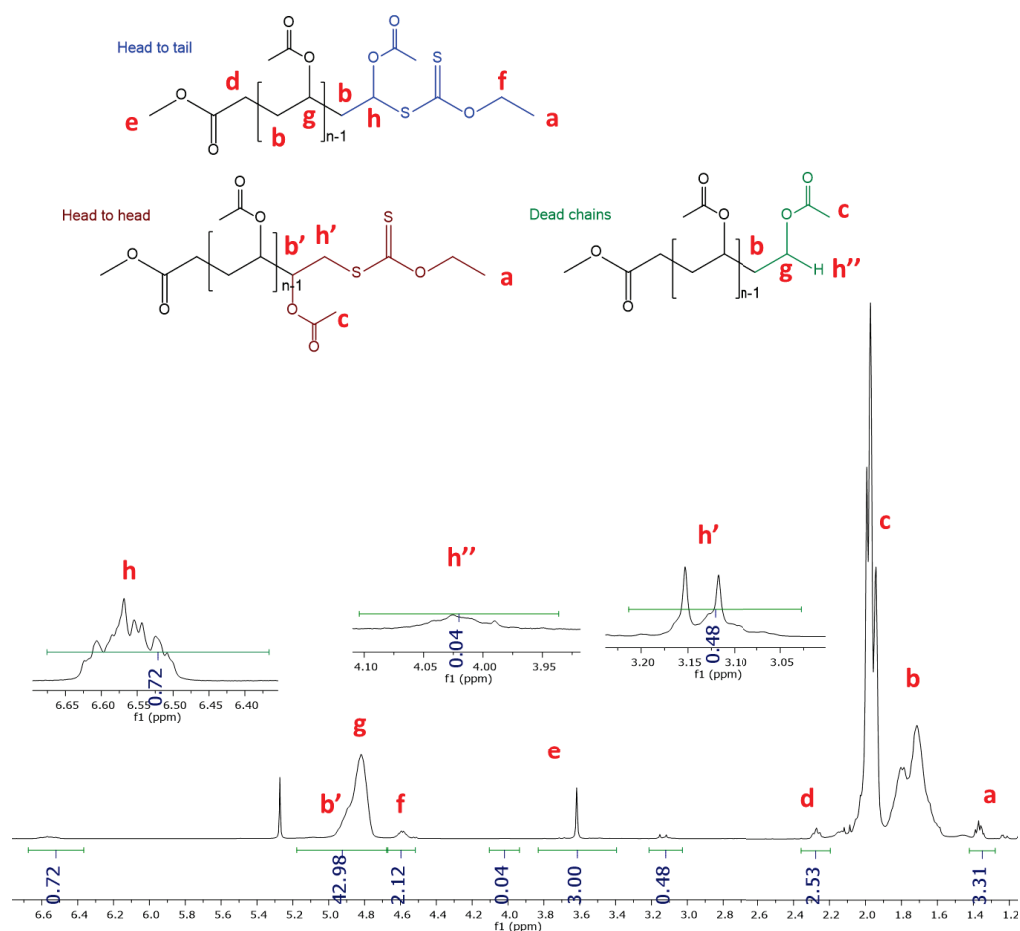


Figure 81. ^1H NMR spectrum of PVAc of target M_n 4 kg mol^{-1} synthesised at 35°C and 20% conversion.

In this case, although dead chains were reduced from 16 to 4%, the percentage of head to head chains increased only slightly from a 23% for conventional reaction conditions to a 24%.

This was confirmed by chain extending this PVAc with VAc and following the reaction by SEC UV. Results are shown in **Table 11** and **Figure 8383**.

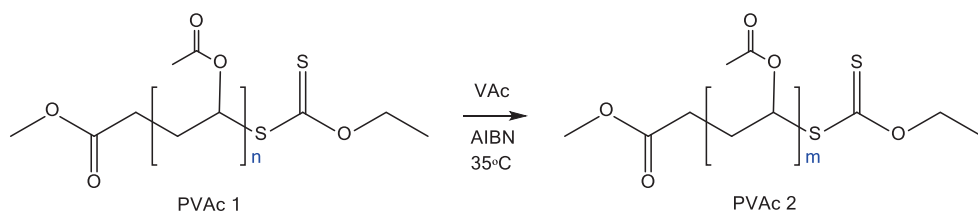


Figure 82: Chain extension of low temperature low conversion PVAc with VAc at 35°C and 20% conversion.

Table 11: Key parameters of low temperature low conversion PVAc before and after chain extension with VAc.

M_{nNMR} PVAc 1	M_{nSEC} PVAc 1	\bar{D}	Conversion % ^c	M_{ntheor} PVAc 2	M_{nNMR} PVAc 2	M_{nSEC} PVAc 2	\bar{D}
kg mol ⁻¹ 1a	kg mol ⁻¹ 1b			kg mol ⁻¹ ^d	kg mol ⁻¹ 1e	kg mol ⁻¹ 1f	
3.7	4.9	1.05	20%	11.7	10.8	13	1.15

a: experimental molar mass of PVAc 1 calculated from end group analysis by ¹H NMR comparing polymer chain end and main chain resonances.

b: experimental molar mass of PVAc 1 calculated by SEC in THF using PMMA standards.

c: conversion of the chain extension from the crude sample calculated by ¹H NMR by comparing monomer and polymer resonances.

d: theoretical molar mass of PVAc 2 calculated from conversion.

e: experimental molar mass of PVAc 2 calculated from end group analysis by ¹H NMR comparing polymer chain end and main chain resonances.

f: experimental molar mass of PVAc 2 calculated by SEC in THF using PMMA standards.

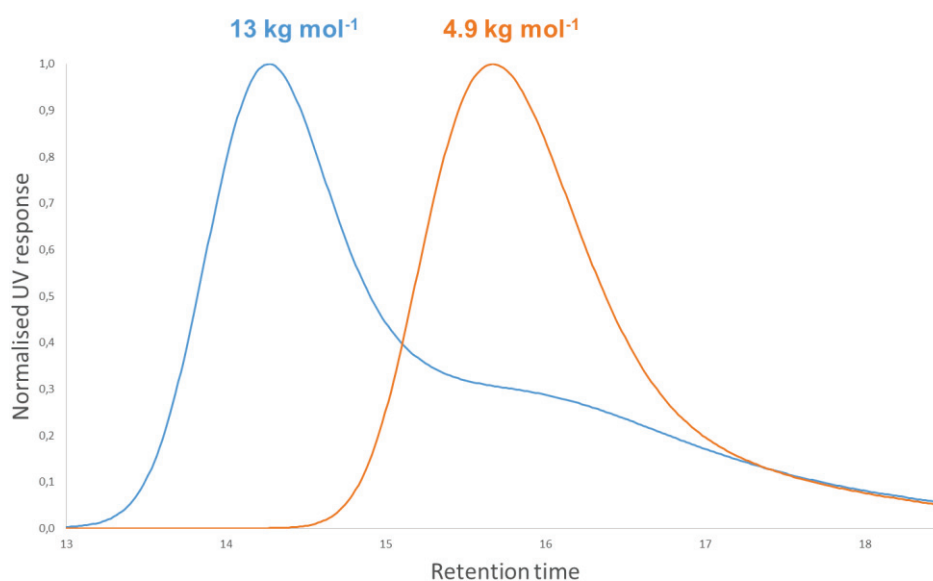


Figure 83: SEC UV chromatograph in THF of chain extension of low conversion low temperature PVAc with VAc at 35 °C.

SEC shows again a peak overlapping with the starting polymer that has been assigned to head to head chains. This result is very similar to the ones for conventional and low temperature reactions (**Figures 70 and 80**). These are

therefore not the best reaction conditions to produce a PVAc of a better quality.

4.3.1.4 Monomer addition

Another possible approach to solving the head to head problem could be switching the monomer addition order, synthesising first a PNVP macro-RAFT with the desired number of NVP units and then extending it with VAc and VPI to make a PNVP-*block*-P(VAc-*stat*-VPi)-X2 block copolymer (**Figure 84**).

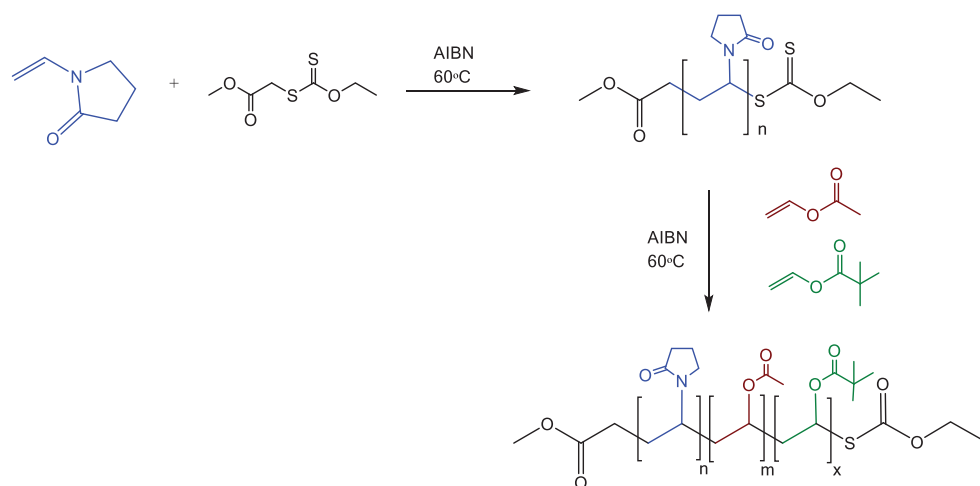


*Figure 84: Reaction scheme for the synthesis of PNVP-*block*-P(VAc-*stat*-VPi)-X2 block copolymers.*

No reference to head to head addition in NVP polymerisation was found in the literature, so it was thought that this material would be free of this type of defects. In order to confirm this, a model 4 kg mol^{-1} PNVP was synthesised. End group analysis of this PNVP by ^1H NMR is very complicated since most of the signals from the end groups overlap with the signals from the polymer making any quantification impossible.

However, it is possible to track the chain extension of this polymer with VAc by SEC UV and see if any material does not extend.

Table 12: Key parameters of PNVP-X2 and PNVP-block-PVAc-X2 synthesised at 60°C.

M_{nNMR} PNVP Kg mol ⁻¹ ^a	M_{nSEC} PNVP Kg mol ⁻¹ ^b	\bar{D}	Conv. % ^c	M_{ntheor} PNVP- <i>block</i> - PVAc Kg mol ⁻¹ ^d	M_{nNMR} PNVP- <i>block</i> - PVAc Kg mol ⁻¹ ^e	M_{nSEC} PNVP- <i>block</i> - PVAc Kg mol ⁻¹ ^f	\bar{D}
4	9	1.90	50%	15.5	13	15.5	2.08

a: experimental molar mass of PNVP 1 calculated from end group analysis by ¹H NMR comparing polymer chain end and main chain resonances.

b: experimental molar mass of PNVP 1 calculated by SEC in DMF using PMMA standards.

c: conversion of the chain extension from the crude sample calculated by ¹H NMR by comparing monomer and polymer resonances.

d: theoretical molar mass of PNVP-*block*-PVAc calculated from conversion.

e: experimental molar mass of PNVP-*block*-PVAc calculated from end group analysis by ¹H NMR comparing polymer chain end and main chain resonances.

f: experimental molar mass of PNVP-*block*-PVAc calculated by SEC in DMF using PMMA standards.

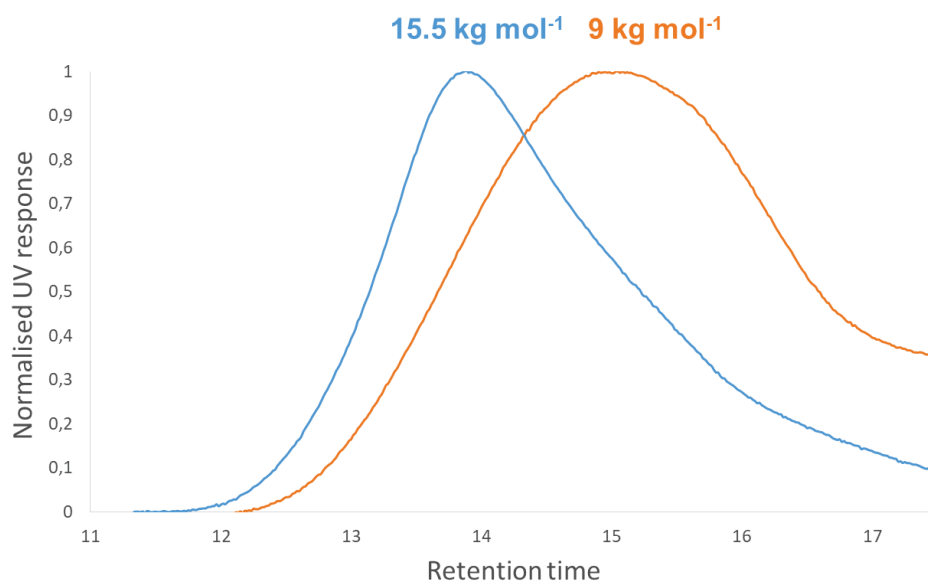


Figure 85: SEC UV chromatograph in THF of chain extension of PNVP with VAc at 60°C.

Due to the difference in hydrodynamic volume of PNVP and most SEC standards, already mentioned in chapter 1, it is not possible to accurately determine the M_n of this starting material. However, a very clear shift without a shoulder was observed, indicating that chain extension is taking place.

This approach, however, is not the most convenient, since it would require making macro-RAFT oligomers of around 4 units of NVP, and these are difficult to purify and handle.

4.3.1.5 Conclusions

In summary, we tried three alternative sets of reaction conditions for the synthesis of PVAc (**Table 13**).

Table 13: Comparison of the livingness of low Mn PVAc synthesised at different reaction conditions.

Entry	Temperature °C	Conversion % ^a	% HT ^b	%HH ^c	%D ^d
1	60	60	53	23	16
2	60	20	84	11	5
3	35	60	68	29	3
4	35	20	72	24	4

a: conversion of the crude sample calculated by ¹H NMR by comparing monomer and polymer resonances.

b: percentage of head to tail chains calculated by ¹H NMR

c: percentage of head to head chains calculated by ¹H NMR

d: percentage of dead chains calculated by ¹H NMR.

The set of conditions that showed the best improvement in terms of proportion of head to head chains compared to the conventional reaction conditions was the one with 20% conversion and a temperature of 60°C.

4.4 Head to head addition in VPi polymerisation.

The stabilisers used for dispersion polymerisation are P(VAc-*stat*-VPi)-X2 copolymers so, although VPi is a very similar monomer to VAc, its behavior in terms of head to head addition and formation of dead chains was also studied in detail.

A model RAFT polymerisation of VPi of target M_n of 4 kg mol⁻¹ was designed (Figure 86).

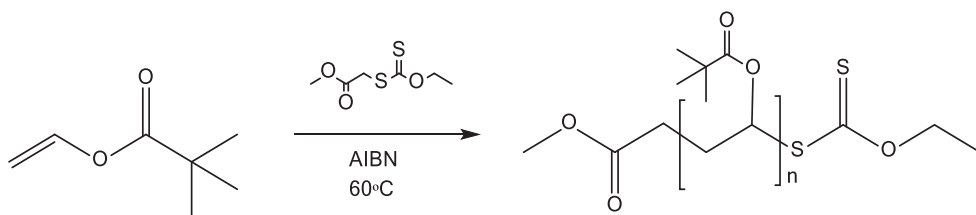


Figure 86: RAFT polymerisation of VPI at 60°C.

A conversion of 50% was achieved in 90 min. $M_{n\text{conversion}} = 4 \text{ kg mol}^{-1}$, $M_{n\text{NMR}} = 5.1 \text{ kg mol}^{-1}$, $M_{n\text{SEC}} = 6.2 \text{ kg mol}^{-1}$, $\mathcal{D} = 1.18$. ^1H NMR is shown in **Figure 87**.

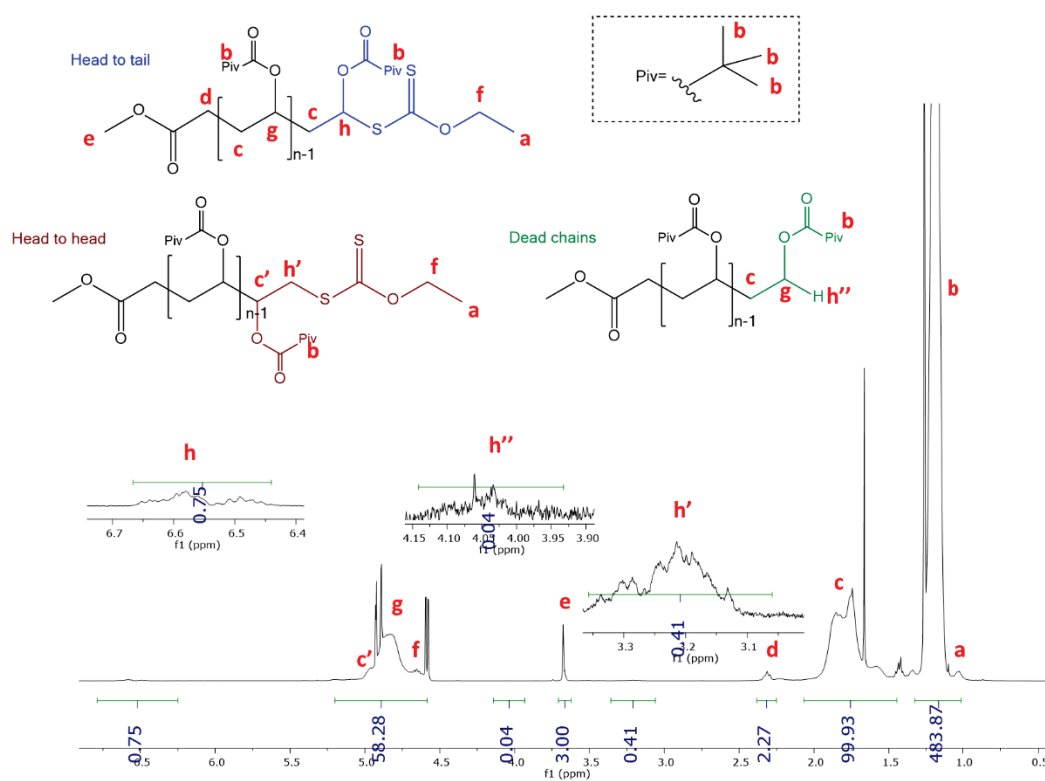


Figure 87. ^1H NMR of low M_n PVPI in CDCl_3 , 256 scans. Unassigned signals belong to leftover monomer.

RAFT end functionality given by the integral of the signal at 6.55 ppm is higher for PVPI (75%) than it was for PVAc (53%). Head to head addition chains are very similar (20%) compared to PVAc (23%). However, dead chains are much lower in this case (4% compared to 16% for PVAc). This was

confirmed by following the chain extension of this material with more VPi by SEC UV (**Figure 88**).

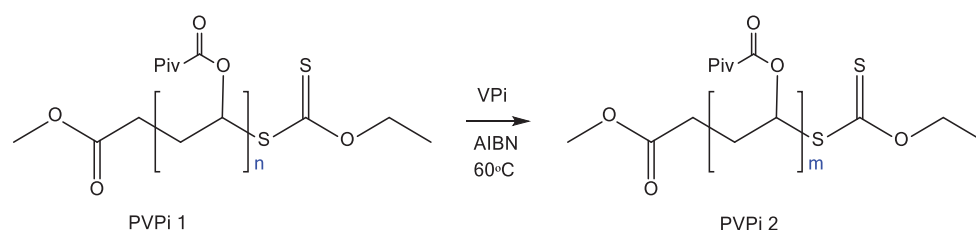


Figure 88: Chain extension of low M_n PVPi with VPi at 60°C.

Results are summarized in **Table 14**.

Table 14: Key parameters of low M_n PVPi before and after chain extension with VPi.

$M_{n\text{NMR}}$ PVPi 1	$M_{n\text{SEC}}$ PVPi 1	\bar{D}	Conv % ^c	$M_{n\text{theor}}$ PVPi 2	$M_{n\text{NMR}}$ PVPi 2	$M_{n\text{SEC}}$ PVPi 2	\bar{D}
Kg mol^{-1} _a	Kg mol^{-1} _b			Kg mol^{-1} ^d	Kg mol^{-1} ^e	Kg mol^{-1} ^f	
5.1	6200	1.18	86	31	42	30	1.32

a: experimental molar mass of PVPi 1 calculated from end group analysis by ^1H NMR comparing polymer chain end and main chain resonances.

b: experimental molar mass of PVPi 1 calculated by SEC in THF using PMMA standards.

c: conversion of the chain extension from the crude sample calculated by ^1H NMR by comparing monomer and polymer resonances.

d: theoretical molar mass of PVPi 2 calculated from conversion.

e: experimental molar mass of PVPi 2 calculated from end group analysis by ^1H NMR comparing polymer chain end and main chain resonances.

f: experimental molar mass of PVPi 2 calculated by SEC in THF using PMMA standards.

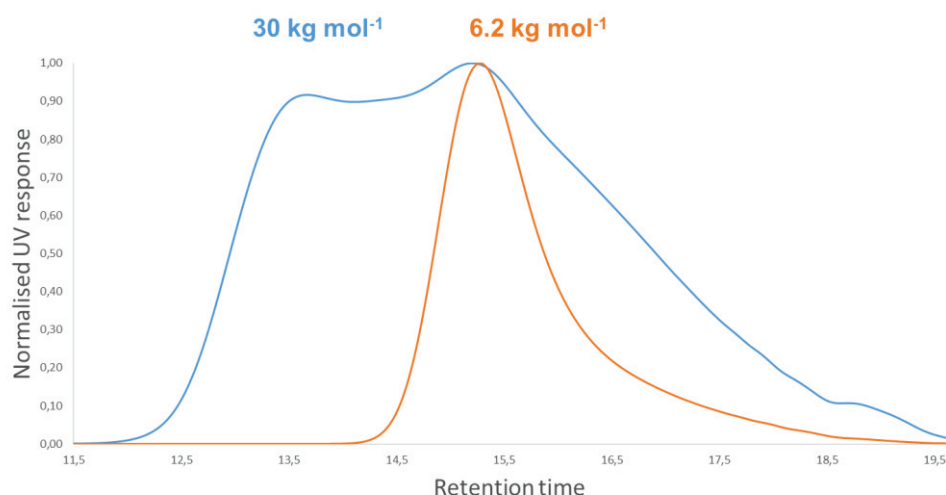


Figure 89: SEC UV in THF of chain extension of low Mn PVPI with VPI.

As predicted, VPI behaves very similarly to VAc, which can be seen both from the NMR data and the SEC trace. In this case, since the reaction proceeded to a higher conversion than expected, a broadening in the lower Mn peak can be observed due to the formation of other side reactions.

4.4.1 Conversion

In order to check if lowering the conversion also reduces head to head defects in the case of VPI, a model polymerisation of VPI was carried out to a conversion of 25%. Again, a target M_n of 4000 g mol⁻¹ was chosen. The polymer obtained was analysed by ¹H NMR.

RAFT end functionality was found slightly higher for low conversion PVPI (87%) than it was for high conversion one (75%). The proportion of head to head chains was reduced from 20 to 11% and dead chains from 4 to 2%, resulting in a better quality material.

This was also confirmed by performing the chain extension of this PVPI with VPI.

Table 15: Key parameters of low Mn PVPI before and after chain extension with VPI at low conversion.

M_{nNMR} PVPI 1 Kg mol ⁻¹ a	M_{nSEC} PVPI 1 Kg mol ⁻¹ b	\bar{D}	Conv % ^c	M_{ntheor} PVPI 2 Kg mol ⁻¹ ^d	M_{nNMR} PVPI 2 Kg mol ⁻¹ ^e	M_{nSEC} PVPI 2 Kg mol ⁻¹ ^f	\bar{D}
4.2	6.1	1.15	25	12	12.5	13.9	1.41

a: experimental molar mass of PVPI 1 calculated from end group analysis by ¹H NMR comparing polymer chain end and main chain resonances.

b: experimental molar mass of PVPI 1 calculated by SEC in THF using PMMA standards.

c: conversion of the chain extension from the crude sample calculated by ¹H NMR by comparing monomer and polymer resonances.

d: theoretical molar mass of PVPI 2 calculated from conversion.

e: experimental molar mass of PVPI 2 calculated from end group analysis by ¹H NMR comparing polymer chain end and main chain resonances.

f: experimental molar mass of PVPI 2 calculated by SEC in THF using PMMA standards.

The product was analysed by SEC UV (**Figure 90**). The trace showed a decrease in the shoulder peak that corresponds to head to head chains.

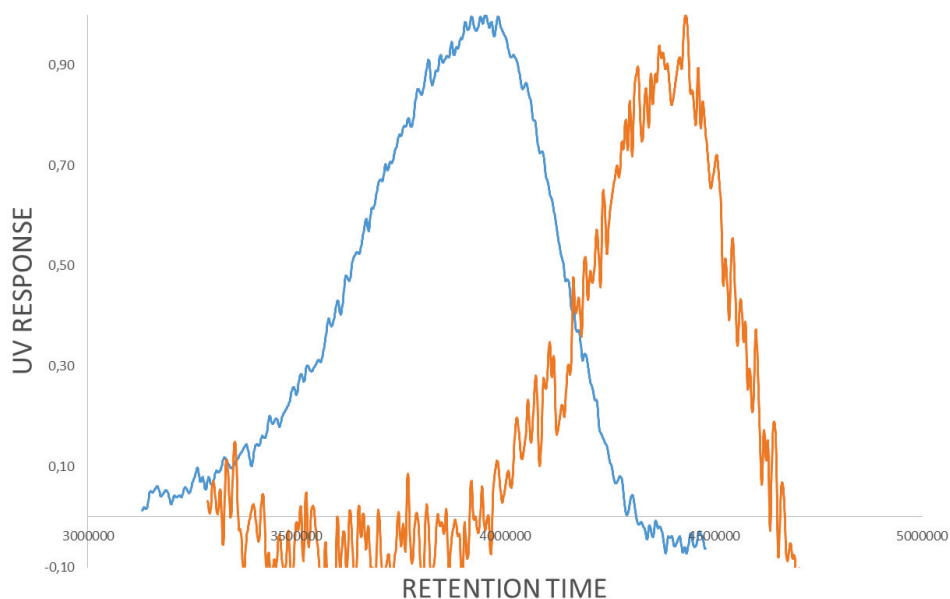


Figure 90: SEC UV in THF of chain extension of low conversion PVPI with VPI at low conversion.

We can therefore conclude that lowering the conversion of the reactions is the best possible approach towards the synthesis of P(VAc-*stat*-VPi)-X2 stabilisers with increased percentage of head to tail chains.

4.5 Synthesis of P(VAc-*stat*-VPi)-X2 with increased head to tail chains

A P(VAc-*stat*-VPi)-X2 of a target M_n of 4 kg mol⁻¹ and a VAc:VPi feed ratio of 50:50 was synthesised in order to analyse the polymer microstructure by NMR and confirm again that defects are reduced. Reaction was stopped at 24% conversion. $M_{n\text{conversion}} = 4.8 \text{ kg mol}^{-1}$, $M_{n\text{NMR}} = 4.7 \text{ kg mol}^{-1}$, $M_{n\text{SEC}} = 6.4 \text{ kg mol}^{-1}$, $\bar{D} = 1.22$. ¹H NMR is shown in **Figure 91**. Having two different monomers complicates the NMR spectrum substantially. For simplicity, only signals corresponding to head to head, head to tail and dead chain ends are shown in this case.

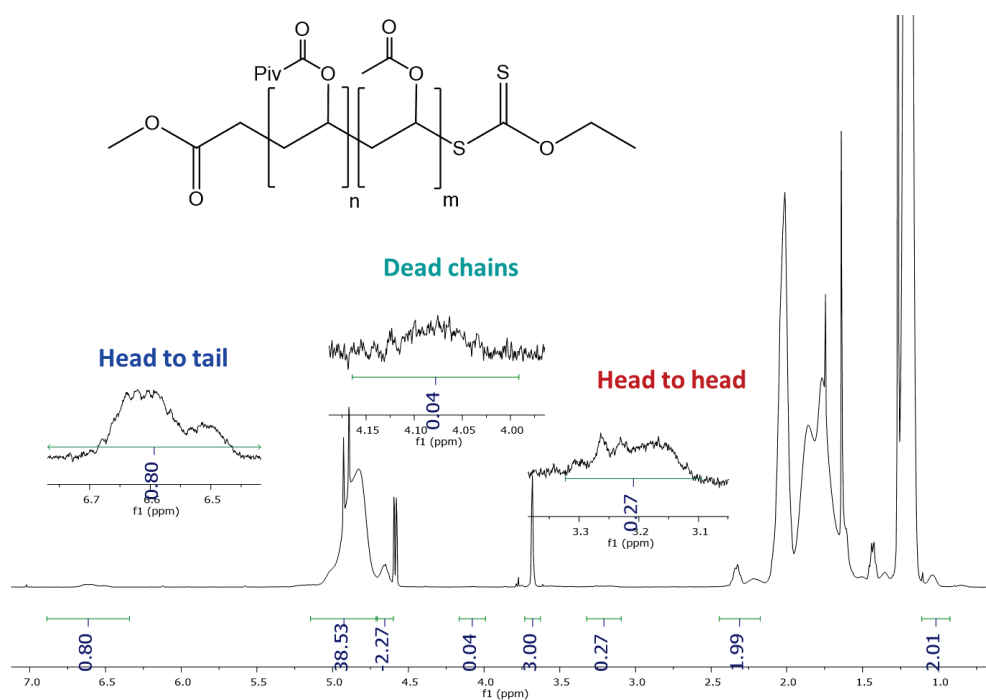


Figure 91: ^1H NMR of low M_n P(VAc-stat-VPI)-X2 in CDCl_3 , 256 scans. Signals at 1.25, 1.7, 4.6 and 5 ppm overlapping with the polymer signals belong to leftover VPI.

There is an increase in the RAFT end functionality (80%) compared to the previously synthesised P(VAc-stat-VPI)-X2 stabilisers (**Table 4**) that presented values ranging from 40 to 60% in the best case.

Similarly to previous results observed for VAc and VPI, the percentage of head to head chains is reduced substantially and dead chains constitute only a small fraction 4%.

This material was then chain extended with more VAc and VPI (**Figure 92**) and the reaction was followed by SEC UV (**Figure 93**). Results are summarized in **Table 16**.

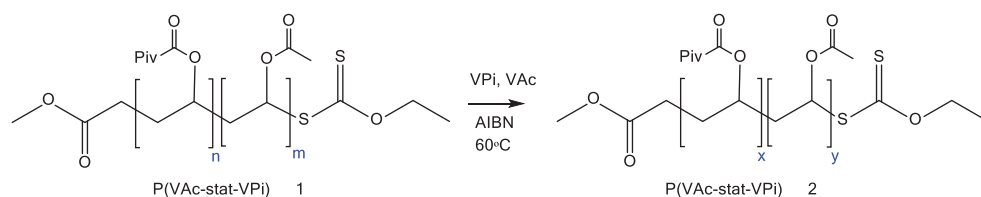


Figure 92: Chain extension of low conversion P(VAc-stat-VPI)-X2 with VAc and VPI at 60°C.

Table 16: Key parameters of low conversion P(VAc-stat-VPI)-X2 before and after chain extension with VAc and VPI.

M_{nNMR}	M_{nSEC}	\bar{D}	Conv	M_{nconv}	M_{nNMR}	M_{nSEC}	\bar{D}
P(VAc-stat-VPI) 1	P(VAc-stat-VPI) 1		% ^c	P(VAc-stat-VPI) 2	P(VAc-stat-VPI) 2	P(VAc-stat-VPI) 2	
Kg mol ^{-1a}	Kg mol ^{-1b}			Kg mol ^{-1d}	Kg mol ^{-1e}	Kg mol ^{-1f}	
4.7	6.4	1.22		9.5	10	14	1.47

a: experimental molar mass of PVAc 1 calculated from end group analysis by ¹H NMR comparing polymer chain end and main chain resonances.

b: experimental molar mass of PVAc 1 calculated by SEC in THF using PMMA standards.

c: conversion of the chain extension from the crude sample calculated by ¹H NMR by comparing monomer and polymer resonances.

d: theoretical molar mass of PVAc 2 calculated from conversion.

e: experimental molar mass of PVAc 2 calculated from end group analysis by ¹H NMR comparing polymer chain end and main chain resonances.

f: experimental molar mass of PVAc 2 calculated by SEC in THF using PMMA standards.



Figure 93: SEC UV in THF of the chain extension of P(VAc-stat-VPI)-X2 with VAc and VPI at 20% conversion.

The expected decrease in the head to head peak was observed similarly to previous experiments carried out with VAc and VPI separately. This is in agreement with ^1H NMR results.

4.6 Conclusions

An in-depth study of head to head addition in RAFT polymerisation of vinyl acetate and vinyl pivalate was carried out. Different reaction parameters like DP_n , conversion, temperature and monomer addition order were tested.

It was found that, while decreasing the DP_n did not seem to have an effect in the formation of head to head chains for the range of M_n that we were investigating (4 to 12 kg mol $^{-1}$), decreasing the conversion decreased the occurrence of head to head substantially. Furthermore, decreasing the reaction temperature resulted in a slight increase in head to head chains.

These results contradict what is reported in the literature for the polymerisation of this kind of monomers.¹⁵⁷

Switching the monomer addition order resulted in polymers with a very small amount of head to head chains. However, this method was more difficult to implement experimentally and was therefore not applied here.

Despite not being able to produce a material with a 100% of RAFT terminated head to tail chains by any of the different methods tried, a very important improvement in the quality of these materials has been observed when decreasing the conversion. This method will be used in the next chapter to synthesise P(VAc-*stat*-VPi)-*block*-PNVP-X2 copolymers to use as stabilisers in dispersion polymerisation of MMA.

Chapter 5: Dispersion polymerisation using P(VAc-*stat*-VPi)-*block*-PNVP-X2

Chapter 5 describes the dispersion polymerisation of two different monomers (NVP and MMA) in scCO₂ using improved P(VAc-*stat*-VPi)-X2 and the PNVP blocks made from them. Solubility in CO₂ will be briefly outlined.

The stabiliser composition (e.g. molar mass of the two blocks) will be discussed in detail.

5.1 Introduction

The importance of different parameters involved in dispersion polymerisation have already been outlined in previous chapters. While the choice of an appropriate solvent is key, the design of an efficient stabiliser is perhaps the most critical step.

The dispersion polymerisation of MMA in scCO₂ has been widely studied by different groups. DeSimone *et al.* studied the influence of concentration and molar mass of a poly(FOA) stabiliser in the dispersion, finding that for high molar mass stabilisers (~200 kg mol⁻¹) smaller and more uniform particles were formed when stabiliser concentration was increased.¹²¹ This was attributed to a more efficient colloidal stabilisation. Furthermore, lower molar mass stabilisers (~11 kg mol⁻¹) yielded smaller particles than the high molar mass ones.

Hems and co-workers designed PMMA-*block*-PFMA block copolymers, where PMMA acted as polymer-philic anchoring group and PFMA (poly (fluoroalkyl methacrylate)) as the CO₂-philic group. They tested them in dispersion polymerisation finding that increasing the stabiliser molar mass led to the production of higher yield and molar mass of the PMMA product obtained.¹⁶⁵ Furthermore, they observed a decrease in particle size when they used higher stabiliser loadings. This was attributed to an increase in

viscosity of the continuous phase that led to an increase in the rates of physical adsorption of the anchoring component of the stabiliser.

Deniz and co-workers studied the effect of varying the concentration of a silicone-containing fluoroacrylate stabiliser (poly (HDFDA-co-SiMA)) upon the polymerisation yield, PMMA molar mass and morphology.¹⁶⁶ As the stabiliser concentration was increased from 5 to 7 wt% the particle size decreased from 7.1 to 3.1 μm , and the yield and molar mass of the product increased.

Hwang *et al* reported the use of random copolymers of FOMA (1*H*,1*H*-perfluorooctyl methacrylate) and DMAEMA (2-dimethylaminoethyl methacrylate) as stabilisers.¹⁶⁷ They observed that the particle size decreased gradually from 1.8 to 1.0 μm with the increase of stabilizer concentration from 2.0 to 7.5% (w/w to MMA).

Giles and coworkers reported the use of graft copolymers based on perfluorohexan-1-ol and or perfluorooctan-1-ol as stabilisers.¹⁶⁸ They observed that increasing the stabiliser loading from 0.1 to 2 wt% resulted in higher molar mass products with narrower molecular weight distributions and more uniform spherical morphology.

McAllister *et al* did a very extensive study on the influence of different parameters on particle size and morphology when using a PDMS-MA macromonomer stabiliser of a molar mass of 10 kg mol^{-1} .¹⁵⁵ An increase in the stabiliser loading from 1 to 20 wt% resulted in a decrease in particle size from 3.6 to 0.6 μm .

The common message that can be taken from all the examples cited above is, firstly, that increasing stabiliser concentration leads to decrease in particle size. Secondly, increasing stabiliser molar mass leads to a more efficient stabilisation and therefore higher conversions and more uniform particle morphology. It is therefore key not only to design stabilisers that anchor effectively to the particles but also to optimise their loading and molar mass in order to produce a material with high yield and controlled morphology.

It has been previously shown in Chapter 3 that the lack of purity of the prepared stabilisers resulted in unsuccessful stabilisation and agglomerated products. A more in-depth study of RAFT polymerisation discussed in Chapter 4 has thrown some light on the defects that can arise from this process and how to tackle them. With this knowledge is now possible to design block copolymer stabilisers with reduced defects and increased purity and tune them to achieve an effective dispersion polymerisation of MMA in $scCO_2$.

5.2 Experimental

Materials

Monomers vinyl acetate (VAc, 99%, with hydroquinone as inhibitor) and methyl methacrylate (MMA, 99%, contains MEHQ as inhibitor) were purchased from Sigma Aldrich. *N*-vinyl pyrrolidone (NVP, 99%, stabilised with NaOH) and vinyl pivalate (VPi, 99%, with hydroquinone as inhibitor)

were purchased from Acros. 2,2'-Azobis(2-methylpropionitrile (AIBN, 98%) was purchased from Sigma Aldrich and 2,2'-Azobis(4-methoxy-2,4-dimethylvaleronitrile (V-70) from Wako. The xanthate RAFT agent (*O*-ethyl-*S*-(1-methoxycarbonyl) ethyl dithiocarbonate) was synthesised as detailed in Chapter 3. All reagents were used without further purification. Dry CO₂ (SFC grade, 99.99%) was purchased from BOC.

Synthesis of P(VAc-*stat*-VPi)-X2

Vinyl acetate (8.03 g, 35.19 mmol), vinyl pivalate (11.96 g, 33.38 mmol), xanthate 2 (68 mg, 0.35 mmol) and AIBN (5 mg, 0.03 mmol) were placed in a round bottom flask with a stirring bar and degassed with argon for 30 minutes in an ice bath. The mixture was stirred at 60°C for 150 minutes until a conversion of 21% was reached. The polymer product was then precipitated into cold petroleum ether and dried under reduced pressure.

In order to remove the residual amount of VPi, the product was dissolved in scCO₂ at 35°C and 83 bar and then flushed with CO₂ at constant temperature and pressure for 20 minutes.

$M_{n\text{theor}} = 12 \text{ kg mol}^{-1}$, $M_{n\text{NMR}} = 11.9 \text{ kg mol}^{-1}$, $M_{n\text{expSEC}}(\text{THF}) = 12.1 \text{ kg mol}^{-1}$, 21% conversion, VAc:VPi 48:52, $\bar{D} = 1.09$. ¹H NMR (CDCl₃): $\delta = 6.4\text{--}6.7 \text{ ppm}$ (m, 0.5 H), 4.7–5 ppm (m, 52 H), 4.5–4.7 ppm (m, 2 H), 3.6 ppm (s, 3H), 2.25–2.35 ppm, 1.5–2.1 ppm (m, 228 H), 1.3–1.4 ppm, 1.1–1.3 ppm (m, 161 H).

Synthesis of P(VAc-*stat*-VPi)-*block*-PNVP-X2

P(VAc-*stat*-VPi)-X2 of 11.9 kg mol^{-1} (3.77 g, 0.31 mmol) was dissolved in 16 g of THF in a round bottom flask with a stirring bar. NVP (290 mg, 2.61 mmol) and AIBN (50 mg, 0.30 mmol) were added. The flask was sealed and degassed for 30 minutes with argon in an ice bath and then heated at 60°C for 180 minutes. The product was precipitated into cold petroleum ether and dried under reduced pressure.

In order to remove the residual amount of NVP, the product was dissolved in scCO_2 at 35°C and 83 bar in a stainless steel autoclave and then flushed with CO_2 at constant temperature and pressure for 20 minutes.

DP of PNVP = 3, $M_{\text{nNMR}} = 12.2 \text{ kg mol}^{-1}$, $M_{\text{nexpSEC}}(\text{DMF}) = 12.0 \text{ kg mol}^{-1}$, $\bar{D} = 1.20$.
. ^1H NMR (CDCl_3): $\delta = 6.4\text{--}6.7 \text{ ppm}$ (m, 0.5 H), $4.7\text{--}5 \text{ ppm}$ (m, 52 H), $4.5\text{--}4.7 \text{ ppm}$ (m, 2 H), 3.9 ppm (m), 3.6 ppm (s), 3.2 (m), 2.25–2.35 ppm, 1.5–2.1 ppm (m, 228 H), 1.3–1.4 ppm, 1.1–1.3 ppm (m, 161 H).

Dispersion polymerisation of NVP and MMA

Dispersion polymerisations were carried out in a 60mL high pressure stainless steel autoclave as thoroughly described in chapter 2. The monomer (MMA, 7.2 g, 0.072 mol or NVP, 8 g, 0.072 mol), 5–10 wt% of the stabiliser (0.04–0.08 mmol) and V-70 (130 mg, 0.42 mmol) were dissolved in CO_2 and heated at 35°C and 4000 psi (276 bar) for 48h. The autoclave was then cooled to room temperature and slowly vented.

Phase Behaviour Measurements

Cloud point data were obtained using a hydraulic variable volume view cell described in Chapter 2. 150 mg of the polymer were dissolved in 3 g of monomer (5 wt% polymer with respect to monomer) and injected into the view cell. 20 g of CO₂ (15 wt% wt monomer with respect to CO₂) were then transferred by means of a high pressure stainless steel CO₂ bomb. The contents of the view cell were stirred using magnetic stirring. The system was heated to the desired temperature (35 to 75 °C) and pressure was increased by means of a movable piston to 345 bar when the sample was fully dissolved. To determine the cloud point, pressure was then decreased until the polymer was precipitated and the back light was totally obscured. All measurements were repeated three times and an average of these values was taken.

5.3. Dispersion polymerisation of NVP with P(VAc-*stat*-VPi)-X2 stabilisers

P(VAc-*stat*-VPi) copolymers with VAc:VPi molar ratios around 50:50 and molar mass ranging from 8 to 14 kgmol⁻¹ were synthesised and purified as described in the experimental part. Results are summarised in **Table 17**.

Table 17: Key parameters of P(VAc-stat-VPI)-X2 copolymer stabilisers synthesised by RAFT polymerisation in bulk at 60°C for 120 minutes.

Entry	VAc:VPI feed ^a	VAc:VPI exp ^b	Conversion % ^c	RAFT % ^d	M_n theor ^e	M_n NMR ^f	M_n SEC ^g	\bar{D}
1	50:50	41:59	22	81	8.8	8.3	8.5	1.11
2	50:50	48:52	21	81	12	11.9	12.1	1.09
3	50:50	48:52	21	82	14	14.5	14.3	1.12
4	50:50	43:57	25	83	18	18.6	18.9	1.19

a: Theoretical VAc:VPI molar ratios.

b: Experimental VAc:VPI molar ratios calculated by NMR.

c: Conversion of the crude sample calculated by NMR by comparing monomer and polymer resonances.

d: Livingness of the chains calculated from end group analysis by NMR comparing polymer chain end and main chain resonances.

e: Theoretical molar mass calculated from conversion.

f: Experimental molar mass calculated from end group analysis by NMR comparing polymer chain end and main chain resonances.

g: Experimental molar mass calculated by SEC in DMF using PMMA standards.

All samples have been synthesised with higher than 80% of head to tail RAFT terminated chains and low dispersity values (<1.2). ¹H and ¹³C NMR of a P(VAc-stat-VPI)-X2 sample (**Table 17, entry 1**) are shown for reference.

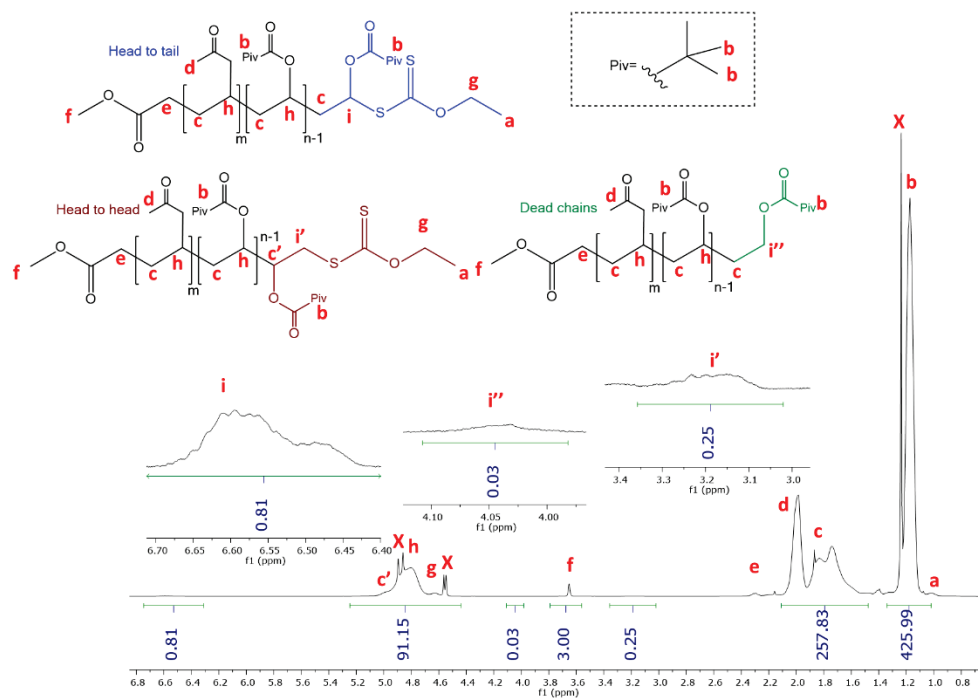


Figure 94: ^1H NMR of $P(\text{VAc-stat-VPI})\text{-X}_2$ synthesised by RAFT polymerisation in bulk at 60°C for 2 hours (Table 17, entry 1) in CDCl_3 , 256 scans. Signals marked X belong to residual VPI.

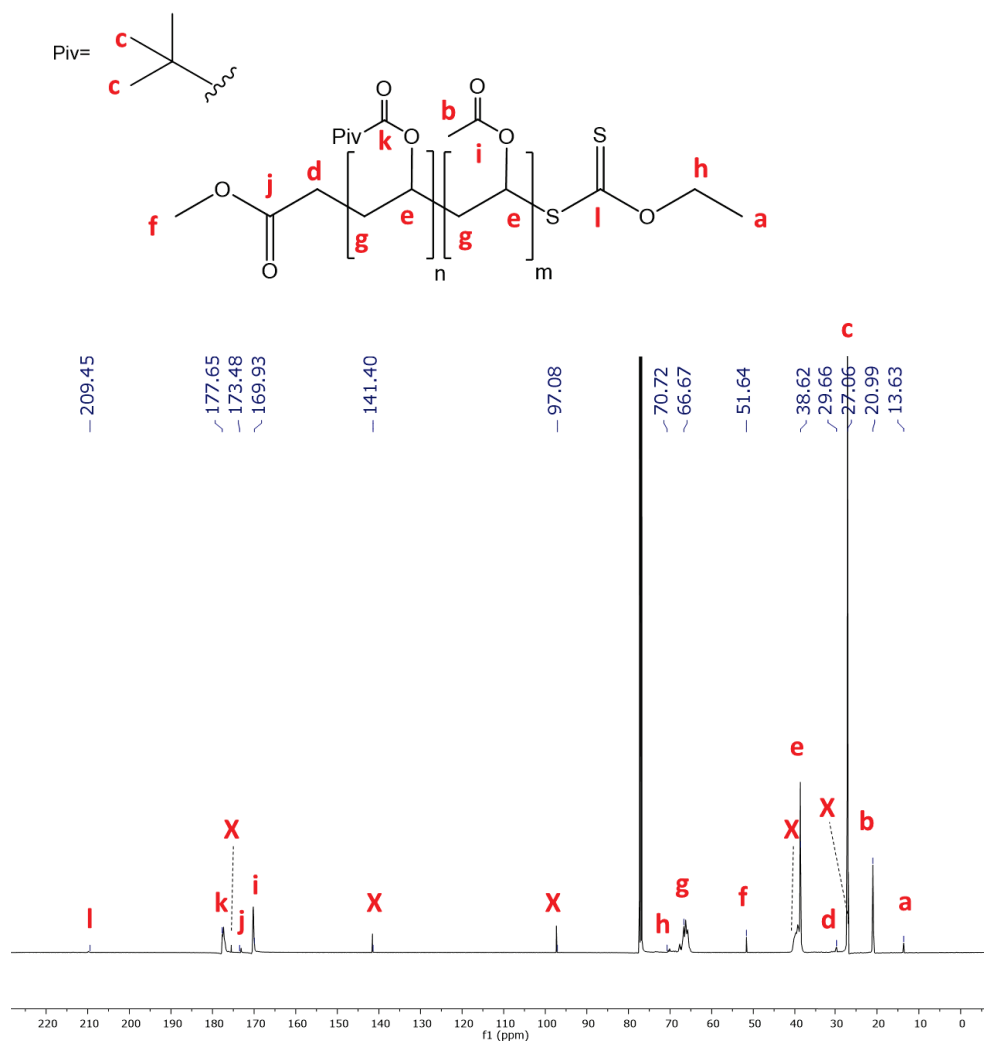


Figure 95: ^{13}C NMR of $P(\text{VAc-stat-VPI})\text{-X2}$ synthesised by RAFT polymerisation in bulk at 60°C for 2 hours (Table 17, entry 1) in CDCl_3 . Signals marked with X belong to residual VPI.

In order to check if the microstructure of the polymer (e.g. percentage of head to head and dead chains) has any impact on its solubility, a cloud point experiment of one of the stabilisers with lower proportion of head to head chains was carried out and compared to a previous stabiliser of similar M_n and VAc:VPI ratio but higher proportion of head to head chains (Figure 9696).

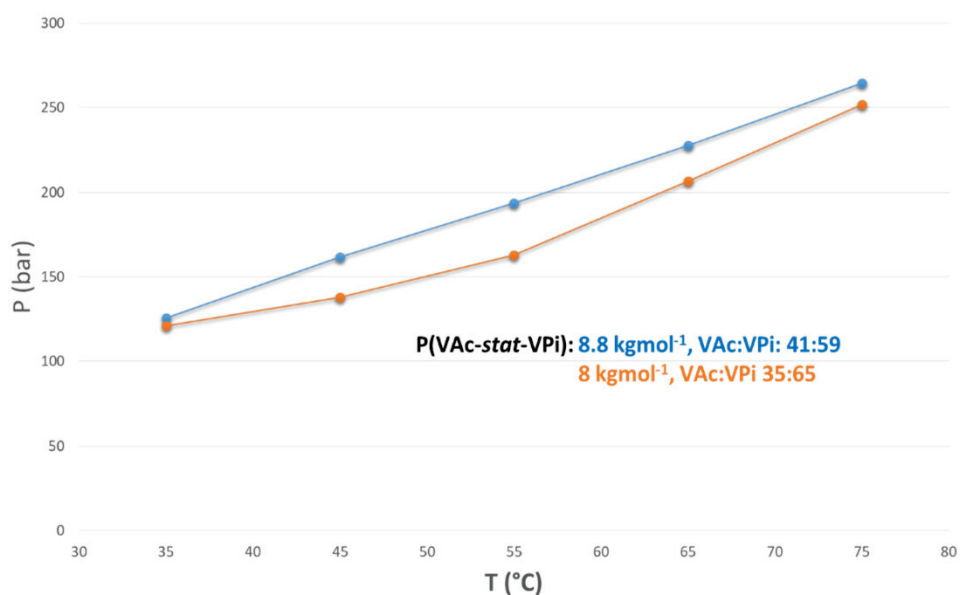


Figure 96: P-T diagram of P(VAc-stat-VPI)-X2 samples of molar mass around 8 kg mol⁻¹, VAc:VPi molar ratios around 40:60 and percentage of head to head chains of 42 (a) and 25 (b) respectively.

Both samples present very similar solubilities in scCO₂ at the different temperatures. Sample a presents a slightly higher solubility but this is due to the slightly smaller M_n and slightly higher amount of VPI. It was therefore concluded that the polymer microstructure does not have a substantial impact in CO₂ solubility in this case.

In order to assess the performance of the synthesised stabilisers (**Table 17, entries 1-4**) and find the optimum molar mass, they were then tested in the dispersion polymerisation of NVP. The procedure is detailed in the experimental part. Experimental data of the polymers obtained are summarised in **Table 18**.

Table 18: Key parameters of PNVP products made by dispersion polymerisation in $scCO_2$ at 35°C and 276 bar using block copolymers of VAc:VPi ratios between 40:60 and 50:50 and M_n between 8 and 18 kg mol⁻¹.

Entry	Stabiliser ^a	Stabiliser VAc:VPi molar ratios ^b	Conversion % ^c
1	17, 1	41:59	99
2	17, 2	48:52	98
3	17, 3	48:52	99
4	17, 4	43:57	99

a: Stabiliser used in the dispersion polymerisation, key parameters shown in Table 17.

b: Experimental VAc:VPi molar ratios calculated by NMR.

c: Conversion of the crude sample calculated by NMR by comparing monomer and polymer resonances.

All products were collected as fine powders (**Figure 97**). SEC of the products could not be carried out in this case since they showed very limited solubility in the most commonly used solvents (Chloroform and THF) likely due to the high M_n associated with dispersion polymerisation.



Figure 97: PNVP polymer powder made by dispersion polymerisation in $scCO_2$ using 5 wt% of P(VAc-stat-VPi)-X2 (Table 188, entry 2).

The morphology of the products was analysed by SEM (**Figure 9898**).

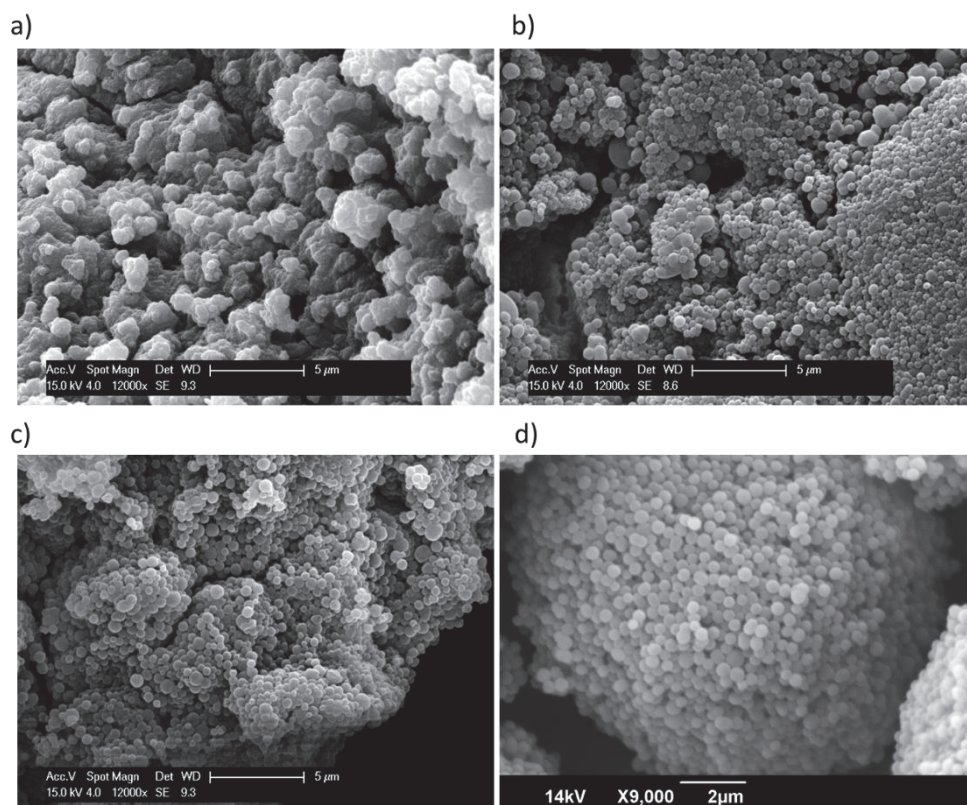


Figure 98: SEM analysis of PNVP samples made using 5 wt% of $P(\text{VAc-stat-VPI})\text{-}X_2$ of varying M_n and VAc:VPI ratios from 4060 to 50:50: a) Table 18, entry 1. b) Table 18, entry 2. c) Table 18, entry 3. d) Table 18, entry 4.

In all the cases a uniform spherical morphology was observed, comparable to that reported for previous stabilisers.¹¹⁶ However, particles seemed to be more uniform in size and shape in the case of higher molecular weight stabilisers (**Table 18, entries 2, 3 and 4**). Particle size could not be estimated for samples a and b due to particle agglomeration. A decrease in particle size was noticed when the stabiliser M_n was increased between sample c (220 ± 10 nm) and d (50 ± 2 nm), which matches observations reported in the literature, as previously discussed in chapter 5 introduction.¹²¹ A molar mass of 12 kg mol^{-1} or superior was hence chosen for the next set of experiments.

5.3.3. Dispersion polymerisation with P(VAc-*stat*-VPi)-*block*-PNVP-X2 stabilisers

P(VAc-*stat*-VPi)-*block*-PNVP copolymers of different DP_{PNVP} were synthesised from the corresponding P(VAc-*stat*-VPi)-X2 macro-RAFTs (**Table 177**). Two different types of stabilisers were synthesised. The first type with a low DP_{PNVP} (3-6), were designed to be soluble in $sc\text{CO}_2$ at the reaction conditions, and it has been hypothesised that they would be either grafted or physically adsorbed to the surface of the particles, stabilising them (**Figure 99, a**) *via* a similar mechanism to that of end capped perfluoropolyethers¹³⁰. The main difference with the previously reported P(VAc-*stat*-VPi)-X stabilisers¹⁶⁹ is the presence of a small PNVP block that should make them more polymer-philic towards PMMA and therefore anchor better compared to the statistical ones.

The second type of stabilisers were synthesised with a high DP of PNVP and were designed to be insoluble in $sc\text{CO}_2$. Hypothetically, since they have a very CO_2 -philic and a very CO_2 -phobic block, they would sit at the CO_2 /polymer interface being buried inside the particles during polymerisation, providing a different anchoring mode (**Figure 99, b**) more similar to that of some fluorinated block copolymers already described in Chapter 3.¹²¹ Woods and co-workers reported the use of perfluoroether PFPE-PMMA block copolymers with PMMA segments of M_n between 2 and 3.3 kg mol⁻¹ as the CO_2 -phobic anchor component, resulting in micron sized

spherical particles.¹²² A DP of PNVP of 35 ($M_n = 3900 \text{ kg mol}^{-1}$) was chosen as a starting point in this thesis due to sample availability.

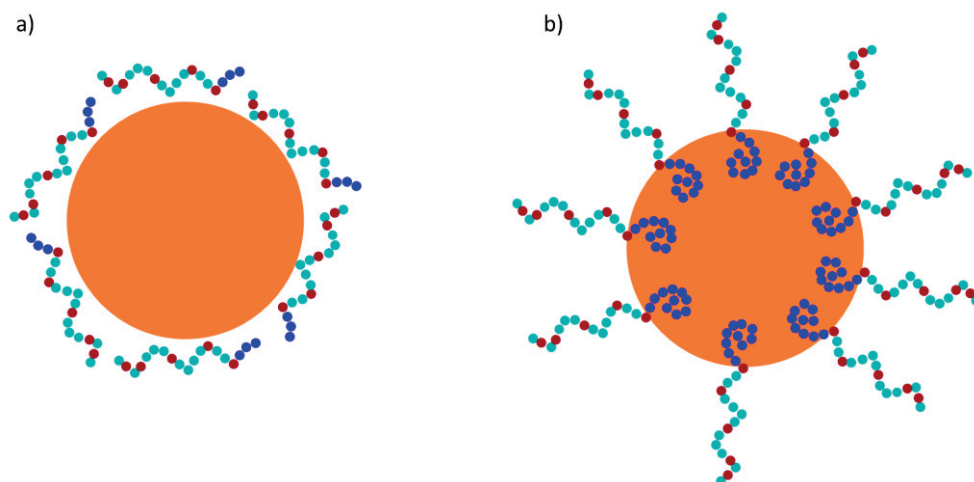


Figure 99: Stabilisation mechanism in dispersion polymerisation of MMA for a) block copolymer stabilisers with low DP of PNVP, b) block copolymer stabilisers with a high DP of PNVP.

5.3.3.1 P(VAc-*stat*-VPi)-*block*-PNVP with low DP_{NVP}

P(VAc-*stat*-VPi) copolymers previously synthesised were used as macro-RAFT agents in the synthesis of P(VAc-*stat*-VPi)-*block*-PNVP block copolymers with 3 and 6 units of NVP. The procedure is described in the experimental section. Results are summarised in **Table 19**.

Table 19: Key parameters of P(VAc-stat-VPi)-block-PNVP-X2 copolymer stabilisers synthesised from P(VAc-stat-VPi)-X2 (Table 17) (by RAFT polymerisation in THF at 60°C for 180 minutes).

Entry	Macro-RAFT ^a	M_{nNMR} (kgmol ⁻¹) ^b	M_{nSEC} (kg mol ⁻¹) ^c	DP target	DP exp ^d	\bar{D}	Cloud Point (bar) 35°C
1	16-2	12.2	12.1	4	3	1.11	149
2	16-3	14.8	14.5	4	3	1.21	170
3	16-4	18.9	18.4	4	3	1.05	195
4	16-2	12.6	12.5	8	6	1.22	167
5	16-3	15.2	14.7	8	6	1.25	194
6	16-4	19.2	18.4	8	6	1.19	220

a: Macro-RAFT agent used, key parameters shown in Table 16.

b: Molar mass calculated from NMR by comparison of *N*-vinyl pyrrolidone unit resonance in the polymer versus vinyl acetate and vinyl pivalate unit resonance.

c: Molar mass calculated from SEC using DMF as solvent and PMMA calibration standards.

d: Degree of polymerisation calculated by integration of the NVP repetitive unit resonances and the resonance of the VAc and VPi units.

All products were analysed by SEC in DMF. Both the RI (**Figure 100100**) and UV (**Figure 101101**) show a clear shift to lower retention time with increasing DP of PNVP. Furthermore, UV shows very little or no overlap with the starting P(VAc-stat-VPi)-X2 macro-RAFT, which indicates that there is a very low amount of head to head chains and all the head to tail chains have extended. Dispersity values are narrow for all the products (<1.5). This confirms the formation of block copolymers with high purity.

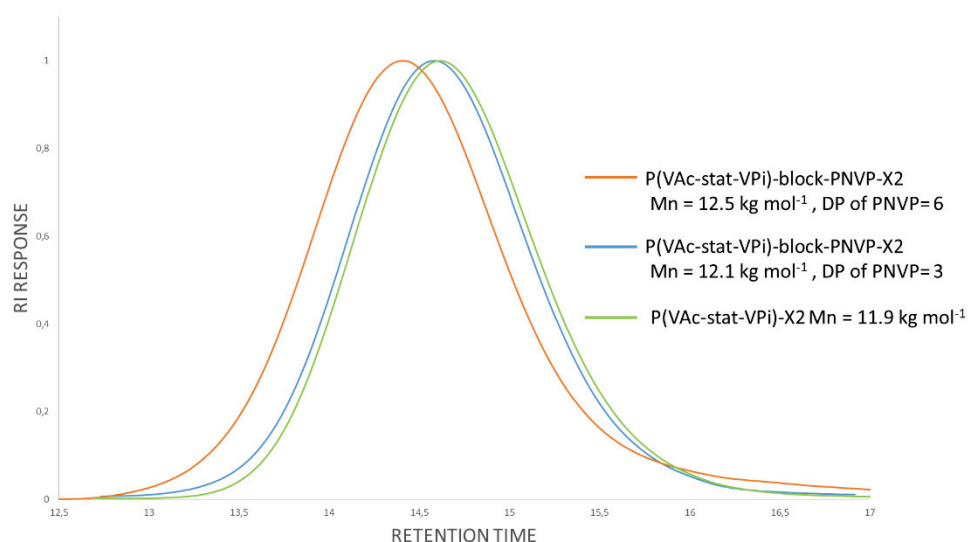


Figure 100: Normalised RI response from SEC in DMF of a) *P*(VAc-stat-VPI)-X2 $M_n=11.9 \text{ kg mol}^{-1}$ (Table 17, entry 2), b) *P*(VAc-stat-VPI)-block-PNVP-X2 $M_n=12.2 \text{ kg mol}^{-1}$ DP of PNVP= 3 (Table 19, entry 1) c) *P*(VAc-stat-VPI)-block-PNVP-X2 $M_n=12.5 \text{ kg mol}^{-1}$ DP of PNVP= 6 (Table 19, entry 4).

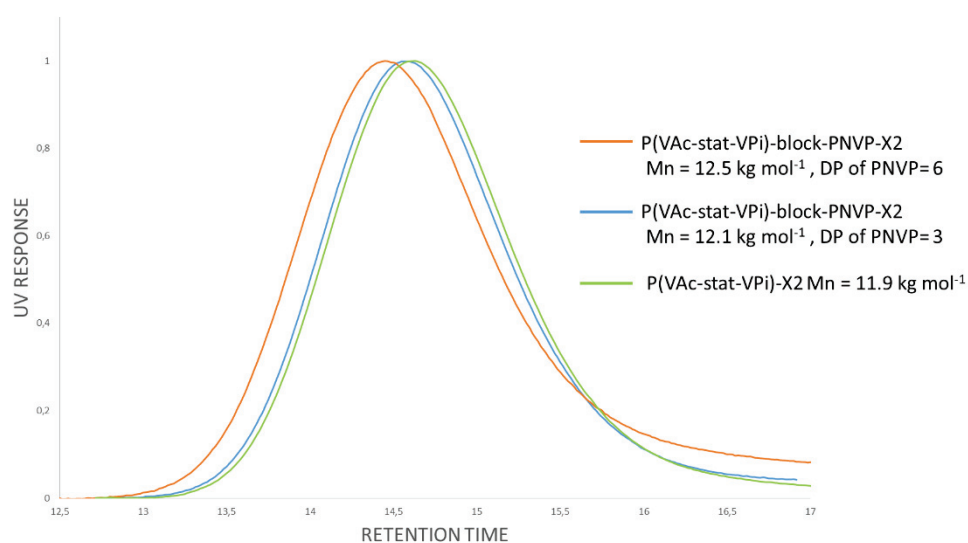


Figure 101: Normalised RI response from SEC in DMF of a) *P*(VAc-stat-VPI)-X2 $M_n=11.9 \text{ kg mol}^{-1}$ (Table 17, entry 2), b) *P*(VAc-stat-VPI)-block-PNVP-X2 $M_n=12.2 \text{ kg mol}^{-1}$ DP of PNVP= 3 (Table 19, entry 1) c) *P*(VAc-stat-VPI)-block-PNVP-X2 $M_n=12.5 \text{ kg mol}^{-1}$ DP of PNVP= 6 (Table 19, entry 4).

Cloud point experiments of the materials were carried out (Table 19). It was hypothesised that, since block copolymers are less soluble in CO₂ than the starting homopolymers, this increase in purity would have a big impact in the solubility of the samples.

However, contrary to what was expected, all samples showed cloud points in the range of those presented by block copolymers of similar molar mass and DP of PNVP synthesised in Chapter 3 (**Figure 5858**). This could be explained by the fact that, although having more block copolymer decreases the solubility, a higher RAFT end functionality results in a lower side formation of PNVP homopolymer and this increases the solubility. Both effects could balance themselves.

In any case, all the stabilisers are completely soluble at dispersion polymerisation conditions (35°C, 276 bar).

In order to compare the performance of the block copolymers with the statistical ones they are made from, in dispersion polymerisation, a standard dispersion polymerisation of NVP using one of these materials (**Table 19, entry 1**) was carried out. A fine polymer powder was obtained upon depressurisation of the autoclave. The product morphology was analysed by SEM (**Figure 102**).

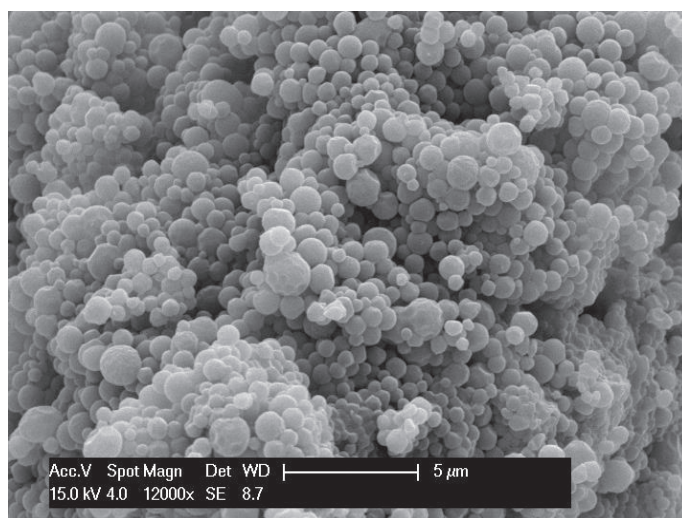


Figure 102: PNVP polymer particles made by dispersion polymerisation in scCO₂ using 5 wt% of P(VAc-stat-VPI)-block-PNVP (Table 19, entry 1).

Spherical particles of homogenous size (220 ± 30 nm) and shape were observed, comparable to those obtained with the equivalent P(VAc-*stat*-VPi)-X2 and improved compared to the ones made with the P(VAc-*stat*-VPi)-*block*-PNVP stabilisers synthesised in chapter 3, that were not uniform in shape and size.

It was then concluded that the new block copolymer stabilisers synthesised from the statistical macro-RAFTs with improved purity perform better in dispersion polymerisation of NVP, producing more uniform particles. This can be explained by a lower amount of undesired side products such as PNVP homopolymer being formed during the chain extension reaction.

Stabiliser loading

In order to find the optimum stabiliser loading for our system of interest, the same P(VAc-*stat*-VPi)-*block*-PNVP-X2 (**Table 19, entry 1**) was tested in dispersion polymerisation of MMA at 5, 10 and 15 wt.% loading. Results are shown in **Table 20**.

*Table 20: Key parameters of PMMA products made by dispersion polymerisation in scCO₂ at 35°C and 276 bar using P(VAc-*stat*-VPi)-*block*-PNVP-X2 (**Table 19, entry 1**) at 5, 10 and 15 wt.%.*

Entry	Stabiliser loading (wt.%)	Product M_n (SEC) ^a kg mol ⁻¹
1	5	18.2
2	10	50.3
3	15	60.1

a: Molar mass calculated from SEC using chloroform as solvent and PMMA calibration standards

The PMMA products were analysed by SEC in THF. For the reaction at 5wt. % stabiliser loading (**Table 2020, entry 1**), a low molar mass polymer was obtained. This indicates an insufficient amount of stabiliser that leads to coagulation of the particles at an early stage.

For reactions at 10 and 15 wt. % stabiliser loading (**Table 2020, entries 2-3**) bimodal M_n distributions were observed (**Figure 103**), meaning there is a higher M_n material which has been stabilised, and a low M_n material that has precipitated most likely due to an insufficient amount of stabiliser. It is worth noting that no improvement is observed when increasing the stabiliser loading from 10 to 15wt. %. Both peaks overlap to some extent, making it difficult to accurately determine the M_n of both materials. M_n data shown in **Table 21** should only be taken as an estimation. For the same reason, dispersity values are not shown.

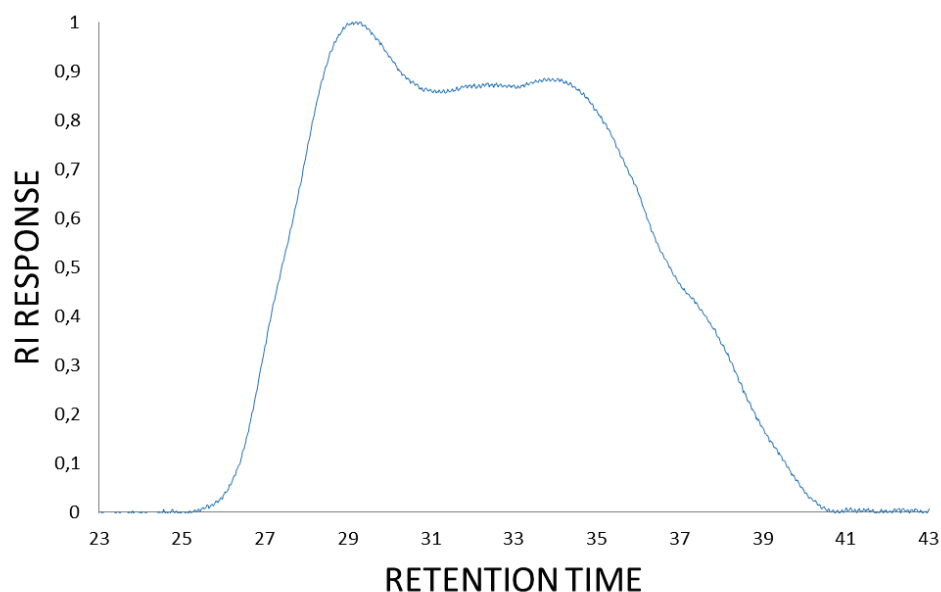


Figure 103: SEC in THF of a PMMA product made by dispersion polymerisation in $scCO_2$ at 35°C and 276 bar using P(VAc-stat-VPI)-block-PNVP-X2 (**Table 19, entry 1**) at 10 wt. %.

In all of the cases a mixture of a solid and a dense liquid (low M_n PMMA) were collected upon depressurisation of the autoclave (**Figure 104**), instead of the expected powder. This indicates that reaction did not proceed to completion, although it is not possible to determine conversion accurately for a heterogeneous mixture. This is also in agreement with SEC observations.



Figure 104: Picture of autoclave contents upon depressurisation for the dispersion polymerisation of PMMA in $scCO_2$ at 35°C and 276 bar using 5 wt.% of P(VAc-stat-VPI)-block-PNVP-X2 (**Table 20, entry 1**).

The particle morphology was analysed by SEM (**Figure 105**).

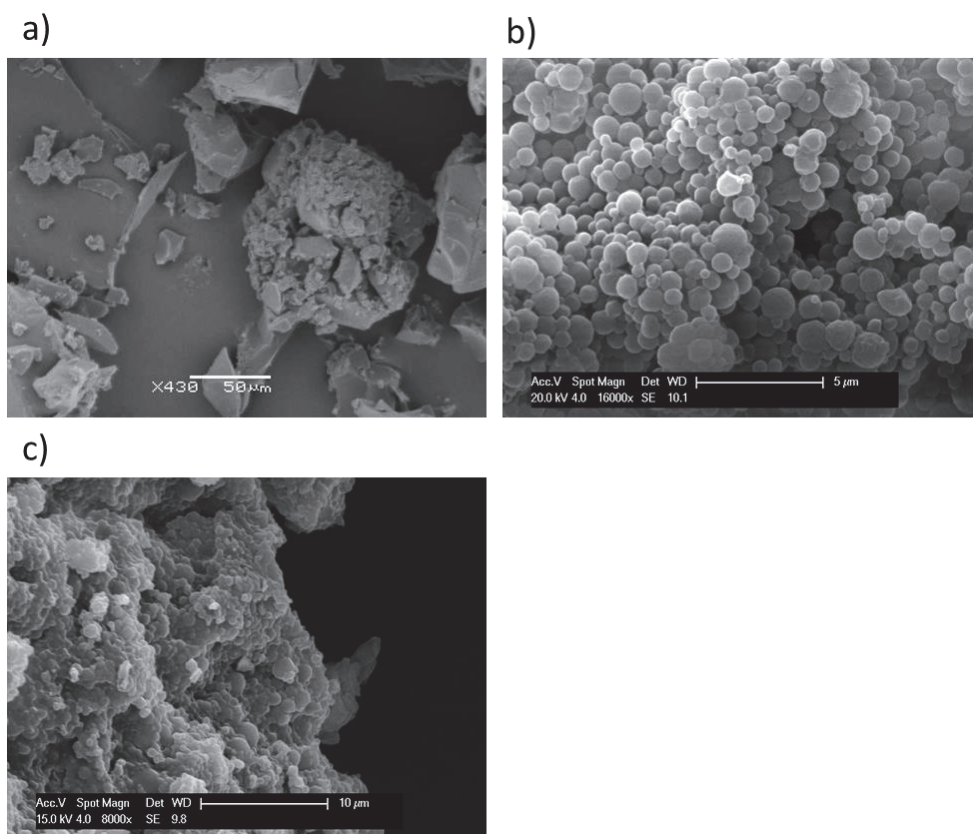


Figure 105: PMMA polymer particles made by dispersion polymerisation in $scCO_2$ using a $P(VAc-stat-VPI)$ -block-PNVP (Table 20, entry 1) loading of a) 5 wt.%, b) 10 wt. %, c) 15 wt. %.

In the case of the reaction at 5wt. % stabiliser loading (**Table 2020, entry 1**), an amorphous product was observed (**Figure 105, a**), which agrees with the SEC data and is the expected result for a precipitation. Well defined spherical particles in the range of 200 to 400 nm were observed for the reaction at 10 wt. % stabiliser (**Table 20, entry 2**) (**Figure 105, b**). Increasing the stabiliser loading to 15 wt. % (**Table 20, entry 3**) not only did not show any improvement in morphology but it also resulted in particle coagulation (**Figure 105, c**). It was therefore decided to use a loading of 10 wt. % for the remaining experiments.

The rest of the stabilisers were then tested in dispersion polymerisation of MMA at 10 wt. % loading. Results are summarised in **Table 21**.

Table 21: Key parameters of PMMA products made by dispersion polymerisation in scCO₂ at 35°C and 276 bar using block copolymers of VAc:VPi ratios between 40:60 and 50:50, M_n between 12 and 18 kg mol⁻¹ and DP of NVP of 3 or 6.

Entry	Stabiliser ^a	Product M_n (SEC) ^b kg mol ⁻¹
1	19-1	50.3
2	19-2	60
3	19-3	61.2
4	19-4	54.8
5	19-5	49.3
6	19-6	49.3

a: stabiliser used in dispersion polymerisation, key parameters shown in table 19.

b: Molar mass calculated from SEC using chloroform as solvent and PMMA calibration standards

The PMMA products were analysed by SEC in THF. Again, a bimodal distribution of M_n can be observed in all cases, indicating the presence of a higher M_n stabilised material and a low M_n precipitated one. As in the previous sets of experiments, a mixture of a solid and a dense liquid were collected upon depressurisation of the autoclave in all cases.

The morphology of the solid products was analysed by SEM. Images are shown in **Figure 106**.

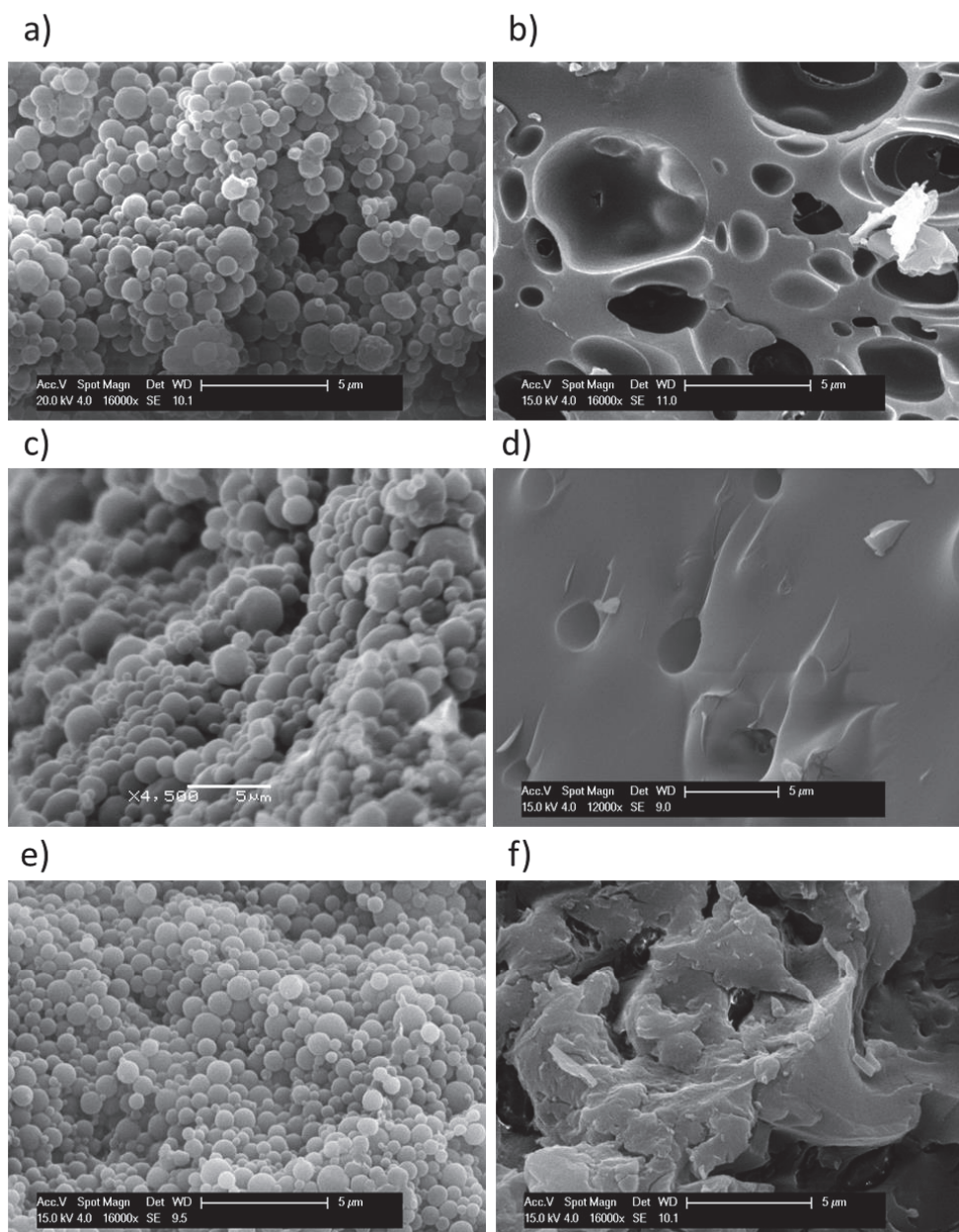


Figure 106: PMMA polymer particles made by dispersion polymerisation in $scCO_2$ using 10 wt% of $P(VAc-stat-VPI)-block-PNVP$: a) $M_n = 12.1 \text{ kg mol}^{-1}$ (Table 21, entry 1), b) 12.6 kg mol^{-1} (Table 21, entry 4), c) 14.8 kg mol^{-1} (Table 21, entry 2), d) 15.2 kg mol^{-1} (Table 21, entry 5), e) 18.9 kg mol^{-1} (Table 21, entry 3), f) 19.2 kg mol^{-1} (Table 21, entry 6).

In the case of $P(VAc-stat-VPI)-block-PNVP$ with DP_{NVP} of 3 units, a trend in the amount and quality of the particles with the M_n was found. The stabiliser of lower M_n (Table 19, entry 1) produced a material that was mainly amorphous although some spherical particles of sizes between 150 and 300

nm could be observed (**Figure 106106, a**). Using a stabiliser with slightly higher M_n (**Table 19, entry 2**) resulted in a material with a higher proportion of spherical particles with sizes in the range of 250-400 nm (**Figure 106106, c**). Finally, the stabiliser of higher M_n (**Table 19, entry 3**) produced well defined, spherical homogenous particles of 180 ± 30 nm. (**Figure 106106, e**). A decrease in the particle size is observed with the highest M_n stabiliser, which matches previous observations reported for these type of stabilisers.¹⁶⁹

In the case of the stabilisers with DP_{NVP} of 6 units we observe in all cases a highly agglomerated amorphous material (**Figure 106106, b, d, f**). This could be partially explained by a lower solubility of these stabilisers compared to the previous ones.

5.3.3.1 P(VAc-*stat*-VPi)-*block*-PNVP with high DP_{NVP}

P(VAc-*stat*-VPi)-*block*-PNVP with high DP_{NVP} were synthesised from the corresponding P(VAc-*stat*-VPi) macro-RAFTs (**Table 17**). A DP of 35 units was chosen as the starting point. All stabilisers are insoluble in $scCO_2$ at the reaction conditions. Results are summarised in **Table 22**.

Table 22: Key parameters of *P*(VAc-stat-VPi)-*block*-PNVP-X2 copolymer stabilisers synthesised from *P*(VAc-stat-VPi)-X2 (Table 17) (by RAFT polymerisation in THF at 60°C for 180 minutes).

Entry	Macro-RAFT ^a	Mn _{NMR} (kgmol ⁻¹) ^b	Mn _{SEC} (kg mol ⁻¹) ^c	DP target	DP exp ^d	\bar{D}
1	16-2	15.9	16.9	38	36	1.38
2	16-3	18.4	18.4	38	35	1.42
3	16-4	21.8	24.6	38	29	1.31

a: Macro-RAFT agent used, key parameters shown in Table 16.

b: Molar mass calculated from NMR by comparison of *N*-vinyl pyrrolidone unit resonance in the polymer versus vinyl acetate and vinyl pivalate unit resonance.

c: Molar mass calculated from SEC using DMF as solvent and PMMA calibration standards.

d: Degree of polymerisation calculated by integration of the NVP repetitive unit resonances and the resonance of the VAc and VPi units.

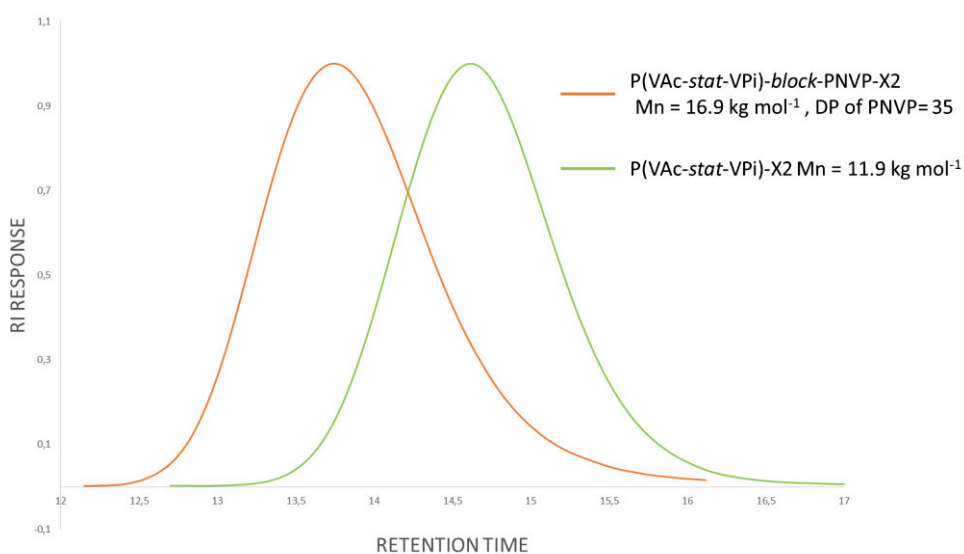


Figure 107: Normalised RI response from SEC in DMF of a) *P*(VAc-stat-VPi)-X2 Mn=11.9 kg mol⁻¹ (Table 17, entry 2), b) *P*(VAc-stat-VPi)-*block*-PNVP-X2 Mn=16.9 kg mol⁻¹ DP of PNVP= 36 (Table 22, entry 1)

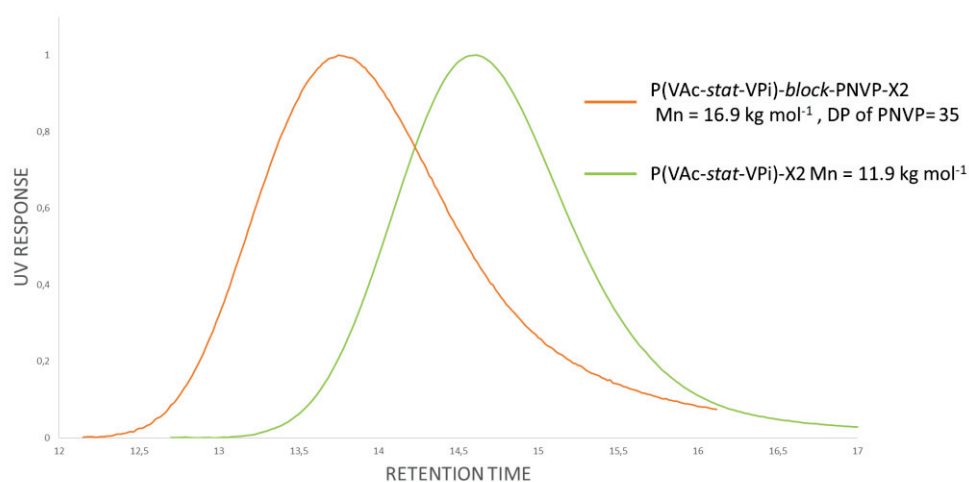


Figure 108: Normalised UV response from SEC in DMF of a) P(VAc-stat-VPI)-X2 Mn=11.9 kg mol⁻¹ (Table 17, entry 2), b) P(VAc-stat-VPI)-block-PNVP-X2 Mn=16.9 kg mol⁻¹ DP of PNVP= 36 (Table 22, entry 1)

Similarly to the low DP block copolymers, both the RI (**Figure 107**) and UV (**Figure 108**) show clear shifts to lower retention time when increasing the DP of PNVP. UV does not show the characteristic peak for head to head chains, indicating a neat chain extension. Dispersity values are narrow for all the products (<1.5). This confirms the formation of block copolymers with high purity.

Stabilisers 1-3 were tested in dispersion polymerisation of MMA. Products were collected as a mixture of solid and dense liquid, as in previous experiments, instead of the expected dry powder, indicating that reaction has not reached high conversion. Results are shown in **Table 23**.

Table 23: Key parameters of PMMA products made by dispersion polymerisation in scCO₂ at 35°C and 276 bar using block copolymers of VAc:VPi ratios between 40:60 and 50:50, M_n between 17 and 25 kg mol⁻¹ and DP of NVP between 29 and 36.

Entry	Stabiliser ^a	Product
		M_n (SEC) kg mol ⁻¹ ^b
1	22-1	62.4
2	22-2	50
3	22-3	165

a: stabiliser used in dispersion polymerisation, key parameters shown in table 22.

b: Molar mass calculated from SEC using chloroform as solvent and PMMA calibration standards

A bimodal distribution is again observed in the SEC plots indicating the presence of a higher and a lower M_n material. It is worth noting that stabiliser 16-3 provides a PMMA material with the highest M_n and lower dispersity. This is an indication of a better stabilisation.

The product morphology was analysed by SEM (**Figure 109**).

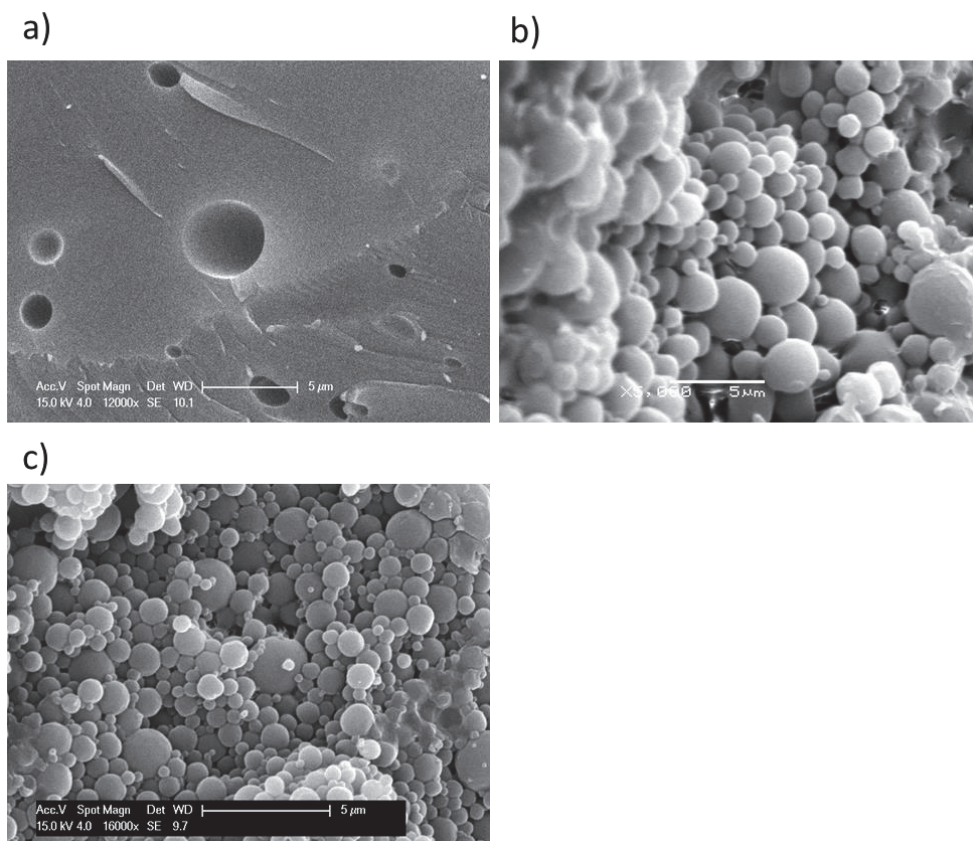


Figure 109: PMMA polymer particles made by dispersion polymerisation in $scCO_2$ using $P(VAc-stat-VPI)$ -block-PNVP with a DP of NVP between 29 and 36. a) Table 23 entry 1, b) Table 23, entry 2, c) Table 23, entry 3.

The same trend as in the case of low DP of PNVP stabilisers was found. Increasing the M_n of the stabiliser resulted in better stabilised materials. In the case of stabiliser **Table 22, entry 1** an amorphous morphology was observed. Using a stabiliser of higher molecular weight (**Table 22, entry 2**) resulted in a material that is mostly constituted by uniform spherical particles, although particle size could not be determined due to particle agglomeration. Finally, the stabiliser with the highest M_n **Table 22, entry 3** provided a very uniform material with a spherical morphology and particle

size in the range of 250 to 350 nm. In addition, particles appeared smaller than for the previous stabiliser.

5.4 Conclusions

P(VAc-*stat*-VPi)-X2 copolymers with a lower amount of head to head chains were synthesised and tested in dispersion polymerisation of NVP in scCO₂, yielding uniform spherical particles comparable to those reported in the literature for the same kind of stabilisers.

Two types of P(VAc-*stat*-VPi)-*block*-PNVP-X2 copolymers were then successfully synthesised from the statistical copolymers, one with a low DP of PNVP (3-6) and the other with a higher one (35). All materials were synthesised with high purity and low dispersity, as confirmed by SEC in DMF.

A P(VAc-*stat*-VPi)-*block*-PNVP-X2 of $M_n = 12.1 \text{ kg mol}^{-1}$ and a DP of PNVP of 3 was then tested in dispersion polymerisation of NVP, producing uniform spherical particles in the same way as the starting statistical copolymer.

The same stabiliser was then tested in dispersion polymerisation of MMA, the monomer of interest. Stabiliser loadings of 5, 10 and 15 wt. % were chosen as the starting point to determine the optimum reaction conditions for this system. Although none of the reactions proceeded to completion and the product was retrieved as a mixture of liquid and solid instead of a powder, spherical particles were found for a loading of 10 wt. %. This is the first time that hydrocarbon based stabilisers are employed in the dispersion polymerisation of MMA in scCO₂ with mild success.

Increasing the loading to 15 wt. % did not show any improvement, contrary to the expected from the literature, and it led to particle coagulation.

The rest of the synthesised block copolymers were then tested at a 10 wt. % loading. Again, conversions were not as high as expected for this kind of process, but an increase in the quality of the particles when increasing the molar mass of the stabiliser was observed in the case of both the blocks of DP of PNVP 3 and 35. The blocks of DP of PNVP 6 yielded amorphous products, likely due to a low solubility of the stabilisers.

It was hypothesised that low DP and high DP block copolymer stabilisers might work *via* a different anchoring mechanism. The first type, being soluble in CO₂, could adsorb to the surface of the particle, while the second type, having a highly CO₂-phobic block would partition between the particles and the CO₂. Further research is necessary in order to confirm this hypothesis and also to solve the issue of reaction conversion and produce better quality materials.

Chapter 6: Conclusions and future research

Dispersion polymerisation in scCO₂ as an alternative green solvent has been widely investigated in recent years.^{113, 121, 123, 125} However, one of the main limitations for the industrial application of dispersion polymerisation in this solvent is the need of highly soluble and effective stabilisers that are both affordable and environmentally friendly. The most widely used stabilisers are fluorinated and silicone based ones, but these are expensive, potentially toxic and bio-accumulative. Hydrocarbon based stabilisers constitute a very promising alternative, however they have only worked for one monomer system so far, NVP.¹¹⁵

Throughout this thesis, the design of new CO₂-soluble hydrocarbon based stabilisers has been investigated. RAFT polymerisation has been used to produce well defined block polymers of a targeted molar mass and architecture. The ability of these materials to stabilise polymeric particles in dispersion polymerisation in scCO₂ has been explored.

Chapter 3 explored the synthesis of P(VAc-*stat*-VPi)-*block*-PNVP-X2 copolymers via RAFT/MADIX polymerisation. A series of polymers of different Mn, VAc:VPi molar ratios and DP of PNVP were prepared and fully characterised by ¹H NMR, SEC and DSC.

The phase behavior of these materials in scCO₂ was then evaluated using a high pressure variable volume view cell. In all cases, it was observed that increasing the VPi content resulted in an increase in solubility, which matched results reported in the literature.¹⁶⁹ Furthermore, increasing the

DP of PNVP led to a decrease in solubility, as expected since PNVP is a CO₂-phobic polymer. Samples were found soluble up to a DP of PNVP of 10 units at dispersion polymerisation conditions (35 °C, 276 bar).

These materials were then tested in dispersion polymerisation of MMA and NVP in scCO₂. None of the stabiliser samples were able to produce PMMA particles with spherical morphology and they did not match the performance of previous stabilisers in the dispersion polymerisation of NVP. This suggested an underlying issue with the way they were synthesised, that was also pointed out by the low RAFT-end functionality seen by ¹H NMR for the P(VAc-*stat*-VPi)-X2 macro-RAFTs they were prepared from.

Chapter 4 investigated the phenomena of head to head addition in RAFT polymerisation of vinyl acetate and vinyl pivalate. Different reaction parameters like DP_n, conversion, temperature and monomer addition order were tested.

It was found that, while decreasing the DP_n did not seem to have a significant effect in the formation of head to head chains for the range of M_n under investigation, decreasing the conversion decreased the occurrence of this side reaction substantially. Furthermore, decreasing the reaction temperature resulted in a slight increase in head to head chains. These results contradicted what is reported in the literature for the polymerisation of this kind of monomers.¹⁵⁷

Despite not being able to produce a material with a 100% of RAFT terminated head to tail chains by any of the different methods tried, a

significant improvement in the quality of these materials was achieved when decreasing the conversion.

This method was used in chapter 5 to synthesise P(VAc-*stat*-VPi)-*block*-PNVP-X2 copolymers with improved purity. Two types of copolymers were successfully prepared from the homopolymers, one with a low DP of PNVP (3-6) and the other with a higher one (35), both with high purity and low dispersity, as confirmed by SEC in DMF.

A stabiliser loading of 10 wt. % was found optimum for the dispersion polymerisation of MMA in scCO₂ with these materials. Conversions were not as high as expected for this kind of process, but an increase in the quality of the particles when increasing the molar mass of the stabiliser was observed in the case of both the blocks of DP of PNVP 3 and 35. The blocks of DP of PNVP 6 yielded amorphous products, likely due to a low solubility of the stabilisers.

It was hypothesised that low DP and high DP block copolymer stabilisers have a different anchoring mechanism. The first type, soluble in CO₂, would adsorb to the surface of the particle, while the second type, having a highly CO₂-phobic block would partition between the particles and the CO₂.

In order to confirm this mechanism, further research needs to be carried out. Techniques like high pressure FTIR or high pressure NMR could help identify the interactions that form between the stabiliser and the polymer.^{134, 170} In addition, washing the particles with an appropriate solvent and

characterizing that solution by NMR and SEC could indicate whether the stabiliser is chemically attached to the particles or just physically adsorbed.

In order to address the issue of low reaction conversions, different approaches could be tried. Firstly, it is necessary to perform a more extensive loading study, with higher stabiliser loadings for different stabilisers. In addition, it is necessary to explore block copolymers with a wider variety of PNVP blocks in order to determine the optimum ASB (anchor soluble balance) for this particular type of stabilisers.

Another approach could be using sequential dispersion polymerisation¹⁵⁵, where the reaction is started with a low amount of monomer, and once the particles are formed, the rest of the monomer is injected.

A completely different approach would be to design new stabilisers with a more polymer-philic block, such as *P(VAc-stat-VPI)-block-PMMA* copolymers. As already discussed in Chapter 3, the synthesis of these is not straightforward and it would be necessary to use a switchable RAFT agent to polymerise both types of monomers¹⁷¹ or a different technique such as ATRP.¹⁷²

References

1. Anastas, P. T.; Heine, L. G.; Williamson, T. C., Green Chemical Syntheses and Processes: Introduction. In *Green Chemical Syntheses and Processes*, American Chemical Society: 2000; Vol. 767, pp 1-6.
2. Anastas, P. T. W., J., Green Chemistry: theory and practice. *Oxford University Press* **1998**.
3. Jessop, P. G., Searching for green solvents, *Green Chemistry* **2011**, *13*, 1391.
4. M., S. G., Physicochemical Principles of Extraction with Supercritical Gases. *Angewandte Chemie International Edition in English* **1978**, *17* (10), 716-727.
5. Reinhardt, D.; Ilgen, F.; Kralisch, D.; König, B.; Kreisel, G., Evaluating the greenness of alternative reaction media. *Green Chemistry* **2008**, *10* (11), 1170.
6. Kainz, S.; Brinkmann, A.; Leitner, W.; Pfaltz, A., Iridium-Catalyzed Enantioselective Hydrogenation of Imines in Supercritical Carbon Dioxide. *Journal of the American Chemical Society* **1999**, *121* (27), 6421-6429.
7. Chatterjee, M.; Ikushima, Y.; Zhao, F.-Y., Highly Efficient Hydrogenation of Cinnamaldehyde Catalyzed by Pt-MCM-48 in Supercritical Carbon Dioxide. *Catalysis Letters* **2002**, *82* (1), 141-144.
8. Leitner, W., Designed to dissolve. *Nature* **2000**, *405*, 129.
9. Licence, P.; Litchfield, D.; Dellar, M. P.; Poliakoff, M., "Supercriticality"; a dramatic but safe demonstration of the critical point. *Green Chemistry* **2004**, *6* (8), 352-354.
10. Oakes, R. S.; Clifford, A. A.; Rayner, C. M., The use of supercritical fluids in synthetic organic chemistry. *Journal of the Chemical Society, Perkin Transactions 1* **2001**, (9), 917-941.
11. P.G., A. P. T. L. W. J., Green Solvents: Supercritical Solvents. *John Wiley and sons* **2014**, *4*.
12. Turner, C., From supercritical carbon dioxide to gas expanded liquids in extraction and chromatography of lipids. *Lipid Technology* **2015**, *27* (12), 275-277.
13. Clifford, T., Fundamentals of Supercritical Fluids. *Oxford University Press* **1999**.
14. (HSE), H. a. S. E., EH40/2005 Workplace Exposure Limits. *HSE Books* **2011**.
15. Darr, J. A.; Poliakoff, M., New Directions in Inorganic and Metal-Organic Coordination Chemistry in Supercritical Fluids. *Chemical Reviews* **1999**, *99* (2), 495-542.
16. Gorbaty, Y. E.; Gupta, R. B., The Structural Features of Liquid and Supercritical Water. *Industrial & Engineering Chemistry Research* **1998**, *37* (8), 3026-3035.
17. Haugen, H. A.; Eldrup, N. H.; Fatnes, A. M.; Leren, E., Commercial Capture and Transport of CO₂ from Production of Ammonia. *Energy Procedia* **2017**, *114*, 6133-6140.
18. Tsouris, C., Separation of CO₂ from Flue Gas: A Review AU - Aaron, Douglas. *Separation Science and Technology* **2005**, *40* (1-3), 321-348.
19. Raventós, M.; Duarte, S.; Alarcón, R., Application and Possibilities of Supercritical CO₂ Extraction in Food Processing Industry: An Overview. *Food Science and Technology International* **2002**, *8* (5), 269-284.
20. Brunner, G., Supercritical fluids: technology and application to food processing. *Journal of Food Engineering* **2005**, *67* (1-2), 21-33.
21. Boyère, C.; Jérôme, C.; Debuigne, A., Input of supercritical carbon dioxide to polymer synthesis: An overview. *European Polymer Journal* **2014**, *61*, 45-63.
22. M., K. F., Alternative Solvents for Green Chemistry. *RSC publishing* **2009**.

23. IUPAC, Glossary of basic terms in Polymer Science (IUPAC Recommendations). **1996**, 68, 2287-2311.
24. Cowie, J., Arrighi, V. , Polymers: Chemistry and Physics of Modern Materials. *CRC Press* **2007**.
25. Mayo, F. R.; Lewis, F. M., Copolymerization. I. A Basis for Comparing the Behavior of Monomers in Copolymerization; The Copolymerization of Styrene and Methyl Methacrylate. *Journal of the American Chemical Society* **1944**, 66 (9), 1594-1601.
26. Jenkins, A. D.; Kratochvíl, P.; Stepto, R. F. T.; Suter, U. W., Glossary of basic terms in polymer science (IUPAC Recommendations 1996). In *Pure and Applied Chemistry*, 1996; Vol. 68, p 2287.
27. Stille, J. K., Step-growth polymerization. *Journal of Chemical Education* **1981**, 58 (11), 862.
28. A., R., Principles of polymer chemistry. *Springer US* **2000**.
29. Flory, P. J., Principles of Polymer Chemistry. *Cornell University Press* **1953**.
30. Costa, M., Step-Growth and Ring-Opening Polymerization. 2013.
31. Matthews, M. S., Polymer Chemistry: Introduction to an Indispensable Science (David M. Teegarden). *Journal of Chemical Education* **2005**, 82 (2), 213.
32. Moad G., Solomon. D. H., The Chemistry of Radical Polymerization. **1995**.
33. Su, W. F., Radical Chain Polymerization. In *Principles of Polymer Design and Synthesis*, Springer Berlin Heidelberg: Berlin, Heidelberg, 2013; pp 137-183.
34. R, H., Polymer Handbook, 4th edn, Edited by J Brandup, EH Immergut and EA Grulke, Associate Editors A Abe and DR Bloch, John Wiley and Sons, New York, 1999, pp 2250, price £210 ISBN 0-471-16628-6. *Polymer International* **2000**, 49 (7), 807-807.
35. Matyjaszewski, K.; Gaynor, S. G., Free radical polymerization. In *Applied Polymer Science: 21st Century*, Craver, C. D.; Carraher, C. E., Eds. Pergamon: Oxford, 2000; pp 929-977.
36. Jenkins Aubrey, D.; Jones Richard, G.; Moad, G., Terminology for Reversible-Deactivation Radical Polymerization Previously Called "Controlled" Radical or "Living" Radical Polymerization.
37. Szwarc, M., Living polymers and mechanisms of anionic polymerization. In: Living Polymers and Mechanisms of Anionic Polymerization. *Advances in Polymer Science* **1983**, 49, 1-177.
38. Destarac, M., Controlled Radical Polymerization: Industrial Stakes, Obstacles and Achievements. *Macromolecular Reaction Engineering* **2010**, 4 (3-4), 165-179.
39. Otsu, T.; Yoshida, M.; Tazaki, T., A model for living radical polymerization. *Die Makromolekulare Chemie, Rapid Communications* **1982**, 3 (2), 133-140.
40. Grubbs, R. B., Nitroxide-Mediated Radical Polymerization: Limitations and Versatility. *Polymer Reviews* **2011**, 51 (2), 104-137.
41. Nicolas, J.; Guillaneuf, Y.; Lefay, C.; Bertin, D.; Gigmes, D.; Charleux, B., Nitroxide-mediated polymerization. *Progress in Polymer Science* **2013**, 38 (1), 63-235.
42. Matyjaszewski, K., Atom Transfer Radical Polymerization (ATRP): Current Status and Future Perspectives. *Macromolecules* **2012**, 45 (10), 4015-4039.
43. Chiefari, J.; Chong, Y. K.; Ercole, F.; Krstina, J.; Jeffery, J.; Le, T. P. T.; Mayadunne, R. T. A.; Meijs, G. F.; Moad, C. L.; Moad, G.; Rizzardo, E.; Thang, S. H., Living Free-Radical Polymerization by Reversible Addition-Fragmentation Chain Transfer: The RAFT Process. *Macromolecules* **1998**, 31 (16), 5559-5562.

44. Destarac, M.; Charmot, D.; Franck, X.; Zard, S. Z., Dithiocarbamates as universal reversible addition-fragmentation chain transfer agents. *Macromolecular Rapid Communications* **2000**, *21* (15), 1035-1039.
45. Hawker, C. J., Molecular Weight Control by a "Living" Free-Radical Polymerization Process. *Journal of the American Chemical Society* **1994**, *116* (24), 11185-11186.
46. Petton, L.; Ciolino, A.; Dervaux, B.; Du Prez, F., *From one-pot stabilisation to in situ functionalisation in nitroxide mediated polymerisation: An efficient extension towards atom transfer radical polymerisation*. 2012; Vol. 3, p 1867-1878.
47. Benoit, D.; Chaplinski, V.; Braslau, R.; Hawker, C. J., Development of a Universal Alkoxyamine for "Living" Free Radical Polymerizations. *Journal of the American Chemical Society* **1999**, *121* (16), 3904-3920.
48. Kamigaito, M.; Ando, T.; Sawamoto, M., Metal-catalyzed living radical polymerization: discovery and developments. *The Chemical Record* **2004**, *4* (3), 159-175.
49. Wang, J.-S.; Matyjaszewski, K., Controlled/"living" radical polymerization. atom transfer radical polymerization in the presence of transition-metal complexes. *Journal of the American Chemical Society* **1995**, *117* (20), 5614-5615.
50. Kwak, Y.; Matyjaszewski, K., Effect of Initiator and Ligand Structures on ATRP of Styrene and Methyl Methacrylate Initiated by Alkyl Dithiocarbamate. *Macromolecules* **2008**, *41* (18), 6627-6635.
51. Keddie, D. J., A guide to the synthesis of block copolymers using reversible-addition fragmentation chain transfer (RAFT) polymerization. *Chemical Society reviews* **2014**, *43* (2), 496-505.
52. Moad, G.; Rizzardo, E.; Thang, S. H., A RAFT Tutorial. *The Strem Chemiker* **2011**, *15* (1), 1-12.
53. Moad, G.; Rizzardo, E.; Thang, S. H., Toward Living Radical Polymerization. *Accounts of chemical research* **2008**, *41* (9), 1133-1142.
54. Moad, G.; Rizzardo, E.; Thang, S. H., Living Radical Polymerization by the RAFT Process. *Australian Journal of Chemistry* **2005**, *58* (6), 379-410.
55. Tang, D.; Jiang, X.; Liu, H.; Li, C.; Zhao, Y., Synthesis and properties of heterografted toothbrush-like copolymers with alternating PEG and PCL grafts and tunable RAFT-generated segments. *Polymer Chemistry* **2014**, *5* (16), 4679.
56. Haraguchi, K.; Kubota, K.; Takada, T.; Mahara, S., Highly Protein-Resistant Coatings and Suspension Cell Culture Thereon from Amphiphilic Block Copolymers Prepared by RAFT Polymerization. *Biomacromolecules* **2014**, *15* (6), 1992-2003.
57. Jennings, J.; Beija, M.; Kennon, J. T.; Willcock, H.; O'Reilly, R. K.; Rimmer, S.; Howdle, S. M., Advantages of Block Copolymer Synthesis by RAFT-Controlled Dispersion Polymerization in Supercritical Carbon Dioxide. *Macromolecules* **2013**, *46* (17), 6843-6851.
58. Liu, J.; Duong, H.; Whittaker, M. R.; Davis, T. P.; Boyer, C., Synthesis of Functional Core, Star Polymers via RAFT Polymerization for Drug Delivery Applications. *Macromolecular Rapid Communications* **2012**, *33* (9), 760-766.
59. Gody, G.; Barbey, R.; Danial, M.; Perrier, S., Ultrafast RAFT polymerization: multiblock copolymers within minutes. *Polym. Chem.* **2015**, *6* (9), 1502-1511.
60. Braslau, R., Handbook of Radical Polymerization Edited by Krzysztof Matyjaszewski (Carnegie Mellon University) and Thomas P. Davis (University of New South Wales). John Wiley & Sons, Inc.: Hoboken. 2002. xvi + 920 pp. \$200.00. ISBN 0-471-39274-X. *Journal of the American Chemical Society* **2003**, *125* (11), 3399-3400.

61. Perrier, S.; Barner-Kowollik, C.; Quinn, J. F.; Vana, P.; Davis, T. P., Origin of Inhibition Effects in the RAFT Polymerization of MA. *Macromolecules* **2002**, *32*, 8300-8306.
62. Perrier, S.; Takolpuckdee, P., Macromolecular design via reversible addition-fragmentation chain transfer (RAFT)/xanthates (MADIX) polymerization. *Journal of Polymer Science Part A: Polymer Chemistry* **2005**, *43* (22), 5347-5393.
63. Moad, G.; Chiefari, J.; Chong, Y. K.; Krstina, J.; Mayadunne, R. T. A.; Postma, A.; Rizzardo, E.; Thang, S. H., Living free radical polymerization with reversible addition – fragmentation chain transfer (the life of RAFT). *Polymer International* **2000**, *49* (9), 993-1001.
64. Feldermann, A.; Coote, M. L.; Stenzel, M. H.; Davis, T. P.; Barner-Kowollik, C., Consistent Experimental and Theoretical Evidence for Long-Lived Intermediate Radicals in Living Free Radical Polymerization. *Journal of the American Chemical Society* **2004**, *126* (48), 15915-15923.
65. Vana, P.; Davis, T. P.; Barner-Kowollik, C., Kinetic Analysis of Reversible Addition Fragmentation Chain Transfer (RAFT) Polymerizations: Conditions for Inhibition, Retardation, and Optimum Living Polymerization. *Macromolecular Theory and Simulations* **2002**, *11* (8), 823-835.
66. Coote, M. L.; Radom, L., Ab Initio Evidence for Slow Fragmentation in RAFT Polymerization. *Journal of the American Chemical Society* **2003**, *125* (6), 1490-1491.
67. Monteiro, M. J.; de Brouwer, H., Intermediate Radical Termination as the Mechanism for Retardation in Reversible Addition–Fragmentation Chain Transfer Polymerization. *Macromolecules* **2001**, *34* (3), 349-352.
68. Wang, A. R.; Zhu, S.; Kwak, Y.; Goto, A.; Fukuda, T.; Monteiro, M. S., A difference of six orders of magnitude: A reply to “the magnitude of the fragmentation rate coefficient”. *Journal of Polymer Science Part A: Polymer Chemistry* **2003**, *41* (18), 2833-2839.
69. McLeary, J. B.; Calitz, F. M.; McKenzie, J. M.; Tonge, M. P.; Sanderson, R. D.; Klumperman, B., Beyond Inhibition: A ¹H NMR Investigation of the Early Kinetics of RAFT-Mediated Polymerization with the Same Initiating and Leaving Groups. *Macromolecules* **2004**, *37* (7), 2383-2394.
70. McLeary, J. B.; Calitz, F. M.; McKenzie, J. M.; Tonge, M. P.; Sanderson, R. D.; Klumperman, B., A ¹H NMR Investigation of Reversible Addition–Fragmentation Chain Transfer Polymerization Kinetics and Mechanisms. Initialization with Different Initiating and Leaving Groups. *Macromolecules* **2005**, *38* (8), 3151-3161.
71. McLeary, J. B.; McKenzie, J. M.; Tonge, M. P.; Sanderson, R. D.; Klumperman, B., Initialisation in RAFT-mediated polymerisation of methyl acrylate. *Chemical communications* **2004**, (17), 1950-1951.
72. Graeme Moad, Y. K. C., Almar Postma, Ezio Rizzardo, San H. Thang, Advances in RAFT Polymerization: The synthesis of polymers with defined end-groups. *Polymer* **2005**, *46*, 8458-8468.
73. Moad, G.; Rizzardo, E.; Thang, S. H., Radical addition–fragmentation chemistry in polymer synthesis. *Polymer* **2008**, *49* (5), 1079-1131.
74. Wood, M. R.; Duncalf, D. J.; Rannard, S. P.; Perrier, S., Selective One-Pot Synthesis of Trithiocarbonates, Xanthates, and Dithiocarbamates for Use in RAFT/ MADIX Living Radical Polymerizations. *Org. Lett.* **2006**, *6* (4), 552-556.
75. Barlow, T. R.; Brendel, J. C.; Perrier, S., Poly(bromoethyl acrylate): A Reactive Precursor for the Synthesis of Functional RAFT Materials. *Macromolecules* **2016**, *49* (17), 6203-6212.
76. Congdon, T.; Shaw, P.; Gibson, M. I., Thermoresponsive, well-defined, poly(vinyl alcohol) co-polymers. *Polym. Chem.* **2015**, *6* (26), 4749-4757.

77. Green, M. D.; Allen, M. H.; Dennis, J. M.; Cruz, D. S.-d. I.; Gao, R.; Winey, K. I.; Long, T. E., Tailoring macromolecular architecture with imidazole functionality: A perspective for controlled polymerization processes. *European Polymer Journal* **2011**, 47 (4), 486-496.
78. Moad, G.; Rizzardo, E.; Thang, S. H., End-functional polymers, thiocarbonylthio group removal/transformation and reversible addition-fragmentation-chain transfer (RAFT) polymerization. *Polymer International* **2011**, 60 (1), 9-25.
79. Arshady, R., Suspension, emulsion, and dispersion polymerization: A methodological survey. *Colloid and Polymer Science* **1992**, 270 (8), 717-732.
80. Chern, C. S., Emulsion polymerization mechanisms and kinetics. *Progress in Polymer Science* **2006**, 31 (5), 443-486.
81. Rudin, A.; Choi, P., Chapter 10 - Dispersion and Emulsion Polymerizations. In *The Elements of Polymer Science & Engineering (Third Edition)*, Rudin, A.; Choi, P., Eds. Academic Press: Boston, 2013; pp 427-447.
82. Guo, J. S.; El-Aasser, M. S.; Vanderhoff, J. W., Microemulsion polymerization of styrene. *Journal of Polymer Science Part A: Polymer Chemistry* **1989**, 27 (2), 691-710.
83. Thickett, S. C.; Gilbert, R. G., Emulsion polymerization: State of the art in kinetics and mechanisms. *Polymer* **2007**, 48 (24), 6965-6991.
84. Distler, D.; Neto, W. S.; Machado, F., Emulsion Polymerization. In *Reference Module in Materials Science and Materials Engineering*, Elsevier: 2017.
85. Warson, H., Emulsion polymerization, a mechanistic approach. R. G. Gilbert. Academic Press, London, 1995. pp. xviii + 362, price £55.00. ISBN 0-12-283060-1. *Polymer International* **1996**, 41 (3), 352-352.
86. Brooks, B., Suspension Polymerization Processes. *Chemical Engineering & Technology* **2010**, 33 (11), 1737-1744.
87. Winslow, F. H.; Matreyek, W., Particle Size in Suspension Polymerization. *Industrial & Engineering Chemistry* **1951**, 43 (5), 1108-1112.
88. Tacidelli, A. R.; Alves, J. J. N.; Vasconcelos, L. G. S.; Brito, R. P., Increasing PVC suspension polymerization productivity—An industrial application. *Chemical Engineering and Processing: Process Intensification* **2009**, 48 (1), 485-492.
89. Jensen, A. T.; Neto, W. S.; Ferreira, G. R.; Glenn, A. F.; Gambetta, R.; Gonçalves, S. B.; Valadares, L. F.; Machado, F., 8 - Synthesis of polymer/inorganic hybrids through heterophase polymerizations. In *Recent Developments in Polymer Macro, Micro and Nano Blends*, Visakh, P. M.; Markovic, G.; Pasquini, D., Eds. Woodhead Publishing: 2017; pp 207-235.
90. Zhang, D.; Yang, X., Precipitation Polymerization. In *Encyclopedia of Polymeric Nanomaterials*, Kobayashi, S.; Müllen, K., Eds. Springer Berlin Heidelberg: Berlin, Heidelberg, 2021; pp 1-10.
91. Pardeshi, S.; Singh, S. K., Precipitation polymerization: a versatile tool for preparing molecularly imprinted polymer beads for chromatography applications. *RSC Advances* **2016**, 6 (28), 23525-23536.
92. Yoshimatsu, K.; Reimhult, K.; Krozer, A.; Mosbach, K.; Sode, K.; Ye, L., Uniform molecularly imprinted microspheres and nanoparticles prepared by precipitation polymerization: The control of particle size suitable for different analytical applications. *Analytica chimica acta* **2007**, 584 (1), 112-121.
93. Li, G. L.; Möhwald, H.; Shchukin, D. G., Precipitation polymerization for fabrication of complex core-shell hybrid particles and hollow structures. *Chemical Society reviews* **2013**, 42 (8), 3628-3646.
94. Barrett, K. E. J., Dispersion polymerisation in organic media. *British Polymer Journal* **1973**, 5 (4), 259-271.

95. Van Der Hoeven, P. C.; Lyklema, J., Electrostatic stabilization in non-aqueous media. *Advances in Colloid and Interface Science* **1992**, *42*, 205-277.
96. Napper, D. H., Steric stabilization. *Journal of Colloid and Interface Science* **1977**, *58* (2), 390-407.
97. Kawaguchi, S.; Ito, K., Dispersion Polymerization. In *Polymer Particles*: Okubo, M., Ed. Springer Berlin Heidelberg: Berlin, Heidelberg, 2005; pp 299-328.
98. Okubo, M.; Izumi, J.; Hosotani, T.; Yamashita, T., Production of micron-sized monodispersed core/shell polymethyl methacrylate/polystyrene particles by seeded dispersion polymerization. *Colloid and Polymer Science* **1997**, *275* (8), 797-801.
99. Ramli, R. A., Hollow polymer particles: a review. *RSC Advances* **2017**, *7* (83), 52632-52650.
100. ten Hove, J. B.; Appel, J.; van den Broek, J. M.; Kuehne, A. J. C.; Sprakel, J., Conjugated Polymer Shells on Colloidal Templates by Seeded Suzuki-Miyaura Dispersion Polymerization. *Small* **2014**, *10* (5), 957-963.
101. Sparnacci, K.; Laus, M.; Tondelli, L.; Magnani, L.; Bernardi, C., Core-shell microspheres by dispersion polymerization as drug delivery systems. *Macromolecular Chemistry and Physics* **2002**, *203* (10-11), 1364-1369.
102. Anwar, N.; Rix, A.; Lederle, W.; Kuehne, A. J. C., RGD-decorated conjugated polymer particles as fluorescent biomedical probes prepared by Sonogashira dispersion polymerization. *Chemical communications* **2015**, *51* (45), 9358-9361.
103. Badila, M.; Hébraud, A.; Brochon, C.; Hadziioannou, G., Design of Colored Multilayered Electrophoretic Particles for Electronic Inks. *ACS Applied Materials & Interfaces* **2011**, *3* (9), 3602-3610.
104. Sabu T., V. P. M., Handbook of Engineering and Specialty Thermoplastics. 429-492.
105. research, G. v., Polymethyl methacrylate (PMMA) Market Analysis By Product (Extruded Sheets, Pellets, And Acrylic Beads), by End-Use (Automotive, Construction, Electronics, Signs & Displays), Competitive Landscape, And Segment Forecasts 2014-2025. **2017**.
106. Ali, U.; Karim, K. J. B. A.; Buang, N. A., A Review of the Properties and Applications of Poly (Methyl Methacrylate) (PMMA). *Polymer Reviews* **2015**, *55* (4), 678-705.
107. Shi, M.; Kretlow, J. D.; Spicer, P. P.; Tabata, Y.; Demian, N.; Wong, M. E.; Kasper, F. K.; Mikos, A. G., Antibiotic-Releasing Porous Polymethylmethacrylate/Gelatin/Antibiotic Constructs for Craniofacial Tissue Engineering. *Journal of controlled release : official journal of the Controlled Release Society* **2011**, *152* (1), 196-205.
108. Richez, A. P.; Yow, H. N.; Biggs, S.; Cayre, O. J., Dispersion polymerization in non-polar solvent: Evolution toward emerging applications. *Progress in Polymer Science* **2013**, *38* (6), 897-931.
109. Perween, M.; Parmar, D. B.; Bhadu, G. R.; Srivastava, D. N., Polymer-graphite composite: a versatile use and throw plastic chip electrode. *Analyst* **2014**, *139* (22), 5919-5926.
110. Kost, J.; Langer, R., Responsive polymeric delivery systems. *Advanced Drug Delivery Reviews* **2001**, *46* (1), 125-148.
111. Shen, J.; Li, Z.; Cheng, R.; Luo, Q.; Luo, Y.; Chen, Y.; Chen, X.; Sun, Z.; Huang, S., Eu³⁺-Doped NaGdF₄ Nanocrystal Down-Converting Layer for Efficient Dye-Sensitized Solar Cells. *ACS Applied Materials & Interfaces* **2014**, *6* (20), 17454-17462.
112. Christian, P.; Sebastian, S.; Hermann, S., Characterization and evaluation of a PMMA-based 3D printing process. *Rapid Prototyping Journal* **2013**, *19* (1), 37-43.

113. Kendall, J. L.; Canelas, D. A.; Young, J. L.; DeSimone, J. M., Polymerizations in Supercritical Carbon Dioxide. *Chemical Reviews* **1999**, 99 (2), 543-564.
114. Mujumdar, A. S., *Handbook of industrial drying* CRC Press: 2015.
115. Birkin, N., New hydrocarbon stabilisers for dispersion polymerisation in supercritical carbon dioxide. *The University of Nottingham* **2012**.
116. Birkin, N. A.; Arrowsmith, N. J.; Park, E. J.; Richez, A. P.; Howdle, S. M., Synthesis and application of new CO₂-soluble vinyl pivalate hydrocarbon stabilisers via RAFT polymerisation. *Polymer Chemistry* **2011**, 2 (6), 1293.
117. Kemmere Maartje, F.; Meyer, T., 2006; p 0.
118. Girard, E.; Tassaing, T.; Marty, J.-D.; Destarac, M., Structure-property Relationships in CO₂-philic (co)polymers: Phase Behavior, Self-assembly and Stabilization of Water/CO₂ Emulsion. *Chemical Reviews* **2015**.
119. Kazarian, S. G.; Vincent, M. F.; Bright, F. V.; Liotta, C. L.; Eckert, C. A., Specific Intermolecular Interaction of Carbon Dioxide with Polymers. *Journal of the American Chemical Society* **1996**, 118 (7), 1729-1736.
120. Coleman, D., Dispersion Polymerization in Organic Media, K. E. J. Barrett, Ed., John Wiley & Sons, Inc., New York, 1975, 322 pp., \$27.50. *Journal of Polymer Science: Polymer Letters Edition* **1975**, 13 (9), 575-576.
121. DeSimone, J. M.; Maury, E. E.; Menciloglu, Y. Z.; McClain, J. B.; Romack, T. J.; Combes, J. R., Dispersion Polymerizations in Supercritical Carbon Dioxide. *Science* **1994**, 265 (5170), 356-359.
122. Woods, H. M.; Nouvel, C.; Licence, P.; Irvine, D. J.; Howdle, S. M., Dispersion Polymerization of MMA in scCO₂. *Macromolecules* **2005**, 38, 3271-3282.
123. Canelas, D. A.; Betts, D. E.; DeSimone, J. M., Dispersion Polymerization of Styrene in Supercritical Carbon Dioxide: Importance of Effective Surfactants. *Macromolecules* **1996**, 29 (8), 2818-2821.
124. Johnston, K. P., Block copolymers as stabilizers in supercritical fluids. *Current Opinion in Colloid and Interface Science* **2000**, 5, 351-356.
125. Shaffer, K. A.; Jones, T. A.; Canelas, D. A.; DeSimone, J. M.; Wilkinson, S. P., Dispersion Polymerizations in Carbon Dioxide Using Siloxane-Based Stabilizers. *Macromolecules* **1996**, 29 (7), 2704-2706.
126. O'Neill, M. L.; Yates, M. Z.; Johnston, K. P.; Smith, C. D.; Wilkinson, S. P., Dispersion Polymerization in Supercritical CO₂ with a Siloxane-Based Macromonomer: 1. The Particle Growth Regime. *Macromolecules* **1998**, 31 (9), 2838-2847.
127. O'Neill, M. L.; Yates, M. Z.; Johnston, K. P.; Smith, C. D.; Wilkinson, S. P., Dispersion Polymerization in Supercritical CO₂ with Siloxane-Based Macromonomer. 2. The Particle Formation Regime. *Macromolecules* **1998**, 31 (9), 2848-2856.
128. Lepilleur, C.; Beckman, E. J., Dispersion Polymerization of Methyl Methacrylate in Supercritical CO₂. *Macromolecules* **1997**, 30 (4), 745-756.
129. Christian, P.; Howdle, S. M.; Irvine, D. J., Dispersion Polymerization of Methyl Methacrylate in Supercritical Carbon Dioxide with a Monofunctional Pseudo-Graft Stabilizer. *Macromolecules* **2000**, 33 (2), 237-239.
130. Wang, W.; Naylor, A.; Howdle, S. M., Dispersion Polymerizations of Methyl Methacrylate in Supercritical Carbon Dioxide with a Novel Ester End-Capped Perfluoropolyether Stabilizer. *Macromolecules* **2003**, 36 (14), 5424-5427.
131. Yang, Y.; Dong, Q.; Wang, Z.; Shen, C.; Huang, Z.; Zhu, H.; Liu, T.; Hu, C. P., Dispersion copolymerization of acrylonitrile-vinyl acetate in supercritical carbon dioxide. *Journal of Applied Polymer Science* **2006**, 102 (6), 5640-5648.

132. Tai, H.; Wang, W.; Howdle, S. M., High molecular weight graft stabilisers for dispersion polymerisation of vinylidene fluoride in supercritical carbon dioxide: the effect of architecture. *Polymer* **2005**, *46* (24), 10626-10636.
133. Molecular multipole moments. *Molecular Physics* **1966**, *11* (4), 371-393.
134. Dardin, A.; Cain, J. B.; DeSimone, J. M.; Johnson, C. S.; Samulski, E. T., High-Pressure NMR of Polymers Dissolved in Supercritical Carbon Dioxide. *Macromolecules* **1997**, *30* (12), 3593-3599.
135. Hu, D. D.; Zhang, Y. N.; Su, M.; Bao, L.; Zhao, L.; Liu, T., Effect of molecular weight on CO₂-philicity of poly(vinyl acetate) with different molecular chain structure. *J. Supercrit. Fluids* **2016**, *118*, 96-106.
136. Shen, Z.; McHugh, M. A.; Xu, J.; Belardi, J.; Kilic, S.; Mesiano, A.; Bane, S.; Karnikas, C.; Beckman, E.; Enick, R., CO₂-solubility of oligomers and polymers that contain the carbonyl group. *Polymer* **2003**, *44* (5), 1491-1498.
137. Rindfleisch, F.; DiNoia, T. P.; McHugh, M. A., Solubility of Polymers and Copolymers in Supercritical CO₂. *The Journal of Physical Chemistry* **1996**, *100* (38), 15581-15587.
138. O'Neill, M. L.; Cao, Q.; Fang, M.; Johnston, K. P.; Wilkinson, S. P.; Smith, C. D.; Kerschner, J. L.; Jureller, S. H., Solubility of Homopolymers and Copolymers in Carbon Dioxide. *Industrial & Engineering Chemistry Research* **1998**, *37* (8), 3067-3079.
139. Drohmann, C.; Beckman, E. J., Phase behavior of polymers containing ether groups in carbon dioxide. *The Journal of Supercritical Fluids* **2002**, *22* (2), 103-110.
140. Tryznowski, M.; Tomczyk, K.; Fraś, Z.; Gregorowicz, J.; Rokicki, G.; Wawrzyńska, E.; Parzuchowski, P. G., Aliphatic Hyperbranched Polycarbonates: Synthesis, Characterization, and Solubility in Supercritical Carbon Dioxide. *Macromolecules* **2012**, *45* (17), 6819-6829.
141. Girard, E.; Tassaing, T.; Camy, S.; Condoret, J. S.; Marty, J. D.; Destarac, M., Enhancement of poly(vinyl ester) solubility in supercritical CO₂ by partial fluorination: the key role of polymer-polymer interactions. *Journal of the American Chemical Society* **2012**, *134* (29), 11920-3.
142. Nelson, M. R.; Borkman, R. F., Ab Initio Calculations on CO₂ Binding to Carbonyl Groups. *The Journal of Physical Chemistry A* **1998**, *102* (40), 7860-7863.
143. Hsiao, Y.-L.; Maury, E. E.; DeSimone, J. M.; Mawson, S.; Johnston, K. P., Dispersion Polymerization of Methyl Methacrylate Stabilized with Poly(1,1-dihydroperfluorooctyl acrylate) in Supercritical Carbon Dioxide. *Macromolecules* **1995**, *28* (24), 8159-8166.
144. Blasig, A.; Shi, C.; Enick, R. M.; Thies, M. C., Effect of Concentration and Degree of Saturation on RESS of a CO₂-Soluble Fluoropolymer. *Industrial & Engineering Chemistry Research* **2002**, *41* (20), 4976-4983.
145. Sarbu, T.; Styranec, T. J.; Beckman, E. J., Design and Synthesis of Low Cost, Sustainable CO₂-philes. *Industrial & Engineering Chemistry Research* **2000**, *39* (12), 4678-4683.
146. Park, E. J.; Richez, A. P.; Birkin, N. A.; Lee, H.; Arrowsmith, N.; Thurecht, K. J.; Howdle, S. M., New vinyl ester copolymers as stabilisers for dispersion polymerisation in scCO₂. *Polymer* **2011**, *52* (24), 5403-5409.
147. Lee, H.; Terry, E.; Zong, M.; Arrowsmith, N.; Perrier, S.; Thurecht, K. J.; Howdle, S. M., Successful Dispersion Polymerization in Supercritical CO₂ Using Polyvinylalkylate Hydrocarbon Surfactants Synthesized and Anchored via RAFT. *Journal of the American Chemical Society* **2008**, *130* (37), 12242-12243.
148. Lee, H.; Pack, J. W.; Wang, W.; Thurecht, K. J.; Howdle, S. M., Synthesis and Phase Behavior of CO₂-Soluble Hydrocarbon Copolymer: Poly(vinyl acetate-alt-dibutyl maleate). *Macromolecules* **2010**, *43* (5), 2276-2282.

149. Arrowsmith, N., *Thesis*.
150. Jin, J.-s.; Chang, C.-w.; Zhu, J.; Wu, H.; Zhang, Z.-t., Solubility of Poly(vinylpyrrolidone) with Different Molecular Weights in Supercritical Carbon Dioxide. *Journal of Chemical & Engineering Data* **2015**, *60* (11), 3397-3403.
151. Destarac, M.; Brochon, C.; Catala, J.-M.; Wilczewska, A.; Zard, S. Z., Macromolecular Design via the Interchange of Xanthates (MADIX): Polymerization of Styrene with O-Ethyl Xanthates as Controlling Agents. *Macromolecular Chemistry and Physics* **2002**, *203* (16), 2281-2289.
152. Stenzel, M. H.; Cummins, L.; Roberts, G. E.; Davis, T. P.; Vana, P.; Barner-Kowollik, C., Xanthate Mediated Living Polymerization of Vinyl Acetate: A Systematic Variation in MADIX/RAFT Agent Structure. *Macromol. Chem. Phys.* **2003**, *204*, 1160-1168.
153. Guinaudeau, A.; Mazières, S.; Wilson, D. J.; Destarac, M., Aqueous RAFT/MADIX polymerisation of N-vinyl pyrrolidone at ambient temperature. *Polym. Chem.* **2012**, *3* (1), 81-84.
154. Yamada, K.; Nakano, T.; Okamoto, Y., Free-radical copolymerization of vinyl esters using fluoroalcohols as solvents: The solvent effect on the monomer reactivity ratio. *Journal of Polymer Science Part A: Polymer Chemistry* **2000**, *38* (1), 220-228.
155. McAllister, T. D.; Farrand, L. D.; Howdle, S. M., Improved Particle Size Control for the Dispersion Polymerization of Methyl methacrylate in Supercritical Carbon Dioxide. *Macromolecular Chemistry and Physics* **2016**, *217* (20), 2294-2301.
156. Parilti, R.; Alaimo, D.; Grignard, B.; Boury, F.; Howdle, S. M.; Jerome, C., Mild synthesis of poly(HEMA)-networks as well-defined nanoparticles in supercritical carbon dioxide. *Journal of Materials Chemistry B* **2017**, *5* (29), 5806-5815.
157. Flory, P. J.; Leutner, F. S., Occurrence of head-to-head arrangements of structural units in polyvinyl alcohol. *Journal of Polymer Science* **1948**, *3* (6), 880-890.
158. Morin, A. N.; Detrembleur, C.; Jérôme, C.; De Tullio, P.; Poli, R.; Debuigne, A., Effect of Head-to-Head Addition in Vinyl Acetate Controlled Radical Polymerization: Why Is Co(acac)₂-Mediated Polymerization so Much Better? *Macromolecules* **2013**, *46* (11), 4303-4312.
159. Iovu, M. C.; Matyjaszewski, K., Controlled/Living Radical Polymerization of Vinyl Acetate by Degenerative Transfer with Alkyl Iodides. *Macromolecules* **2003**, *36* (25), 9346-9354.
160. Koumura, K.; Satoh, K.; Kamigaito, M., Mn₂(CO)₁₀-Induced RAFT Polymerization of Vinyl Acetate, Methyl Acrylate, and Styrene. *Polym. J* **2009**, *41* (8), 595-603.
161. Guerre, M.; Semsarilar, M.; Godiard, F.; Ameduri, B.; Ladmiral, V., Polymerization-induced self-assembly of PVAc-b-PVDF block copolymers via RAFT dispersion polymerization of vinylidene fluoride in dimethyl carbonate. *Polymer Chemistry* **2017**, *8* (9), 1477-1487.
162. Yu, H.; Chen, Q.; Zhang, Z.; Zhu, J.; Cheng, Z.; Zhou, N.; Zhang, W.; Zhu, X., ⁶⁰Co γ -irradiation-initiated RAFT polymerization of VAc at room temperature. *Reactive and Functional Polymers* **2012**, *72* (2), 153-159.
163. Britton, D.; Heatley, F.; Lovell, P. A., ¹³C NMR Spectroscopy Studies of Branching and Sequence Distribution in Copolymers of Vinyl Acetate and n-Butyl Acrylate Prepared by Semibatch Emulsion Copolymerization. *Macromolecules* **2001**, *34* (4), 817-829.
164. Britton, D.; Heatley, F.; Lovell, P. A., Chain Transfer to Polymer in Free-Radical Bulk and Emulsion Polymerization of Vinyl Acetate Studied by NMR Spectroscopy. *Macromolecules* **1998**, *31* (9), 2828-2837.

165. P. Hems, W.; Yong, T.-M.; L. M. van Nunen, J.; I. Cooper, A.; B. Holmes, A.; A. Griffin, D., Dispersion polymerisation of methyl methacrylate in supercritical carbon dioxide-evaluation of well defined fluorinated AB block copolymers as surfactants. *Journal of Materials Chemistry* **1999**, 9 (7), 1403-1407.
166. Deniz, S.; Baran Acarali, N.; Akgun, M.; Uzun, İ.; Dincer, S., *Dispersion polymerization of methyl methacrylate in supercritical carbon dioxide using a silicone-containing fluoroacrylate stabilizer*. 2005; Vol. 54, p 1660-1668.
167. Hwang, H. S.; Yuvaraj, H.; Kim, W. S.; Lee, W.-K.; Gal, Y.-S.; Lim, K. T., Dispersion polymerization of MMA in supercritical CO₂ stabilized by random copolymers of 1H,1H-perfluorooctyl methacrylate and 2-(dimethylaminoethyl methacrylate). *Journal of Polymer Science Part A: Polymer Chemistry* **2008**, 46 (4), 1365-1375.
168. Giles, M. R.; O'Connor, S. J.; Hay, J. N.; Winder, R. J.; Howdle, S. M., Novel Graft Stabilizers for the Free Radical Polymerization of Methyl Methacrylate in Supercritical Carbon Dioxide. *Macromolecules* **2000**, 33 (6), 1996-1999.
169. Birkin, N. A.; Wildig, O. J.; Howdle, S. M., Effects of poly(vinyl pivalate)-based stabiliser architecture on CO₂-solubility and stabilising ability in dispersion polymerisation of N-vinyl pyrrolidone. *Polymer Chemistry* **2013**, 4 (13), 3791.
170. Dardin, A.; DeSimone, J. M.; Samulski, E. T., Fluorocarbons Dissolved in Supercritical Carbon Dioxide. NMR Evidence for Specific Solute–Solvent Interactions. *The Journal of Physical Chemistry B* **1998**, 102 (10), 1775-1780.
171. Moad, G.; Keddie, D.; Guerrero-Sanchez, C.; Rizzardo, E.; Thang, S. H., Advances in Switchable RAFT Polymerization. *Macromolecular Symposia* **2015**, 350 (1), 34-42.
172. Nicolaÿ, R.; Kwak, Y.; Matyjaszewski, K., Synthesis of poly(vinyl acetate) block copolymers by successive RAFT and ATRP with a bromoxanthate iniferter. *Chemical communications* **2008**, (42), 5336-5338.